NTNU

Norwegian University of
Science and Technology

Modification of Existing Permeameters to Estimate Hydraulic Conductivity of Groundwater in Unconsolidated Sand in the Laboratory

Runa Aronsen Solberg

Petroleum Geoscience and Engineering
Submission date: June 2018
Supervisor: Randi Kalskin Ramstad, IGP
Co-supervisor: Ole Torsæter, IGP

Norwegian University of Science and Technology
Department of Geoscience and Petroleum

Thesis Description

Title: Modification of Existing Permeameters to Estimate Hydraulic Conductivity of Groundwater in Unconsolidated Sand in the Laboratory

Student: Runa Aronsen Solberg

Supervisor: Associate Professor Randi Kalskin Ramstad

Co-supervisor: Professor Ole Torsæter

Objective: The objective of this thesis is to modify three already existing permeameters to better estimate the hydraulic conductivity of groundwater in unconsolidated sand. The permeameters are originally used for hydraulic conductivity measurements in the laboratory for petroleum (liquid and gas) and groundwater (Darcy-cell) purposes, respectively.

Thesis description:

- Relevant background theory and literature study on important hydrogeological parameters for estimation of hydraulic conductivity.
- Literature study on different laboratory methods used to estimate hydraulic conductivity. The work will focus on three methods; the air permeameter, the liquid permeameter and the Darcy-cell.
- Literature study on other laboratory methods important when estimating hydraulic conductivity.
- Modify the existing Darcy-cell to better estimate hydraulic conductivity of groundwater in unconsolidated sand in the laboratory. Include a description of the process and equipment.
- Modify the existing core permeameters to enable testing with unconsolidated sand.
- Estimate and compare hydraulic conductivity of groundwater in unconsolidated sand using the modified Darcy-cell and the modified air- and liquid permeameters. Evaluate and discuss these values.
- Evaluate and discuss how implemented modifications to the modified Darcy-cell and the modified air- and liquid permeameters can have affected estimated hydraulic conductivity.
- Conclusion and suggestions of further work.

Abstract

"Modification of Existing Permeameters to Estimate Hydraulic Conductivity of Groundwater in Unconsolidated Sand in the Laboratory" is a master thesis written by Runa Aronsen Solberg in the spring of 2018. The thesis is the final work of the course *TPG4920 – Petroleum Engineering, Master's Thesis*, at the Department of Geoscience and Petroleum at the Norwegian University of Science and Technology (NTNU). The thesis is a continuation of the author's specialization project completed during autumn 2017. The thesis contains a total of 116 pages.

Hydraulic conductivity describes how easily a fluid is transported through a porous medium and can be estimated using several methods. A simple and cost-efficient method used to estimate hydraulic conductivity is by permeameter testing in the laboratory. It has proved to be a challenge to estimate hydraulic conductivity in the laboratory because the sample material does not represent an undisturbed "in situ" material in the field, because the grain structure of the sample is disturbed during the drilling process of groundwater wells and when transported from the well to the laboratory. The objective of this thesis is to modify 3 already existing permeameters; the Darcy-cell, the air permeameter and the liquid permeameter (the latter 2 collectively called core permeameters), to better calculate the hydraulic conductivity of groundwater in unconsolidated sand in the laboratory. The purpose of this is to obtain results for hydraulic conductivity of groundwater that can be used as an estimate of the "in-situ" hydraulic conductivity in unconsolidated sand in the field.

The smallest average value of hydraulic conductivity is estimated using the liquid permeameter with a value of $2{,}19 \times 10^{-6}$ m/s, followed by the air permeameter with a value of $2{,}25 \times 10^{-5}$ m/s. The largest value was estimated using the Darcy -cell with an average of $1{,}26 \times 10^{-3}$ m/s. The results show that it is not possible to use the modified core permeameters to estimate the hydraulic conductivity of groundwater in unconsolidated sand. Further modifications of the setup and collection of more data is needed. The modified Darcy-cell provides the most reliable values for hydraulic conductivity, but methods of fully saturating the sample needs to be further investigated to obtain results for hydraulic conductivity of groundwater that can be used as an estimate of the "in-situ" hydraulic conductivity of unconsolidated sand in the field.

Sammendrag

"Modifisering av eksisterende permeametere for å estimere hydraulisk konduktivitet til grunnvann i ukonsolidert sand i laboratoriet" er en masteroppgave skrevet av Runa Aronsen Solberg våren 2018. Masteroppgaven er skrevet i forbindelse med emnet *TPG4920 – Petroleumsteknologi, masteroppgave*, ved Institutt for geovitenskap og petroleum ved Norges teknisk-naturvitenskapelige universitet (NTNU). Oppgaven er en videreføring av forfatterens fordypningsprosjekt gjennomført høsten 2017. Oppgaven er på totalt 116 sider.

Hydraulisk konduktivitet beskriver hvor lett en væske beveger seg gjennom et porøst medium og kan estimeres ved bruk av flere metoder. En enkel og kostnadsbesparende metode for å estimere hydraulisk konduktivitet er ved permeametertesting i laboratoriet. Det har vist seg å være en utfordring å estimere hydraulisk konduktivitet i laboratoriet fordi prøvematerialet ikke representerer et uforstyrret "in-situ" materiale i felt, fordi kornstrukturen til prøven blir forstyrret under boreprosessen av grunnvannsbrønner og når den transporteres fra brønn til laboratoriet. Målet med denne oppgaven er å modifisere 3 allerede eksisterende permeametere; Darcy-cellen, luft permeameteret og væske permeameteret (de 2 sistnevnte samlet kalt kjerne permeametere), i et forsøk på å bedre beregne hydraulisk konduktivitet til en ukonsolidert sand i laboratoriet. Formålet med dette er å få resultater for hydraulisk konduktivitet av grunnvann som kan brukes som et estimat av "in situ" hydraulisk konduktivitet i ukonsolidert sand i felt.

Den minste gjennomsnittlige verdien for hydraulisk konduktivitet estimeres ved bruk av væske permeameteret og gir en verdi lik $2{,}19 \times 10^{-6}$ m/s, etterfulgt av luft permeameteret med en verdi lik $2{,}25 \times 10^{-5}$ m/s. Den største verdien estimeres ved bruk av Darcy-cellen med et gjennomsnitt lik $1{,}26 \times 10^{-3}$ m/s. Resultatene fra oppgaven viser at det ikke er mulig å bruke de modifiserte kjerne permeameterne til estimering av hydraulisk konduktivitet til grunnvann i ukonsolidert sand. Ytterligere modifikasjoner av oppsett og innsamling av mer data er nødvendig. Den modifiserte Darcy-cellen gir de mest pålitelige verdiene for hydraulisk konduktivitet, men metoder for å fullstendig mette prøven med saltvann må undersøkes ytterligere for å få resultater for hydraulisk konduktivitet av grunnvann som kan brukes som et estimat av «in-situ» hydraulisk konduktivitet til en ukonsolidert sand i felt.

Preface

The objective of this thesis is to modify 3 already existing permeameters to better estimate the hydraulic conductivity of unconsolidated sand in the laboratory. The purpose of this is to obtain results for hydraulic conductivity of groundwater that can be used as an estimate of the "in-situ" hydraulic conductivity in unconsolidated sand in the field. The laboratory work has been conducted in the Reservoir laboratory and in the Engineering Geology laboratory at the Department of Geoscience and Petroleum.

I would like to extend my gratitude to Staff Engineer Roger Overå for great assistance during my work in the laboratory. A special thank you to Staff Engineer Håkon Myhren, Staff Engineer Terje Bjerkan, Senior Engineer Noralf Vedvik and Senior Engineer Steffen Wærnes Moen for priceless help in building and programming the components for the Darcy-cell and for helping with the modifications of the core permeameters.

I would like to thank my supervisor Randi Kalskin Ramstad, Associate Professor at the Department of Geoscience and Petroleum and my co-supervisor Ole Torsæter, Professor at the Department of Geoscience and Petroleum, for providing good guidance and advice. I would also like to express my gratitude to Researcher Atle Dagestad from the Geological Survey of Norway (NGU) for his excellent guidance, advice and good discussions regarding my work. Thank you to PhD Candidate Sondre Gjengedal for his assistance in the Engineering Geology laboratory and for his advice on designs for the Darcy-cell.

Thank you to friends and classmates for everything we have experienced together, both socially and academically, during these five years of ups and downs at NTNU.

Thank you, Matias, for always providing support and comfort and for being who you are.

Lastly, a special thank you to my family for all their support during my five years at NTNU. Thank you, pappa, for our academic discussions and your support. Thank you, mamma, for always being there when I needed moral support and someone to talk to. Thank you, Njord, for your guidance and advice regarding my work.

Runa Aronsen Solberg

Trondheim, 11. June 2018

Table of Contents

List of Figures

List of Tables

Nomenclature

μ	Viscosity
γ	Specific weight
ρ	Fluid density
A	Cross-sectional area
C_u	Uniformity coefficient
C	Proportionality factor
d	Grain diameter
d_n	The grain-size that is n percent finer by weight
h_i	Hydraulic head level at level i
ID	Inner diameter
K	Hydraulic conductivity
k	Permeability
k_f	Filter permeability
k_s	Sand permeability
K_s	Hydraulic conductivity of groundwater in sand
K_T	Total hydraulic conductivity. Includes hydraulic conductivity through filters and sand
L	Length
L_{Bottom}	Length of Darcy-cell top lid
L_{Top}	Length of Darcy-cell bottom lid
L_s	Length of sand sample
L_{swc}	Length of saltwater column above sand sample
$L_{cyl.\ -sample}$	length from the top of the sample inside the matrix cup to the top of the matrix cup
m	Mass
m_{sw}	Mass of saltwater
m_{cws}	Mass of cylinder with wet sand sample
m_{cds}	Mass of cylinder with dry sand sample
n	Porosity
n_{eff}	Effective porosity
OD	Outer diameter

P	Pressure
Δp	Pressure drop/pressure loss/pressure difference
Q	Flow rate
q	Darcy velocity
R	Reynolds number
S_i	Fluid saturation, where i is fluid type
t	Time
V_p	Pore volume
V_{tot}	Total soil or rock volume
V_b	Bulk volume
V_g	Volume of solid material
V_f	Fluid volume
V_{eff}	Interconnected pore volume
V_{sw}	Volume of saltwater
V_{swc}	Volume of saltwater column above sand sample
V_s	Total volume of sand
V_1	volume of the empty matrix cup
V_2	volume of the matrix cup and sand sample

Abbreviations

EDS	Energy-dispersive X-ray spectroscopy
PC	Polycarbonate
POM	Polyoxymethylene
PVC	Polyvinyl chloride
SE	Secondary electron
SEM	Scanning electron microscopy

1 Introduction

Hydraulic conductivity is considered one of the most important parameters within hydrogeological contexts and describes how easily a fluid is transported through a porous medium. The parameter can be estimated using several different methods, where permeameter testing, grain-size distribution analysis and pumping tests are considered the most common. Pumping tests are considered the most accurate method because the soil sample in this test represents an undisturbed "in situ" material, but the tests are time-consuming and costly. Estimation of hydraulic conductivity using empirical formulas based on grain size distribution is a simpler and less expensive method, but it is often difficult to predict the precision of these. Estimation of hydraulic conductivity can also be easily accomplished by permeameter testing in the laboratory. A weakness in estimating the hydraulic conductivity in the laboratory is that the sample material does not represent an undisturbed "in situ" material because the grain structure of the sample is disturbed during the drilling process of the groundwater well and when transported from the well to the laboratory.

The most common method of permeameter testing is performed using a type of permeameter cell known as a Darcy-cell. To be able to correctly estimate the hydraulic conductivity of groundwater in a soil one must assume that the sample is fully saturated with water. However, fully saturating a soil sample in the Darcy-cell has proven to be a challenge, as gas bubbles may be trapped in the pore spaces. Extracting the air in the sample by applying vacuum to the cell will make it easier to fully saturate the sand sample. It has however not been possible to apply vacuum on the existing cell at the Department of Geoscience and Petroleum because the existing cell-wall is too weak to withstand the difference in pressure on its inside and outside when vacuum is applied. It is therefore a wish to modify the existing apparatus to make it possible to apply vacuum on the cell, to better estimate the hydraulic conductivity in soils.

There is, however, a variety of permeameter tests that can be used to estimate hydraulic conductivity. Two permeameter types (collectively called core permeameters), the air permeameter and the liquid permeameter, are commonly used in the petroleum industry to estimate the permeability of core samples. It is in theory possible to estimate the hydraulic conductivity in an unconsolidated soil sample using the core permeameters, but it has not yet been conducted successfully because the apparatuses are not designed to contain

unconsolidated material. It is therefore necessary to modify the existing core permeameters to enable testing of unconsolidated soil samples in the laboratory.

The objective of this thesis is therefore, to modify the existing Darcy-cell to better estimate the hydraulic conductivity of groundwater in soils in the laboratory, with the purpose of obtaining results for hydraulic conductivity that can be used as an estimate of the "in-situ" hydraulic conductivity of groundwater in soils in the field. Further, the objective is to modify the core permeameters to enable testing of unconsolidated soils in the laboratory, with the purpose of obtaining results that can estimate what the hydraulic conductivity is in the field.

The data in this project is based on the testing of an unconsolidated sand collected from 2 wells in the city center of Elverum. The sand sample consists of fluvial/glacifluvial deposits and is collected during a project named "*Optimal ressursutnyttelse av grunnvann til oppvarming og kjøling i Melhus og Elverum (ORMEL*)", in English named *"Optimal resource utilization of groundwater for heating and cooling in Melhus and Elverum"*.

1.1 Thesis structure

The thesis is structured into 7 main parts:

- *Chapter 2: Theory* addresses hydrogeological concepts important for estimation of hydraulic conductivity. A description of different permeameter types used to estimate hydraulic conductivity and an insight into relevant international standard test methods is also given. The chapter also covers theory on other laboratory methods important when estimating hydraulic conductivity. This chapter includes some material from the author's specialization project, autumn 2017 (Solberg, 2017).

- *Chapter 3: Method* describes the modification process for the core permeameters and Darcy-cell. Laboratory procedures and setups used in the thesis are also explained and observations during the tests are described. This chapter also includes some material from the author's specialization project, autumn 2017 (Solberg, 2017).

- *Chapter 4: Results* gives an overview of the most relevant results obtained from the laboratory work. Raw data is found in appendices A-J.

- *Chapter 5: Discussion* evaluates the results and assesses its reliability. Suggestions to further modifications to the permeameters used in the thesis is made. Potential sources of error will also be studied.
- *Chapter 6: Conclusion* gives a summary of the major findings and results.
- *Chapter 7: Further Work* gives suggestions to further work.

2 Theory

The following chapter addresses hydrogeological concepts that are relevant for estimating hydraulic conductivity. Further, a description of different permeameter types used to estimate hydraulic conductivity and an insight into relevant international standard test methods is given. Lastly, the chapter covers theory on relevant laboratory methods.

2.1 Groundwater and aquifers

The ground can be divided into a saturated and an undersaturated zone based on water content present in the soil. The water content in the undersaturated zone varies, whereas it remains constant in the saturated zone. The movable water present in the saturated zone is termed groundwater (Brattli, 2009). The groundwater surface is known as the water table and is an undulating surface representing the boundary between the undersaturated and the saturated zone. In this divide, the hydrostatic pressure is equal to the atmospheric pressure (Freeze & Cherry, 1979). The depth at which the water table appears depends upon topography and climate. The water table surface normally follows the topographical surface, but also appears in rivers, lakes and at sea level (Brattli, 2009). Damp climate can cause the water table to lie quite high in the groundwater profile, whilst a drier climate will cause it to lie deeper.

An aquifer can be defined as a saturated permeable geological unit that can store and release water with flow rates high enough to deliver usable amounts of water to groundwater wells (Fetter, 2001; Freeze & Cherry, 1979). An aquifer can be divided into three types: unconfined, confined and semi-confined, see Figure 2.1. An unconfined aquifer is bound by an underlying impermeable layer, also termed aquiclude, whilst the water table is in direct contact with the atmosphere (Fetter, 2001). This means that the water table has a pressure corresponding to atmospheric pressure. Examples of unconfined aquifers are unconsolidated soils such as sand or gravel and fractured rocks that do not have an overlying impermeable layer.

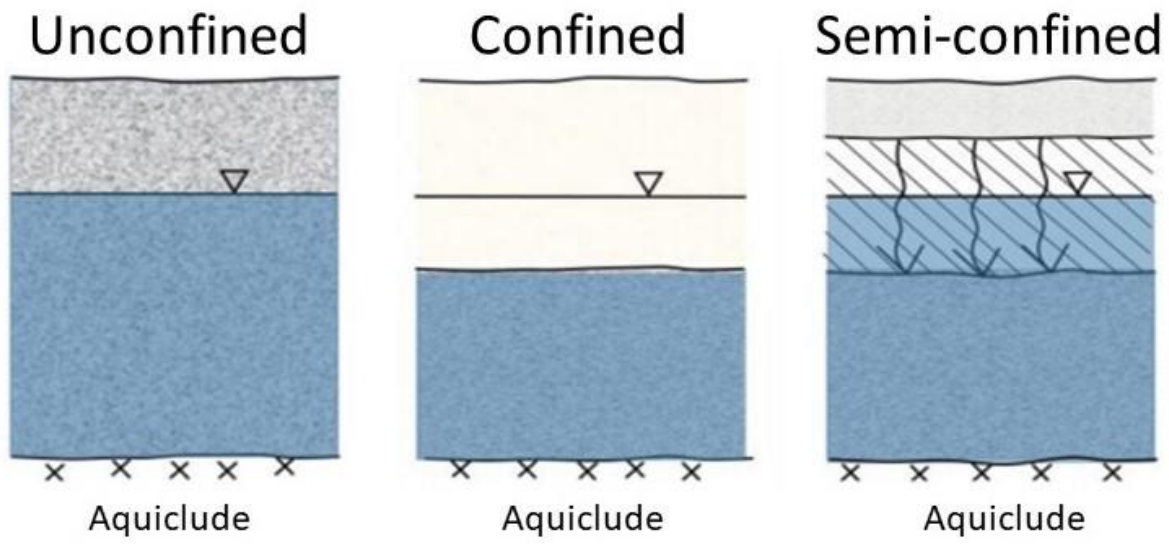

Figure 2.1:Unconfined, confined and semi-confined aquifers (Brattli, 2009).

A confined aquifer is bound by an overlying and underlying impermeable layer, and is fed with water from higher topographical locations (Fetter, 2001). This causes the water in the aquifer to be over pressured. Installing a well through the overlying dense layer causes the groundwater in the well to rise to a height higher than the water table surface (Schwartz & Zhang, 2003). Semi-confined aquifers are bound by an overlying low-permeable layer and an underlying impermeable layer. The overlying layer allows for a certain supply of water. The water pressure in a semi-confined aquifer is higher than in an unconfined aquifer, but lower than in a confined aquifer.

2.2 Hydrogeological concepts

The following subchapter describes hydrogeological concepts relevant for estimation of hydraulic conductivity.

2.2.1 Porosity

Porosity greatly affects the fluid flow rate in a soil and hydraulic conductivity greatly relies on fluid flow rate. Consequently, the soil porosity influences the value of hydraulic conductivity. A higher porosity tends to yield a higher value for hydraulic conductivity and similarly a lower porosity yields a lower hydraulic conductivity. Porosity indicates how much volume of soil or rock, that consists of pore space. Porosity is defined as the relationship between the pore space and the total volume and can be expressed as a fraction or a percentage (Torsæter & Abtahi, 2000).

Porosity can be expressed mathematically as:

$$n = \frac{V_p}{V_{tot}} \times 100 \tag{2.1}$$

Where *n* is porosity expressed as a percentage, V_p is the pore volume and V_{tot} is the total volume of the soil or rock.

Porosity can be classified as primary or secondary. Primary porosity occurs during the deposition of sediment that forms the soil or rock, while secondary porosity is caused by geological processes subsequent to the sediment deposition (Torsæter & Abtahi, 2000). An example of secondary porosity is fractured rock. In soils, porosity is dependent on packing, grading, grainsize, grain shape and grain orientation (Schwartz & Zhang, 2003). Fetter (2001) explains that spherical grains of the same size form a cubic packing, see Figure 2.2, and is the packing with the highest theoretical porosity of 47,65%. Applying a load to the grains causes them to shift with respect to one another and creates a rhombohedral packing with a theoretical porosity of 25,95%, see Figure 2.2. He explains that these two packing types constitute extreme cases for porosity when packing spherical grains of the same size. The porosity decreases if a sediment contains grains of different sizes because the smaller grains fill the free pore space in the sediment. An example of a soil containing two different grain sizes forming a cubic packing can be seen in Figure 2.2, where the porosity has been reduced from 47,65% to 14% (Torsæter & Abtahi, 2000). Introducing additional grain sizes causes the porosity to decrease further. Geological agents such as running water, wind and wave activity often contributes to the formation of well-sorted deposits, while ice erosion and avalanches contribute to poorly sorted sediments, also called well-graded sediments (Brattli, 2009; Fetter, 2001).

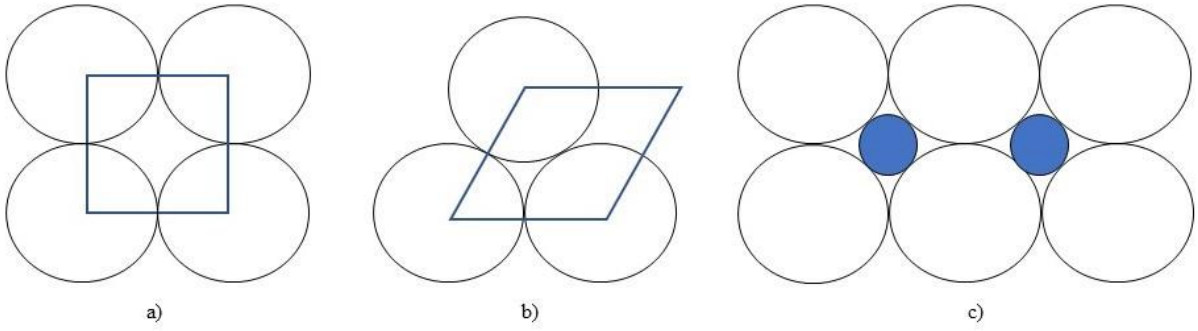

Figure 2.2:Packing types. a) Cubic packing, b) rhombohedral packing, c) cubic packing with two grain sizes. Sketch based on (Fetter, 2001).

Grain shape also affects the porosity of a soil. Spherical grains form a denser packing with less pore space causing a lower porosity as opposed to irregularly shaped grains (Fetter, 2001). In addition, the grain orientation of the irregular grains will affect the porosity of the soil (Brattli, 2009). Lastly, the grade of cementation describes how much cement is present in the soil. An increase in cement present in the soil contributes to a reduced porosity.

A distinction is made between total porosity and effective porosity. Total porosity considers the total pore space of a soil or rock, including pores that are not interconnected. It is common to only look at the interconnected pores when studying the flow in porous media because this pore volume is what contributes to fluid flow. Thus, the concept of effective porosity is applied to describe the relationship between the interconnected pore volume and the total volume of the soil or rock (Jacob Bear, 1972). Effective porosity can be expressed mathematically as:

$$n_{eff} = \frac{V_{eff}}{V_{tot}} \times 100 \tag{2.2}$$

Where n_{eff} is the effective porosity [%] and V_{eff} is the interconnected pore volume. Table 2.1 shows the porosity of a variety of sediments. Sand and gravel have a high porosity ranging between 24-53% which, among other things, is due to the irregular shape of the grains. Clays also have a high porosity, but the pores are very small, making it difficult for water to flow through the pore system. In addition, the surface properties of the clay mineral cause the water molecules to stick to the clay particles hindering the flow of water. These characteristics affect the hydraulic conductivity of the clay and results in it being low (Brattli, 2009).

Table 2.1: The porosity of a variety of sediments (Schwartz & Zhang, 2003).

Sediment	**Porosity [%]**
Coarse gravel	24-36
Fine gravel	25-38
Coarse sand	31-46
Fine sand	26-53
Silt	34-61
Clay	34-60

2.2.2 Grain size distribution

The diameter of each grain in a soil sample is of importance when performing a Darcy-cell experiment. This is because when a soil sample is inserted into a cylinder like the one in the Darcy-cell, the orientation of the grains touching the cylinder will be different from what the grain orientation is like in the field. The wall of the cylinder pushes on the grains closest to the wall. This in turn causes these grains to push on the neighbouring grains, and so on. So, identifying the largest grain diameter in the sample is important when flowing fluid through a soil sample in a cylinder. Knowing the largest grain diameter in the sample makes it possible to estimate how far into the sample the "push" from the wall on the grains will travel. A requirement described by Chapuis (2012) says that the inner diameter of the cylinder must be eight to ten times the largest grain diameter in the sample. This requirement is also described in the international test method *D2434-68 Permeability of Granular Soils (Constant Head)* by ASTM International (2006). However, in this standard the requirement says that the inner diameter of the cylinder must be between 8 and 12 times the maximum grain size in the sample. Since the requirement varies between 8 to 12 times the largest grain diameter, this thesis will apply a requirement that says the inner diameter of the cylinder must be ten times the largest grain diameter. Applying this requirement means that when fluid flows through the sample, the inner part of the cylinder will not be affected by the "wall effect", and the fluid in the middle of the cylinder is more likely to flow similar to how fluid flows in field. It should however be noted, that other disturbances such as the method used to pack the sample and disturbances during the test can affect the fluid flow, causing it to change its flow path.

Classification of sediments is based on the diameter of each grain in a sample. Table 2.2 shows how soils are classified based on their grain size. Gravel, sand and silt are further divided into sub-sections of coarse, medium and fine. The divide between silt and clay represents the transition between particles visible and invisible to the human eye. How the grains are distributed in a sample greatly affects the hydraulic conductivity of a soil (Fetter, 2001). The grain size distribution of a soil can be represented by plotting the grain sizes in a logarithmic scale on the x-axis and the cumulative percent finer by weight on an arithmetic scale on the y-axis, see Figure 2.3. Determining the grain size of the sand fraction is done by shaking the sand through multiple sieves with decreasing mesh openings, called a sieve analysis. The grain size of the silt and clay fractions are too small to determine in a sieve analysis, so a hydrometer test is normally used to determine the silt and clay fractions. The hydrometer test determines the grain sizes based on the time it takes for the sediments to settle in water (Fetter, 2001). The

hydrometer test will not be used in this master thesis, and will not be discussed any further. The sieve analysis is discussed in further detail in subchapter 3.3.

Table 2.2: Grain-size classification (Brattli, 2015).

Section	Sub-section	Grain size [mm]
Boulder		>600
Cobble		60-600
Gravel	Coarse	20-60
	Medium	6-20
	Fine	2-6
Sand	Coarse	0.6-2
	Medium	0.2-0.6
	Fine	0.06-0.22
Silt	Coarse	0.02-0.06
	Medium	0.006-0.02
	Fine	0.002-0.006
Clay		<0.002

It is possible to determine if a sediment is well- or poorly sorted using the uniformity coefficient C_u (Fetter, 2001). The parameters needed to determine C_u can be read from the grain-size distribution curve. Mathematically the uniformity coefficient, C_u, can be expressed as:

$$C_u = \frac{d_{60}}{d_{10}} \tag{2.3}$$

Where d_{60} and d_{10} is the grain-size that is 60% and 10% finer by weight, respectively. Brattli (2015) classifies the uniformity coefficient in the following manner; if C_u is less than 5, the soil is well sorted. If C_u is between 5-15, the soil is medium sorted and if C_u is more than 15, the soil is poorly sorted.

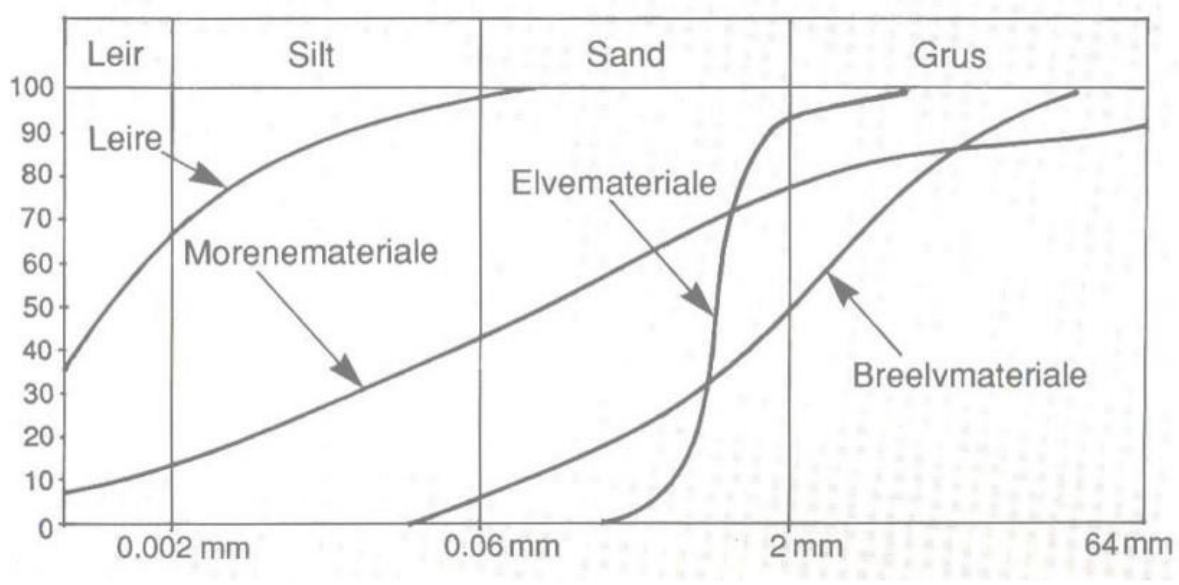

Figure 2.3: Grain-size distribution curve displaying a variety of sediments (Brattli, 2015). The figure shows characteristic graphs for a variety of depositional environments; where "leir", "silt", "sand" and "grus" is clay, silt, sand and gravel, respectively. "Leire", "morenemateriale", "elvemateriale" and "breelvmateriale" is clay deposits, till deposits, fluvial deposits and glacial river deposits, respectively.

2.2.3 Homogeneity and isotropy

The ability of an aquifer to store or release water is not only dependent on the hydraulic conductivity of the unit, but also the thickness of the aquifer and its associated properties (Fetter, 2001). If an aquifer has the same properties throughout the unit, it is considered homogeneous. When considering soils, this means that the grain distribution, grade of cementation, porosity and other hydraulic properties, such as the hydraulic conductivity, are relatively equal in the entire formation. An aquifer is said to be inhomogeneous if the hydraulic properties vary laterally or horizontally in the unit. Hydraulic conductivity is affected by inhomogeneity in formations. For example, aquifers consisting of alternating coarse-grained and fine-grained layers can have alternating values of hydraulic conductivity if the fluid flow direction is perpendicular to the layers (Fetter, 2001). A formation with a hydraulic conductivity equal in all directions is referred to as isotropic, and anisotropic in the opposite case (Brattli, 2009). Figure 2.4 shows combinations of homogeneity, inhomogeneity, isotropy and anisotropy.

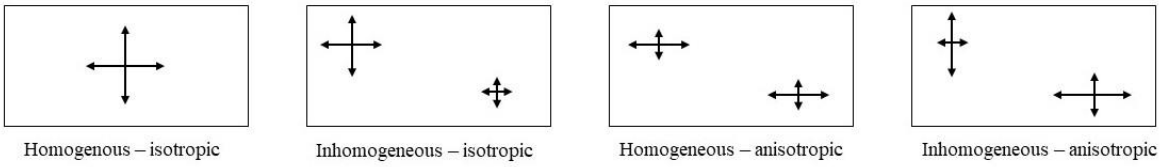

Figure 2.4: Combinations of homogeneity/inhomogeneity, isotropy/anisotropy Sketch based on (Brattli, 2009).

2.2.4 Permeability and hydraulic conductivity

Hydraulic conductivity *K* describes how easily a liquid can be transported through a porous medium. Hubbert (1956) stated that hydraulic conductivity is a function of the flow properties of the porous medium and the fluid that flows through it. It is the rock or soil's ability to transport water along with its ability to store water, that constitutes the most important hydrogeological properties (Fetter, 2001). Porosity is an important element with respect to the hydrogeological properties of a porous media. A rock or soil can have a high porosity, but low hydraulic conductivity. This is due to lack of connections between the pores in the media and results in the liquid being unable to flow through the pore system. Vesicular basalt is an example of such a rock type (Fetter, 2001). As described in subchapter 2.2.1, some soils and rocks have a high porosity, such as clay, but small pores making it difficult for liquid flow between the pores (Fetter, 2001). The flow rate is affected by the liquid flow properties, where thick liquids flow slower through a porous medium than thin liquids. Viscosity μ [Pas, kg/ms] is a measure of the shear resistance required for a liquid to be able to flow. Thick liquids have a high viscosity whereas thin liquids have a low viscosity (Brattli, 2009; Fetter, 2001).

The flow rate *Q* is proportional to the specific weight of the liquid and inversely proportional with respect to the viscosity μ, of the fluid. If a liquid is flowing through a porous media consisting of spherical grains of equal diameters, the flow rate will be proportional to the square diameter of the grains (Fetter, 2001). These relationships can be expressed mathematically as:

$$Q \propto d^2$$
$$Q \propto \gamma \qquad (2.4)$$
$$Q \propto \frac{1}{\mu}$$

where *d* is the diameter of the spherical grains [m] and γ is the specific weight of the liquid [N/m^3].

By combining these relationships, one obtains:

$$Q \propto \frac{Cd^2\gamma}{\mu} \tag{2.5}$$

Where C is a proportionality factor [-]. Equation 2.5 gives an expression of the liquid flow rate based on the flow properties of the porous medium, C and d, and the properties of the liquid, γ and μ (Fetter, 2001). Permeability can be defined by introducing a new constant k. Permeability only considers the properties of the porous medium and can be written:

$$k = Cd^2 \tag{2.6}$$

where k is the permeability of the porous medium [m^2]. Further, the relationship between hydraulic conductivity and permeability can be expressed mathematically as:

$$K = \frac{k\rho g}{\mu} \tag{2.7}$$

where K is the hydraulic conductivity of the porous medium [m/s] and ρ is the fluid density [kg/m^3]. Table 2.3 shows the hydraulic conductivity of a selection of soils.

Table 2.3: Hydraulic conductivity of a selection of soils (Lindmark, 2014).

Soil	**Hydraulic conductivity [m/s]**
Fine gravel	10^{-1}-10^{-3}
Coarse sand	10^{-2}-10^{-4}
Medium sand	10^{-3}-10^{-5}
Fine sand	10^{-4}-10^{-6}
Coarse Silt	10^{-5}-10^{-7}
Medium silt	10^{-7}-10^{-9}
Clay	< 10^{-9}

2.2.5 Tortuosity

J. Bear & Bachmat, (1967) suggests that the permeability of a porous medium is dependent on three key properties: porosity, cross-sections of the elementary channels and tortuosity. Since hydraulic conductivity is dependent on permeability, it makes tortuosity an important parameter when estimating the hydraulic conductivity.

Carman, (1997) discovered through his studies on fluid flow through granular beds, that the streamlines in a porous media are not linear or parallel. He discovered that the actual flow path of a fluid in a granular bed L_e is always greater than the depth of the bed L. Carman proposed a tortuosity factor to take this into account: $\left(\frac{L_e}{L}\right)^2 > 1$. In other words, the tortuosity is always greater than or equal to 1. It is not possible to measure the tortuosity factor of a porous media directly. Numerical estimates on the tortuosity factor are given by different authors. Irmay suggests a value of 2.5 for the tortuosity factor $\frac{L_e}{L}$ (J. Bear, Zaslavsky, & Irmay, 1968), whilst Carman suggests a value $\frac{L_e}{L} = \sqrt{2} \approx 1.4$. Other values suggested in literature vary from 0.56 to 0.8 (Jacob Bear, 1972). Although the value of the tortuosity factor is not applied in this master thesis, the theory is important in understanding the flow of fluids in porous media.

2.2.6 Groundwater flow

Groundwater flow is driven by the difference in hydraulic potential from one location to another. In 1854, Dupuit performed the first experiments on flow of fluids using water filters. His results showed that the pressure drop across the filter is proportional to the water filtration rate (Zolotukhin & Ursin, 2000). Further attempts were made by Henry Darcy in 1856 by flowing water through sand filters at different pressures. The experiments showed that the flow rate Q is proportional to the difference in water levels at two levels in the sand sample, h_1-h_2, and the cross-sectional area of the sample. The experiments also showed that the flow rate is inversely proportional to the length of the sample (Verruijt, 1982). Based on these results, Darcy derived what is today known as Darcy's law:

$$Q = -KA\frac{h_1 - h_2}{L} \tag{2.8}$$

Where Q is the fluid flow rate [m^3/s], K is the proportionality constant, also known as hydraulic conductivity [m/s], A is the cross-sectional area [m^2], h_1 and h_2 is the hydraulic head level at levels 1 and 2 in the sample respectively and L is the length of the sample [m]. The negative sign in Darcy's law indicates that the groundwater flows in the direction of decreasing hydraulic potential (Brattli, 2009). Darcy assumed the flow to be isothermal, incompressible, homogeneous and with a negligible kinetic energy. He also assumed laminar flow, with stationary flow conditions in a fully water saturated material.

When Darcy performed his experiment he only used water and solely changed the sand type. This affected the value of the proportionality constant *K*, but meant that the effect of the fluid parameters, viscosity and density, on the flow rate were left undetermined (Dake, 1983). Experiments performed at later times have shown that Darcy's law is valid for fluids with viscosities and densities different to that of water. It has further been shown that if the difference in hydraulic head h_1-h_2 is constant, the flow rate *Q* will remain the same regardless of the orientation of the sand filter (Zolotukhin & Ursin, 2000).

One can apply Reynolds number to determine if groundwater flow is laminar:

$$R = \frac{\rho_w q d}{\mu_w} \tag{2.9}$$

Where ρ_w is the water density [kg/m^3], *q* is the Darcy velocity [m/s], *d* is the average grain size in the soil or rock [m] and μ_w is the dynamic viscosity of water [Pas, kg/ms]. Laminar flow occurs if Reynolds number is between 1 and 10. The flow is considered turbulent if Reynolds number is beyond these values (Verruijt, 1982). Laminar flow is most often the case in aquifers, but turbulent flow may occur near groundwater wells where the flow rate is high. Laminar flow is assumed in all flow tests made in this thesis.

2.3 Soil composition

The hydraulic conductivity is largely affected by soil composition. When flowing water through a sand sample, the flow rate can be affected if clay is present in the sand sample. Some clay minerals, like smectites and illites, can expand up to 20 times their original volume by absorbing water in between their layers (PetroWiki, 2016). This volume expansion is known as swelling. In the petroleum industry, one normally looks at swelling in sandstones. However, the theory applies for unconsolidated sands as well. When clays swell they reduce the permeability of the sand by plugging the pore throats in the pore system. Swelling of clay is not common in unconsolidated soils in Norway and since the sand sample used in this thesis is from Norway, one assumes that the swelling of clay in the sample is unlikely.

In later years however, it has been observed that fines migration are a larger cause of flow rate reduction (PetroWiki, 2016). Fines migration occurs when flooding a sand sample with fluid. The fine particles are transported through the pore system and eventually gets stuck in pore throats. This causes a reduction in flow rate since no, or little, water can pass the blocked pore channels.

Further, soils containing clay and fines will contain more intricate flow channels, causing highly tortuous paths (O'Geen, 2013). This in turn affects the flow rate of fluid and therefore the hydraulic conductivity of the soil. As was mentioned in subchapter 2.2.1, the surface properties of the clay mineral causes the water molecules to stick to the clay particles (Brattli, 2009), hence reducing the flow rate and consequently the hydraulic conductivity.

2.4 Permeameter types

Two general types of permeameters exist; the rigid-wall permeameter, also called fixed-wall permeameter, and the flexible-wall permeameter. The type of permeameter used to measure the hydraulic conductivity of soils depends on the soil type used. A fixed-wall permeameter is normally preferred when conducting experiments using sand and coarse-grained soils with a high hydraulic conductivity (US20100089124A1, 2010), whereas flexible-wall permeameters are generally preferred when conducting experiments using fine-grained soils with a low hydraulic conductivity. Sidewall leakage is a concern when conducting experiments in permeameter cells, and is caused by clay particles in the samples reacting with the permeating liquid. Depending on what the clay reacts with it can cause smaller or larger pore spaces between the sidewall and the soil sample. This can cause fluid to flow faster at the sidewalls, and leads to an error in the hydraulic conductivity, giving values that are too high (D. Daniel, Anderson, & Boynton, 1985). The two main types of permeameters and their advantages and disadvantages, is based on D. Daniel et al. (1985) and the United States Patent Application US20100089124A1 (2010), and will be discussed further in 2.4.1 and 2.4.2.

2.4.1 Rigid-wall

Rigid-wall permeameters can be divided into three categories: compaction-mold, consolidation-cell and fixed-cylinder. The compaction-mold permeameters are often preferred when measuring the hydraulic conductivity of samples containing high amounts of clay (D. Daniel et al., 1985). A common design for this permeameter type is used in the ASTM Standard Test method D5856-15, and is described further in subsection 2.5. In general, the soil sample is first compacted in the mold, then fluid is flown through the sample. The permeating liquid can either be stored above the soil sample, inside the compaction-mold, or in a separate reservoir connected to the permeameter with tubing, see Figure 2.5. The permeating liquid can be pressurised before conducting the experiment, to reduce the time taken for it to flow through the sample. Atmospheric pressure is maintained in the effluent line. The flow rate is estimated by measuring the flow at the outlet or the inflow rate.

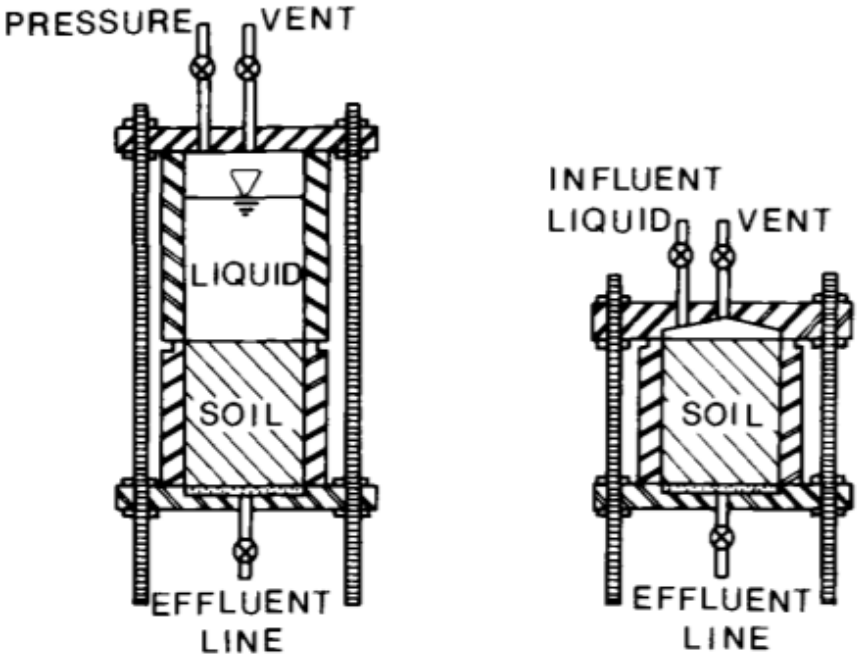

Figure 2.5: Compaction-mold permeameter, with permeant liquid inside permeameter and in a separate reservoir respectively (D. Daniel et al., 1985).

The compaction-mold permeameter is simple and economical, but can lead to unsaturated soil in some parts of the cell if back pressure is not used. Further, it is not possible to monitor how the particles in the sample react with the permeating liquid when conducting the experiment, which can lead to sidewall leakage and errors in the calculated hydraulic conductivity.

A modified, less common, version of the compaction-mold permeameter, is the double-ring permeameter. It monitors the rate of flow at the sidewalls and in the middle of the soil sample, making it possible to determine if there is a large amount of sidewall leakage. The rings are situated at the bottom of the permeameter, separating the flow at the sidewalls from the flow in the centre see Figure 2.6. If the sidewall leakage is large then the flow through the outer outlet will be significantly larger than the flow through the inner outlet.

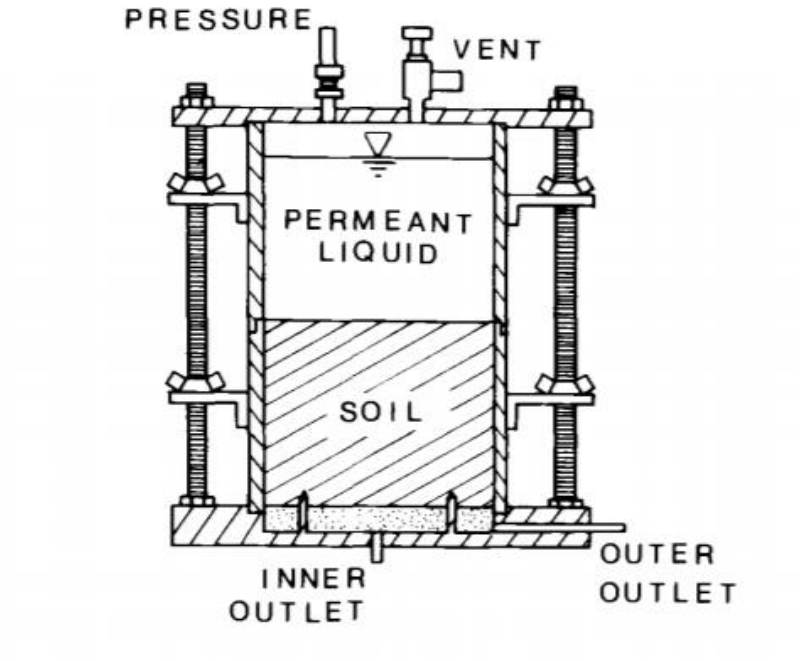

Figure 2.6: Double-ring permeameter (D. Daniel et al., 1985).

Another type of rigid-wall permeameter is the consolidation-cell, see Figure 2.7. This permeameter allows for vertical consolidation and thus better simulates the in-situ conditions of soil in the field. The soil is consolidated by applying vertical pressure on the sample, indicated by the black arrow in Figure 2.7. The vertical pressure also contributes to less sidewall leakage, since the soil particles are pushed against the wall when pressure is applied. Then, the sample is permeated with fluid, from the bottom of the sample and upwards (D. Daniel et al., 1985).

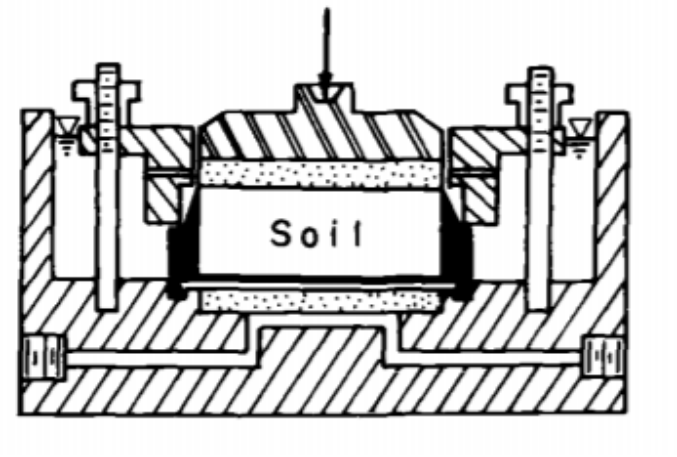

Figure 2.7: Consolidation-cell permeameter (D. Daniel et al., 1985).

The fixed-cylinder permeameter, see Figure 2.8, comprises of a cylinder and two end-plates at each end (D. Daniel et al., 1985). The permeating fluid is stored in separate reservoirs, one connected to the tubing at the inlet, and one connected to the tubing at the outlet. Before the experiment, the sample is permeated from the bottom of the sample to the top. During the experiment, the fluid flows from the upper reservoir, through the sample and into the bottom reservoir, where the flow rate is measured. To reduce the risk of sidewall leakage, Hawley & Northey, (1981) suggests using undersized porous disks at the top- and bottom plate, which helps evenly spread and direct the fluid flow to the outlet.

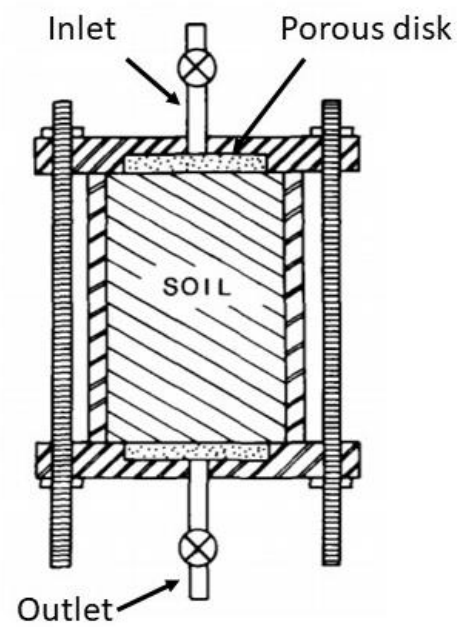

Figure 2.8: Fixed-cylinder permeameter (D. Daniel et al., 1985).

The consolidation-cell has similar traits to the Darcy-cell, discussed further in subsection 2.10. A disadvantage of the consolidation cell is the inability to apply vertical pressure on the soil samples in the cell.

2.4.2 Flexible-wall

Flexible-wall permeameters are normally triaxial cells, or modified versions of these (D. E. Daniel, Trautwein, Boynton, & Foreman, 1984). D. E. Daniel et al., (1984) describe the flexible-wall permeameter used at The University of Texas, see Figure 2.9. Other flexible-wall designs exist, but will not be discussed in this thesis. The design in Figure 2.9 has interchangeable base pedals, to allow experiments on soil samples with differing diameters.

Also, the apparatus contains double drainage lines at the top and bottom of the cell and help remove air bubbles in the sample (D. E. Daniel et al., 1984). The pressure drop is measured directly using a differentially acting pressure transducer. The pressure in the cell is separated from the pressure at the ends of the cell by pressure controls (D. Daniel et al., 1985). It is common to assume that the soil sample is fully saturated in this design. Back pressure is applied to the sample in an attempt at achieving full saturation.

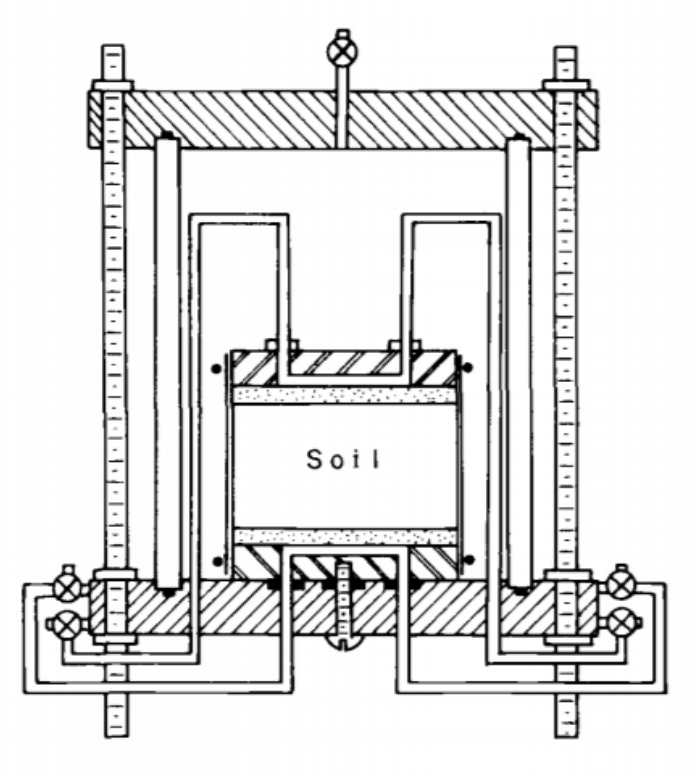

Figure 2.9: Flexible-wall permeameter(D. E. Daniel et al., 1984).

Advantages of this design include being able to fully saturate samples because of the use of back pressure, being able to measure the vertical and volumetric deformations of the soil sample, and the vertical and horizontal stresses (D. Daniel et al., 1985). Disadvantages include broken membranes if certain types of chemicals are used in the permeating fluid and the equipment is generally expensive.

2.5 International standard test methods for measuring hydraulic conductivity

This subsection gives a description of international standard test methods for measuring hydraulic conductivity in the laboratory. Although the international standards cover many different aspects, the focus in subsection 2.5 will be on initial test conditions and apparatus

types used in the research. The aim of investigating existing permeameter types is to gain knowledge of apparatuses used today and build on the existing knowledge to be able to modify the core permeameter and the Darcy – cell.

D2434-68 Permeability of Granular Soils (Constant Head) by ASTM International (2006), covers the standard laboratory test method for permeability of granular soils using a constant head hydraulic system using a fixed-wall permeameter, and is similar to the Darcy-cell method in subchapter 2.10. It should be noted that this standard was withdrawn in 2015 because it had not been updated by the end of the eighth year since last approval date, causing it to be withdrawn in accordance with the regulations of ASTM. Since the reason for its withdrawal is because it had not been updated, the author decided to still use the standard because it contains relevant information for this thesis.

The following description is based upon this standard test method. The method may be used with laboratory compacted samples that have a hydraulic conductivity higher than 1×10^5 m/s. The procedure assumes laminar flow of water through the granular soil and is limited to disturbed granular soils consisting of no more than 10% soil passing a 75-μm sieve. The following initial test conditions need to be held to be able to have a laminar flow of water through the sample with a constant head. The flow must be continuous and with no change in volume of the soil sample. The pore spaces in the soil must be fully saturated with water. To achieve this, a vacuum pump is used to remove the air from the sample and fully saturating it with water, see Figure 2.10. Lastly, steady-state flow is assumed, with a constant hydraulic gradient.

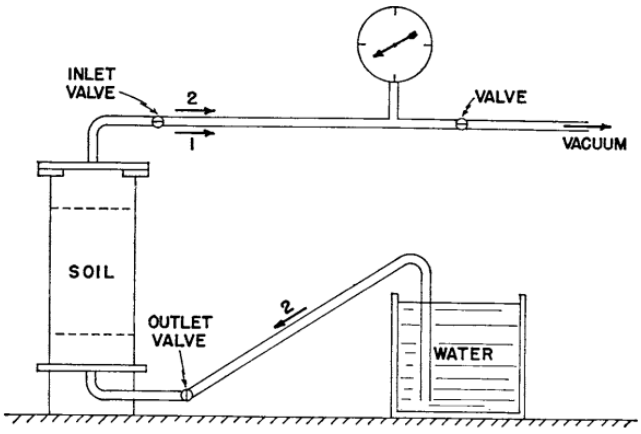

Figure 2.10: Vacuum pump. Used to remove air from the sample and fully saturating it with water (ASTM International, 2006).

Figure 2.11 shows a possible layout of what a constant-head permeameter following this standard would look like. The cylinder must have a diameter of 8 or 12 times the diameter of the sample grain size, depending on the percentage of total soil left on the sieve opening. The material of the cylinder can either be metal or a transparent acrylic plastic cylinder. The permeameter should have a porous disk both in the top and bottom of the cylinder with a permeability higher than that of the soil sample. In addition, the top disk should be fitted with a spring that applies a spring pressure of 22-45 N total load when the top plate is installed onto the apparatus. The distance *L*, between the manometers that are used to measure head loss *h*, should be equal to or greater than the diameter of the cylinder.

Further, a constant-head filter tank is placed above the permeameter, and another filter tank is placed below the permeameter or as seen in Figure 2.11. The constant-head filter tank above the permeameter delivers water to the soil sample and removes overflow of water in the tank. Removing the overflow of water assures that the head remains constant throughout the test.

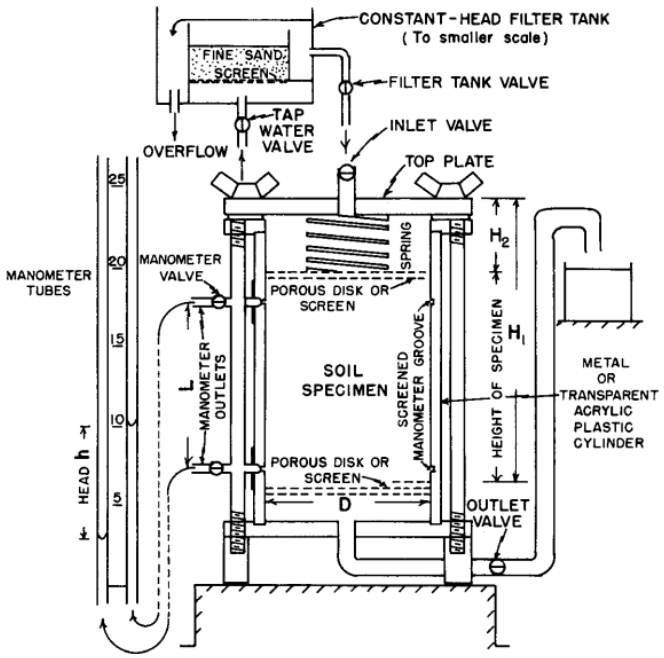

Figure 2.11: Constant-head permeameter (ASTM International, 2006).

To better represent an undisturbed soil sample in the field the compaction grade of the sample is important. The laboratory compaction method can be decided by preference. For a full description of the test method, including preparation of sample and procedure, see the standard test method D2434-68 by ASTM International (2006).

D5856-15 Measurement of Hydraulic Conductivity of Porous Material Using a Rigid-Wall, Compaction-Mold Permeameter by ASTM International (2015), covers the standard laboratory test method for measuring the hydraulic conductivity of porous materials using a fixed-wall, compaction-mold permeameter. The following description is based on this standard test method. The method may be used with laboratory compacted samples that have a hydraulic conductivity less than or equal to 1×10^5 m/s. The test method is valid for one dimensional, laminar flow with laboratory compacted porous materials where Darcy's law is assumed to be valid. Initial test conditions include a fully or close to fully saturated sample with water, where little or none of the pores contain air. If a fully saturated sample is crucial, Test Method D5084-16a (ASTM International, 2016) may be used. This test method is discussed later in this subchapter. Further, it is possible to use a range of permeating liquids if test method D5856-15 is modified, however for this exact method the permeating liquid must be water. "Sidewall" leakage between the test sample and the compaction/permeameter ring could be a problem. The leakage is caused by loss of contact between the soil and the compaction/permeameter ring and can cause overestimation of hydraulic (D. Daniel et al., 1985).

The apparatus can vary depending on the hydraulic system used, where constant-head and falling-head are the two most common methods. The apparatus consists of a permeameter cell comprising of a rigid compaction-mold composed of a strong material like plastic, metal or steel. Further, the permeameter is designed with two plates on top and bottom of the cell. These control the flow into and out of the sample in the permeameter. The design of the top plate varies depending on whether the test sample can swell during the test, see Figure 2.12.

Porous disks are placed in the top and bottom of the compaction-mold permeameter allowing fluid flow through the permeameter. If the soil sample is of a fine grade, filter paper should be placed on top of the porous plates preventing finer particles blocking the pores in the plates. For a full description of the test method, including preparation of sample and procedure, see the standard test method D5856-15 by ASTM International, 2015.

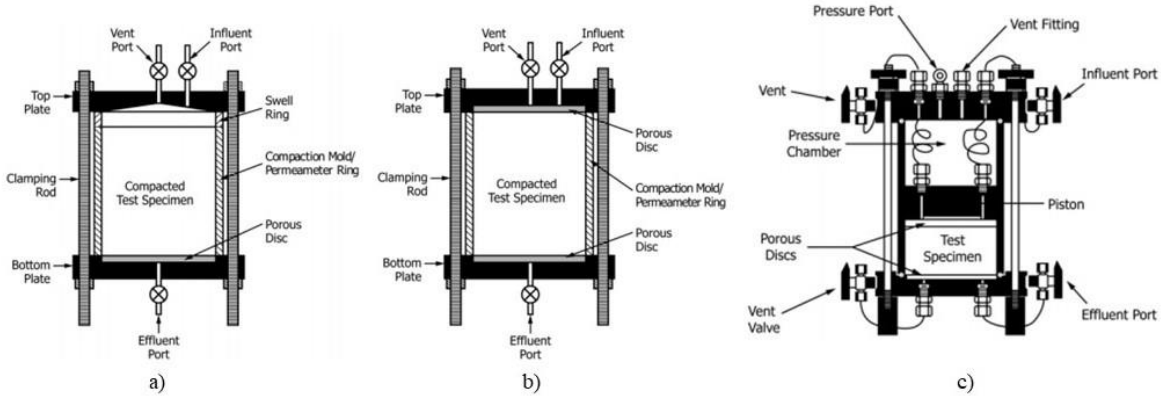

Figure 2.12: Compaction-mold permeameters with varying top plates (ASTM International, 2015). Figure a) shows a permeameter with no restraint on the top of the sample allowing sample to swell. Figure b) shows a permeameter with a restraint on the top of the test sample. Figure c) shows a permeameter with a controlled vertical stress on top of the sample.

D5084-16a Measurement of Hydraulic Conductivity of Saturated Porous Materials Using a Flexible Wall Permeameter by ASTM International (2016), covers the standard test methods for measurement of hydraulic conductivity of saturated porous materials using a flexible-wall permeameter. The following description is based on this standard test method. The method may be used for samples that have a hydraulic conductivity less than or equal to 1×10^5 m/s. Water is used as the permeating liquid; however, it is possible to use a range of permeant liquids if the test method is modified.

The method can be applied to a variety of hydraulic systems, numbered *A* to *F*, where *Method E – Constant Volume-Constant Head (by mercury)* and *Method F – Constant Volume-Falling Head (by mercury), rising tailwater elevation*, are two relevant methods for this thesis and will be further discussed below. The test method is valid for one dimensional, laminar flow in porous materials where Darcy's law is assumed to be valid. Further, the test method is applicable to fully water saturated samples, assuming no air is present in the pore system.

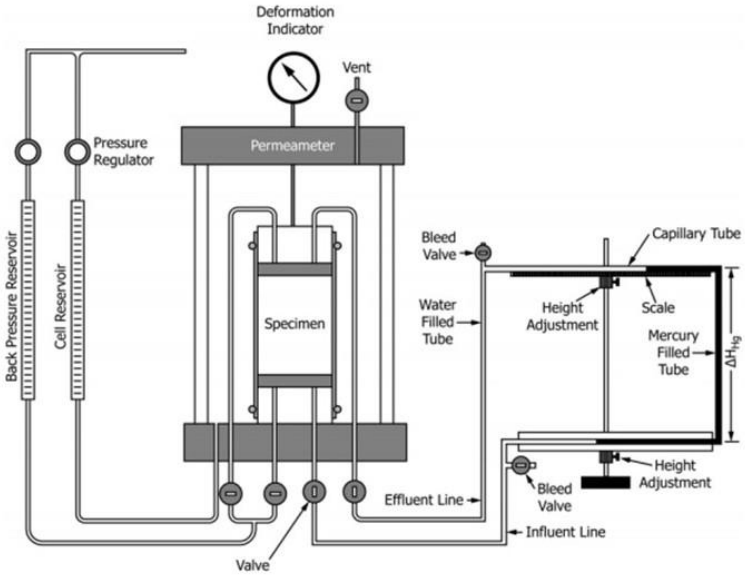

Figure 2.13: Method E – Constant Volume - Constant Head (by mercury)(ASTM International, 2016).

Both method *E* and method *F* use mercury to create the head loss in the system. The head loss in Figure 2.13 remains constant if the water-mercury interface in the upper part of the tube stays in the upper horizontal tube and the water-mercury interface in the lower part of the tube stays in the lower horizontal tube. The head in Figure 2.14 is falling if the mercury extends from the headwater- to the tailwater tubes. In this method the tailwater tube has a smaller diameter than the headwater tube, making it possible to flush water through the system without affecting the position of the mercury in the headwater tube. A potential problem one may encounter when using mercury to measure head loss in the two methods is that some water can be trapped within the mercury altering the head loss measurement. Cleaning the headwater and tailwater tubes can help prevent this from occurring.

Both methods apply a backpressure reservoir to enable full water saturation of samples. Backpressure can be applied to the system by using a deadweight acting on a piston or using a compressed gas supply. Similarly, compressed gas or a deadweight acting on a piston may be used to apply pressure on the permeameter cell. However, a pressure regulator, to control the gas pressure and a pressure gauge to measure the gas pressure is required. For a full description of the test method, including preparation of sample and procedure, see the standard test method D5084-16a by ASTM International (2016).

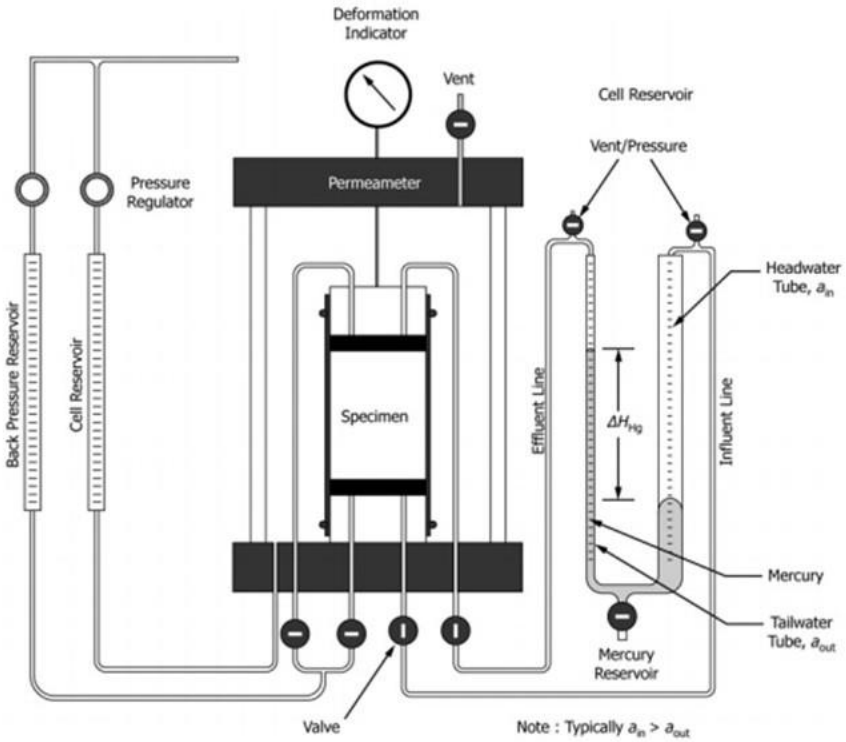

Figure 2.14: Method F – Constant volume - Falling head (by mercury), rising tailwater elevation (ASTM International, 2016).

2.6 Measuring effective porosity in the laboratory

This subchapter describes the method used to estimate the effective porosity of a porous media using a helium porosimeter. This method is commonly used to measure the effective porosity of core samples; hence some modifications are done to enable the estimation of effective porosity of unconsolidated soil samples. These modifications are described in subchapter 3.3. The effective porosity of porous media is estimated using a helium porosimeter by applying the principle of gas expansion, described by Boyle's law, see equation 2.10 (Torsæter & Abtahi, 2000). The porosity of a sample can be calculated using helium gas which penetrates the pore space of the sample material under a given pressure. The equipment used during the test is a cylinder with two connected pressure chambers, separated by a valve, see Figure 2.15. When the valve is closed, the reference chamber contains a known volume of gas V_1 [cm^3] and a known reference pressure p_1 [psig]. The other chamber consists of the sample material and has an unknown volume V_2 [cm^3] and a known pressure p_2 [psig]. The pressure in the reference chamber p_1 is larger than the pressure in the sample chamber. Thus, when the valve opens, helium gas with a known volume V_1 and known pressure p_1 will flow from the reference

chamber to the sample chamber, penetrating the pore system of the sample. An equilibrium pressure p and equilibrium volume V is then established (Torsæter & Abtahi, 2000).

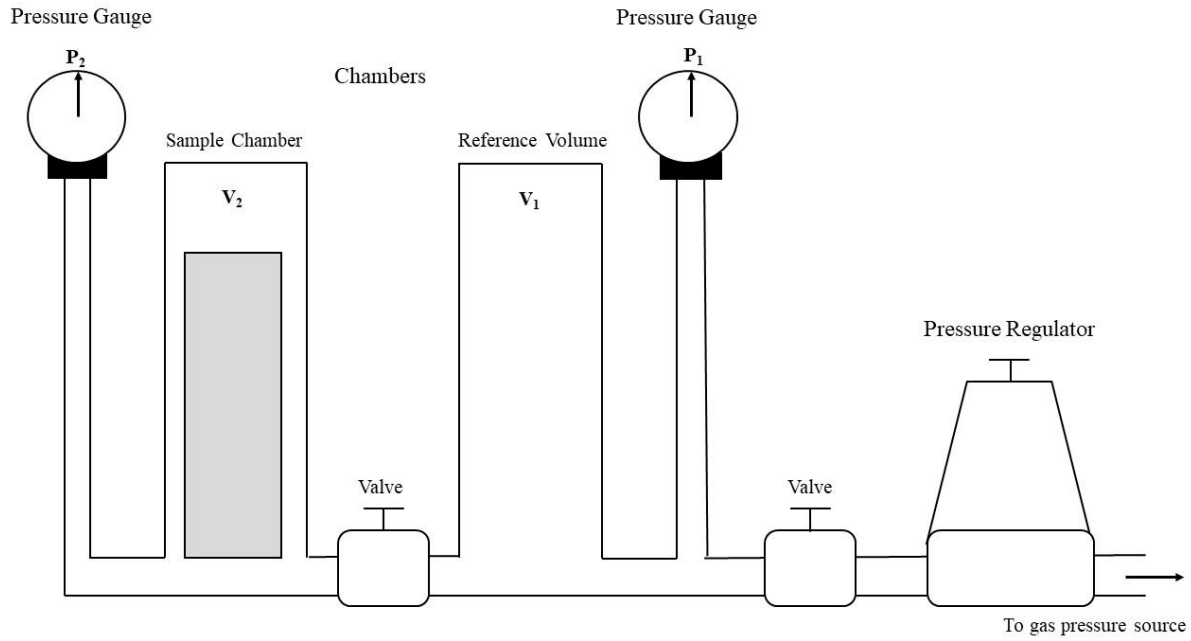

Figure 2.15: Schematic diagram of helium porosimeter method. Sketch based on (Torsæter & Abtahi, 2000).

The volume V_2 can be calculated using Boyle's law, assuming an isothermal expansion of the helium gas in the sample:

$$p_1V_1 + p_2V_2 = p(V_1 + V_2) \tag{2.10}$$

Where p is the equilibrium pressure read off the pressure gauge [psig]. Solving equation 2.10 with respect to V_2 gives the following expression:

$$V_2 = \frac{(p_1 - p)V_1}{p - p_2} \tag{2.11}$$

The pressures are expressed as absolute pressures when calculating V_2 which means that the atmospheric pressure is set to equal 0 psig. If the pressure in the sample chamber is equal to the atmospheric pressure p_2 = 0 psig and the pressure in the reference chamber is set to p_1 = 100 psig, then equation 2.11 can be simplified to:

$$V_2 = \frac{(100 - p)V_1}{p} \tag{2.12}$$

The pore volume of the sample is given as the difference between the bulk volume of the sample V_b and the volume of solid material V_g.

This can be described mathematically by:

$$V_p = V_b - V_g \tag{2.13}$$

Where V_p is the pore volume of the sample [cm^3] and the bulk volume of the sample can be expressed as:

$$V_b = h \times \frac{\pi d_i^2}{4} \tag{2.14}$$

Where h is the height from the bottom of the sample chamber to the top of the sample [cm] and d_i is the inner diameter of the sample chamber [cm]. Further, the volume of solid material V_g can be expressed as:

$$V_g = V_1 - V_2 \tag{2.15}$$

The effective porosity of the porous media can then be calculated using a variation of equation 2.2:

$$n = \frac{V_p}{V_b} \tag{2.16}$$

2.7 Measuring density in the laboratory

Density is defined as the mass of fluid per unit volume (Jacob Bear, 1972) and can be expressed mathematically as:

$$\rho = \frac{m}{V} \tag{2.17}$$

Where ρ is the density of the fluid [kg/m^3], m is the mass of fluid [kg] and V is the fluid volume [m^3]. A commonly used method to measure density is by using a pycnometer, which is a glass flask with a known volume and a stopper and is described by Torsæter & Abtahi (2000). The empty pycnometer is first weighed before fluid is added to fill the whole volume of the flask. Then the stopper is added to the top of the flask and the total weight is recorded. The weight of the fluid can be calculated by subtracting the weight of the empty pycnometer from the total weight. Since the volume of the pycnometer is known, and the mass of fluid can be calculated, the density can be calculated using equation 2.17.

2.8 Saturation determination

Saturation determination is commonly used in core analysis (Torsæter & Abtahi, 2000). When using core samples, the saturation is defined as the ratio of the fluid volume in a core to its pore volume:

$$S = \frac{V_f}{V_p} \tag{2.18}$$

Where S is fluid saturation [%], V_f is fluid volume [m^3] and V_p is the pore volume of the core sample. The same definition can be applied when determining the fluid saturation in unconsolidated sand. The fluids present in sand are water and gas (air) and together they constitute the total amount of fluid in the sand:

$$S_w = \frac{V_w}{V_p} \tag{2.19}$$

$$S_g = \frac{V_g}{V_p} \tag{2.20}$$

$$S_w + S_g = 100 \tag{2.21}$$

Where S_w and S_g are water and gas saturations, respectively, and V_w and V_g is the volume of water and gas present in the sand sample, respectively.

2.9 The core permeameter

The absolute permeability of a rock or soil can be measured using either liquid or gas. A core permeameter is used to measure the absolute permeability of core samples in the field of petroleum. The following subchapter gives a description of two types of permeameters used to measure absolute permeability of core samples using liquid and gas as the permeating fluid, respectively. First, a general description of the core permeameter apparatus and method is given, followed by a description and method of the core permeameter using liquid as the permeating fluid. Finally, a description and method of the core permeameter using gas as the permeating fluid is given.

In general, the core permeameter laboratory test is performed by flowing a liquid or gas with known viscosity and density through a core sample of known dimensions. The measured parameters during the test are pressure drop Δp and the fluid flowrate Q. The apparatus, see Figure 2.16, can be used for single- and multiple phase flow and for compressible fluids. Further, this method can be used for high temperatures and pressures, which is of great

importance in the petroleum industry since a petroleum reservoir is located at great depths with high temperatures and pressures. The Darcy-cell, described in subchapter 2.10, operates in a very different temperature and pressure range because aquifers are located at much shallower depths where the groundwater temperatures are 1-2 °C higher than the annual average air temperature on site (Geological Survey of Norway, 2015). Also, significantly lower pressures are observed, since the thickness of the overburden is relatively thin when compared with the overburden above a typical petroleum reservoir.

A core permeameter consists of what is called a core holder and two manometers or pressure sensors, that measure the pressure at the inlet and outlet of the core holder, also known as the line pressure. Next, gas or liquid is flooded through the core holder. It is essential that fluid is flooded through the core and not on the sides of the core. A Hassler core holder, see Figure 2.17, is normally used for this purpose. The Hasler core holder contains a rubber sleeve that tightens around the core once confining pressure is applied to the system. This creates a sealed system, only allowing the fluid to flow though the core sample. For the system to be sealed the confining pressure must be 7 bars or higher than the line pressure in the system (Torsæter & Abtahi, 2000).

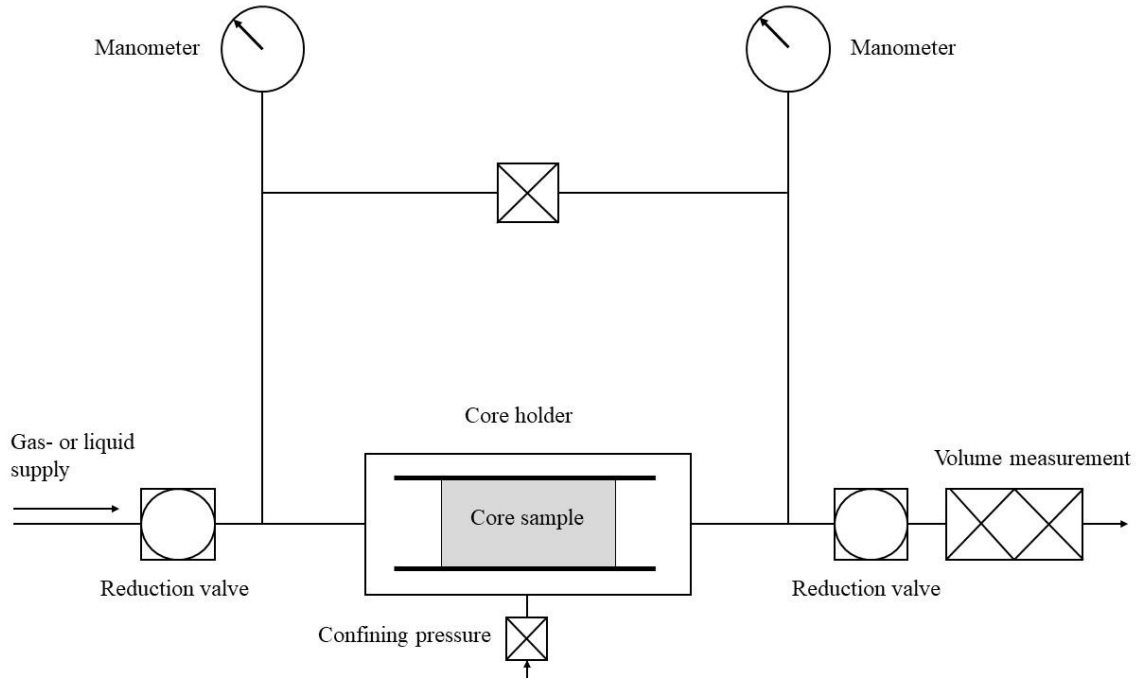

Figure 2.16: Schematic diagram of a core permeameter with constant head. Sketch based on (Torsæter & Abtahi, 2000).

Prior to the experiment, a core is placed in the core holder. The inner diameter of the core holder is 3,81 cm and its length allows for a core sample with length 10 cm. This means the outer diameter of the core placed in the core holder cannot exceed 3.81 cm and its length cannot exceed 10 cm. Once the core is placed in the core holder, a confining pressure is applied to the system. A gas or liquid is then flowed through the core sample. Next, the pressure difference across the core sample is measured using manometers or pressure sensors on either side of the core holder. The flow rate is either decided by using a pump with a constant rate, that pumps liquid from the supply or it is measured using a flow meter at the outlet of the core holder. Once the flow rate and pressure difference is known, it is possible to estimate the permeability k [D] of the core sample using altered versions of Darcy's law (Torsæter & Abtahi, 2000). The derived equations vary depending on whether liquid or gas is the permeating fluid, see subchapters 2.9.1 and 2.9.2.

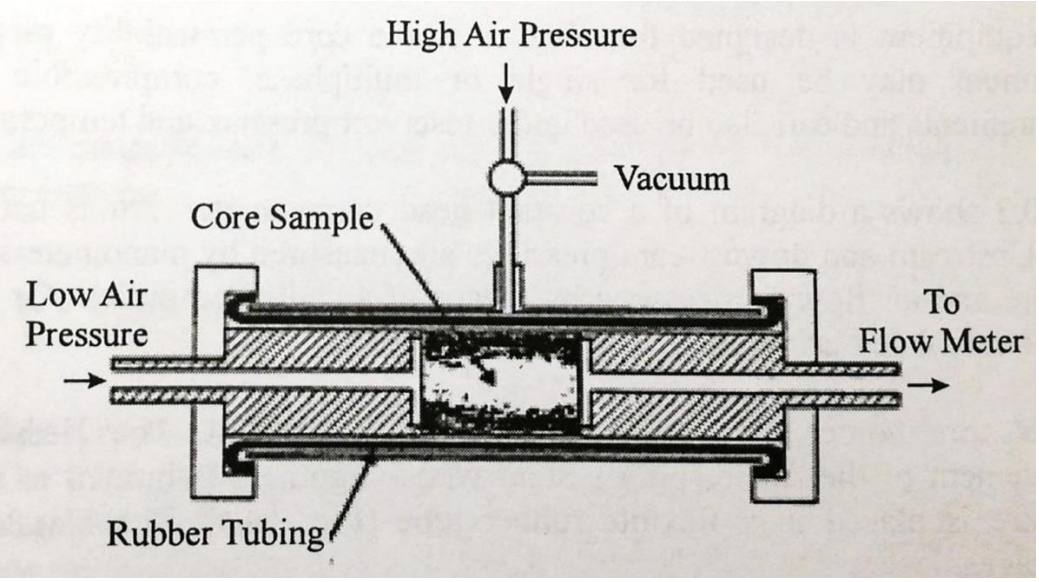

Figure 2.17: Hassler core holder (Torsæter & Abtahi, 2000).

2.9.1 Liquid permeability measurements using a core permeameter

Measuring the permeability of liquid in core samples is done by flooding a liquid through a core sample. To be able to calculate the permeability the flow of fluid must be horizontal with a stationary flow current. Further, one assumes that the core sample is fully saturated with fluid, incompressible and the flow laminar. Lastly, no reactions between the fluid and the porous medium is assumed (Zolotukhin & Ursin, 2000).

Darcy's equation for horizontal flow can be expressed as:

$$Q = \frac{kA\Delta p}{\mu L} \tag{2.22}$$

Where Q is expressed in m^3/s, A in m^2, Δp is the pressure difference at the inlet and outlet of the core holder expressed in Pa, μ in Pa and L in m. Rearranging equation *2.22* with respect to permeability gives:

$$k = \frac{Q\mu L}{A\Delta p} \tag{2.23}$$

2.9.2 Gas permeability measurements using a core permeameter

Although no fluid and porous rock interaction is assumed when conducting the liquid permeability method, this is not always the case (Zolotukhin & Ursin, 2000). Liquid can sometimes interact with the porous rock potentially resulting in other measured values of permeability. As mentioned in subchapter 2.3, the composition of a soil sample may affect the flow of liquid. Similarly, the composition in a core sample may affect the liquid flow. To avoid this interaction between the core and the liquid, a method of measuring the absolute permeability is done by using gas.

The apparatus used in gas permeability measurements is normally the same as the one described previously in subchapter 2.9, see Figure 2.16 and Figure 2.17, using gas as the fluid supply. The gas supply used is normally air.

Gas is highly compressible and means that a higher pressure will cause the gas molecules to pack closer together, i.e. the gas is dependent upon pressure. Darcy's law assumes an incompressible substance and may not be applied directly. The following derivation of absolute permeability of gas is based on Zolotukhin & Ursin, (2000, p.71). The mass flow of gas can be written $Q\rho$.

Substituting this into equation 2.22 gives:

$$Q\rho = -A\frac{k\rho}{\mu}\frac{dp}{dx} \tag{2.24}$$

where Q is the flow of gas [cm^3/s], ρ is the density of gas [g/cm^3] at a given pressure p [bar], k is the absolute permeability [D]. Applying the ideal gas law ($pV=nRT$) and the expression for density, rearranged with respect to volume of gas ($V = \frac{m}{\rho}$), one can express gas density as:

$$\rho = \frac{\rho_0}{p_0}p \tag{2.25}$$

where the subscript "*0*" refers to reference conditions, for example standard conditions. Substituting this expression for density into equation 2.24 gives:

$$Q\rho = -A\frac{k\rho_0 p}{\mu p_0}\frac{dp}{dx} \tag{2.26}$$

Taking into account mass balance one can express Qρ:

$$Q\rho = Q_0\rho_0 \tag{2.27}$$

Substituting the expression for $Q_0\rho_0$ into equation 2.26 and rearranging with respect to Q_0 gives:

$$Q_0 = -A\frac{kp}{\mu p_0}\frac{dp}{dx} \tag{2.28}$$

Where $\frac{dp}{dx}$ is the pressure difference across the core sample, and p_1 to p_2 is the inlet and outlet pressures in the core holder. Integrating from p_1 to p_2 gives:

$$Q_0 = A\frac{k}{2\mu p_0}\frac{{p_1}^2 - {p_2}^2}{\Delta l} \tag{2.29}$$

where Δl is the length of the core and can thus be expressed as L [cm]. Rearranging for permeability k gives:

$$k = \frac{2\mu p_0 Q_0 L}{({p_1}^2 - {p_2}^2)A} \tag{2.30}$$

Equation 2.30 can be used to calculate the absolute permeability of a core sample. In theory this equation can also be used to calculate the absolute permeability of a soil sample, for example unconsolidated sand.

2.10 The Darcy-cell

The following subchapter describes the theory of the Darcy-cell in general. Then, a description of the existing Darcy-cell at the Department of Geoscience and Petroleum and the method used to calculate the hydraulic conductivity of a soil sample in the cell is described. The purpose of this is to give the reader insight into the original setup of the cell before modifications were made to it.

2.10.1 The Darcy-cell in general

The Darcy-cell consists of a permeameter cell, an upper and lower water tank and piezometers or manometers. A soil sample is added to the permeameter cell and before the start of the experiment, the soil sample is saturated with water by flowing water through the bottom of the sample to the top of the cell. Fully saturating the sample with water means that the pore spaces in the soil are completely filled with water. The density of air is lower than that of water and means that it is easier to push the air out of the pores if water is flowing in the opposite direction of gravity, in this case, from the bottom of the sample to the top of the cell.

The upper and lower water tank is continuously filled with water, maintaining a constant hydraulic head, see Figure 2.18. The hydraulic head in the cell is measured by means of piezometers connected with tubing to the cell wall. The difference between the water levels in the piezometers is the difference in head Δh. If the pressure difference is equal between every level, then it is reasonable to assume a constant hydraulic head in the cell.

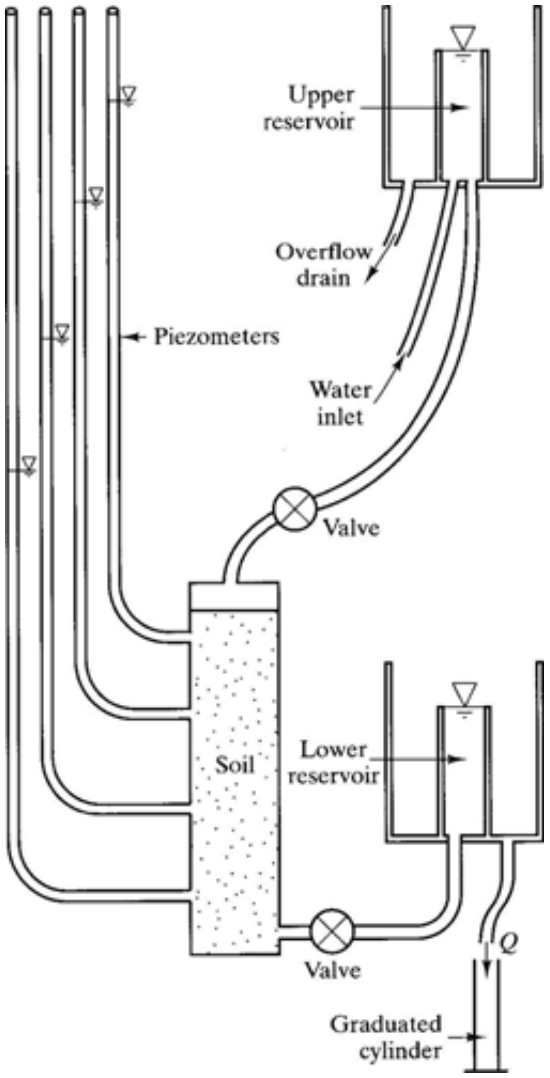

Figure 2.18: Constant head Darcy-cell apparatus (Geotechdata.info, 2010).

2.10.2 The existing Darcy-cell

Figure 2.19 shows the layout of the existing Darcy-cell at the Department of Geoscience and Petroleum. In addition to the design in Figure 2.18, this apparatus has four different nozzle levels, with three nozzles in each level. The four nozzle levels make it possible to control that the difference in hydraulic head is equal between the levels. Also, the three nozzles in each level are placed at different locations. If the head measured at the different nozzles in the level are equal then it is reasonable to assume that the hydraulic head is the same in the whole sample in that level. This is however, only an assumption, and is not always the case, since disturbances from the packing process, or during the test, can affect the flow rate and consequently the hydraulic head.

To be able to estimate a hydraulic conductivity that is realistic when compared to expected values of unconsolidated sand in the field, one needs to imitate the “in-situ” compaction grade present in a soil in the field when compacting the sample in the laboratory. If the sample is packed too loose compared to what it would be packed like in the field, then the hydraulic conductivity calculated in the laboratory will be too high. An attempt at imitating the “in-situ” compaction grade can be done by packing the sand sample in steps and between each step drop a circular weight on the sample. If the drop in hydraulic head is linear along the flow line, one can assume that the sample has been packed properly and an adequate compaction grade has been reached. If the compaction grade varies within the sample, then the pore volume between the grains will vary, causing a non-linear drop in head along the flow line. This in turn will cause a difference in hydraulic head at the different nozzle levels.

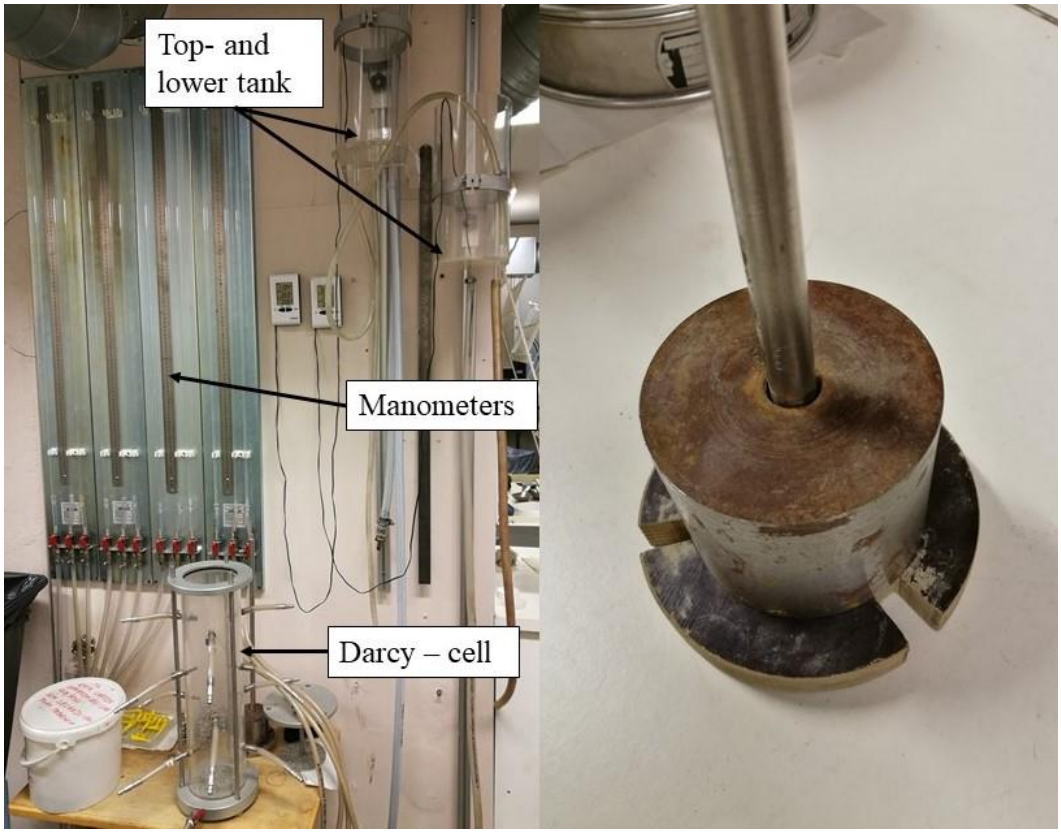

Figure 2.19: Existing Darcy-cell apparatus, showing the Darcy-cell apparatus on the left and the circular weight used to imitate the “in-situ” compaction grade in the field on the right. Photo: Runa A. Solberg.

During the experiment, water flows from the upper tank through the sample and out through the bottom tank and into a measuring cylinder. The time it takes for a certain volume of water to reach the measuring cylinder is recorded and the flow rate Q [m^3/s] is calculated using the following equation:

$$Q = \frac{V}{t} \tag{2.31}$$

Where t is time [s] and V is the volume of water in the measuring cylinder [m^3]. By measuring the length of the cell L [m], the cross-sectional area A [m^2] and the constant difference in hydraulic head Δh [m], the hydraulic conductivity K can be estimated using another version of Darcy's law:

$$K = \frac{QL}{A\Delta h} \tag{2.32}$$

3 Method

The laboratory work described in this chapter was conducted in the reservoir laboratory at the Department of Geoscience and Petroleum during the period January to May 2018. The work is conducted by the author with guidance from Staff Engineer Roger Overå. An exception is the sieve analysis described in subchapter 3.3, which was conducted in the Engineering Geology laboratory at the Department of Geoscience and Petroleum with guidance from PhD Candidate Sondre Gjengedal.

3.1 Modifying the core permeameter

The original core permeameter is not designed for unconsolidated soils. This subchapter describes the modifications done to the original setup in an attempt at enabling testing of unconsolidated sand in this apparatus. There exists several challenges with using unconsolidated soils in a core permeameter. A core has a solid grain structure, making it possible to flow fluid through the pore system. This solid structure means that there is no need for any filters at the inlet or outlet of the core holder. Unconsolidated soils, however, have a loose grain structure. This causes some grains to flow with the fluid which can eventually block the outlet. Installing filters at the inlet and outlet of the existing apparatus could be a solution to this problem, but this is both time consuming and expensive. An alternate solution could be to create a cylinder that can be inserted into the already existing core holder. Then the soil sample can be packed into the cylinder that is inserted into the core holder. A hypothesis is that using two filters on either side of the cylinder will behave as a barrier for the grains and not the fluid, allowing the fluid to pass through the filters and to the outlet of the existing apparatus, whilst the grains remain in the cylinder. Figure 3.1 shows a proposed design of the cylinder with filters.

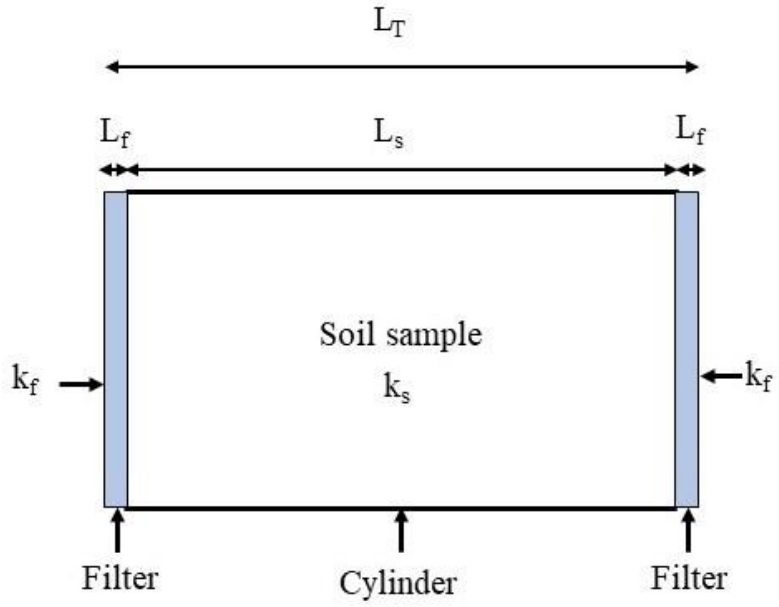

Figure 3.1: Sketch of cylinder and filters. Sketch by: Runa A. Solberg.

If permeability is calculated using the same method as mentioned in subchapter 2.9 in this new setup, one would calculate the average permeability across the whole length of the core holder, including the permeability of the filters and the soil sample. If the two permeabilities of the filters are known or measured beforehand, the only unknown permeability is that of the soil sample. Figure 3.2 shows flow in series through three layers of different dimensions, and is similar to the flow of fluid through the cylinder and filters in Figure 3.1.

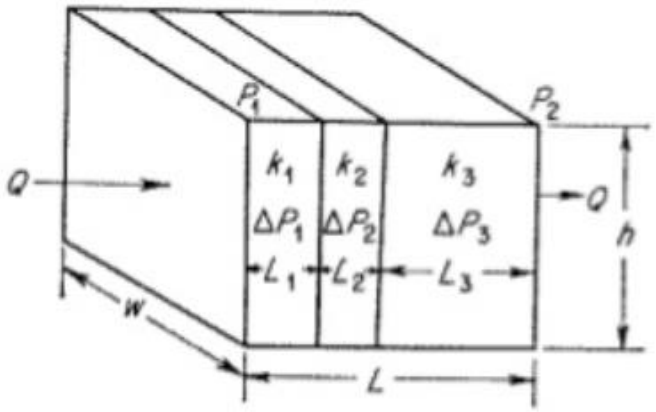

Figure 3.2: Flow in series (M.T.H Corporation, 2014).

Given that the total length L of the unit can be expressed as:

$$L = L_1 + L_2 + L_3 \tag{3.1}$$

Where L_1, L_2 and L_3 are the lengths of layer 1, 2 and 3 in Figure 3.2 respectively [cm]. The total flow rate can be expressed mathematically, assuming that the flow rate is equal in every layer, as:

$$Q = Q_1 = Q_2 = Q_3 \tag{3.2}$$

Where Q is the constant flow rate through all layers [cm^3/s] and Q_1, Q_2 and Q_3 are the flow rates of layers 1, 2 and 3 respectively [cm^3/s]. The total pressure loss in the unit can be expressed as:

$$p_1 - p_2 = \Delta p_1 + \Delta p_2 + \Delta p_3 \tag{3.3}$$

Where p_1 is pressure at the inlet of the unit [bar], p_2 is pressure at the outlet of the unit, Δp_1, Δp_2 and Δp_3 are the pressure losses in layer 1, 2 and 3 [bar]. One can express average permeability of the unit by applying another version of Darcy's law, expressed in pressure loss instead of head loss:

$$Q = \frac{\bar{k} A \Delta p}{\mu L} \tag{3.4}$$

Solving equation 3.4 with respect to $\Delta p = p_1 - p_2$:

$$p_1 - p_2 = \frac{Q \mu L}{\bar{k} A} \tag{3.5}$$

Where $\bar{k}$ is average permeability [darcy], $A = wh$ the cross-sectional area of the unit [cm^2] and μ the viscosity of the fluid [cP]. Using equation 3.5 with respect to the three layers gives:

$$p_1 - p_2 = \frac{Q \mu L}{\bar{k} A} = \frac{Q \mu L_1}{k_1 A} + \frac{Q \mu L_2}{k_2 A} + \frac{Q \mu L_3}{k_3 A} \tag{3.6}$$

Solving equation 3.6 with respect to $\frac{L_2}{k_2}$ and then for k_2, gives the following expressions:

$$\frac{L_2}{k_2} = \frac{L}{\bar{k}} - \frac{L_1}{k_1} - \frac{L_3}{k_3} \tag{3.7}$$

$$k_2 = \frac{L_2}{\frac{L_T}{\bar{k}} - \frac{L_1}{k_1} - \frac{L_3}{k_3}} \tag{3.8}$$

Relating this to Figure 3.1, L_1 and L_3 would correspond to L_f, and L_2 to L_s. Further, k_1 and k_3 would correspond to k_f and k_2 to k_s, giving the following expression:

$$k_s = \frac{L_s}{\frac{L_T}{\bar{k}} - \frac{L_{f1}}{k_{f1}} - \frac{L_{f2}}{k_{f2}}} \tag{3.9}$$

If one assumes that the filter permeability of the two filters are equal, then equation 3.9 can be simplified to:

$$k_s = \frac{L_s}{\frac{L_T}{\bar{k}} - \frac{L_{fT}}{k_f}} \tag{3.10}$$

Where L_{fT} is the total length of the two filters. All parts of equation 3.9 and are known and thus, k_s can be calculated. The hydraulic conductivity can then be calculated by converting the permeability from darcy to square meter and inserting this value for permeability into equation 2.7.

The following paragraphs describe the method used to modify the core permeameter applying the suggested layout seen in Figure 3.1. Trial and error led to several modifications to this original idea, and these modifications are described below. In all modifications, metal cylinders of length 6 cm and outer diameter 3,81 cm are used. The metal in the cylinder is of acidproof steel Type 316. A circular metal filter with outer diameter of 3,81 cm is placed on either side of the cylinder. The filters are made of sintered metal.

3.1.1 First modification

The first modification was carried out by cutting metal cylinders into pieces with length 6 cm, outer diameter 3,81 cm and inner diameter 3,54 cm. The metal was cut into pieces by Staff Engineer Håkon Myhren. The metal filters had previously been used during a flooding experiment where the permeating fluid was oil. To remove the oil, the filters were left in toluene for a day and then dried in a drying cabinet at 60 °C. The first modification was based on the layout in Figure 3.1. The cylinder and filters were inserted into the core holder of an existing air permeameter, see Figure 3.3. It is not possible to insert the cylinder or filters into the core holder at atmospheric pressure because the rubber sleeve inside the core holder has a smaller diameter at such pressure. Applying vacuum to the core holder causes the rubber sleeve to get "sucked" to the inner wall of the core holder, allowing the filters and cylinders to be placed inside it. It was not possible to fill the cylinder with the soil sample before inserting the cylinder into the core holder, without losing some sand at the transition between the filters and cylinder.

If the sand spilt in these transitions when packing the soil sample in the cylinder in the laboratory, some of the grains in the transitions could potentially spill into the core holder when inserting the filled cylinder and filters. The free grains would be free to flow from the core holder and into the tubing of the apparatus and flow meter once the sample was flooded with air. These grains could in turn cause problems with the readings of the flow meter and in a worst-case scenario, break it.

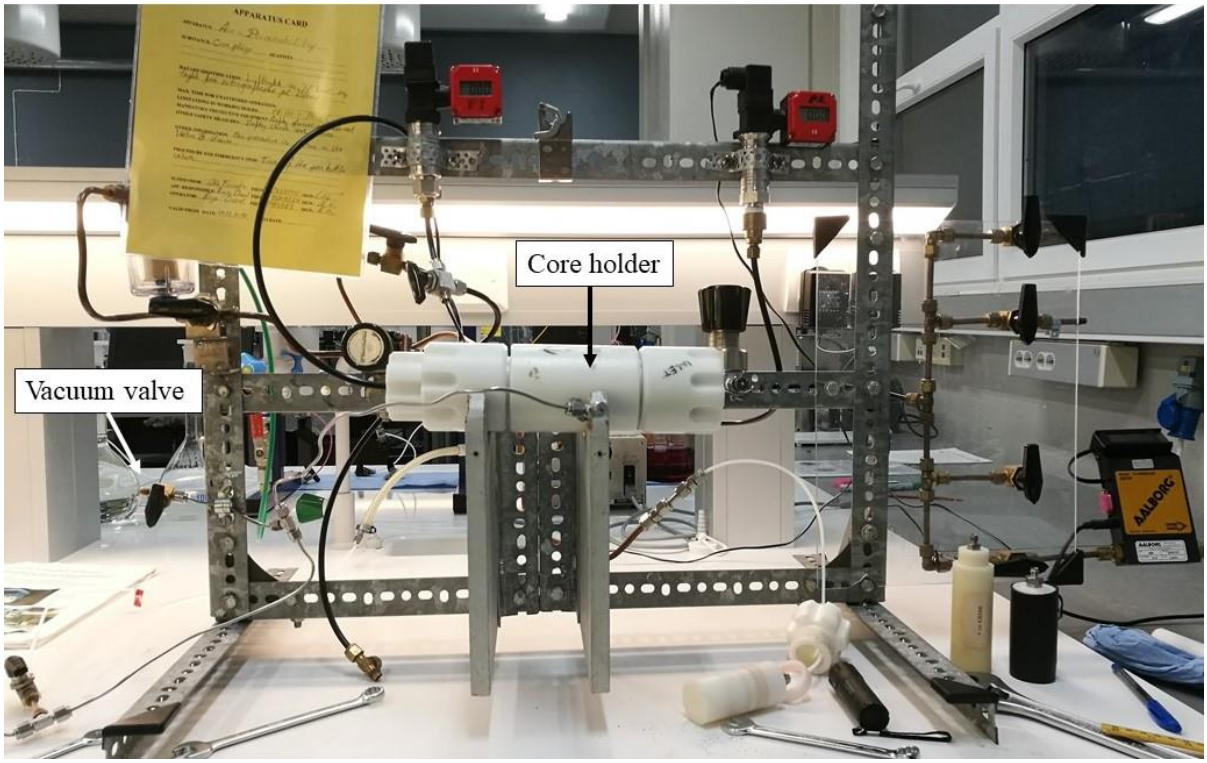

Figure 3.3: Existing air permeameter Photo: Runa A. Solberg.

To test the first modification, the bottom filter was placed in the core holder first, by holding the core holder vertically. Then, the cylinder was placed inside the core holder and filled in steps with the sand sample. The second filter was placed on top of the sand filled cylinder. Sand grains were observed between the outside of the cylinder and the rubber sleeve, which meant that it was not possible to run the experiment since grains of sand would travel though the rest of the system once flooding was initiated. Further modifications was needed to run the experiment without sand grains escaping from the cylinder.

3.1.2 Second modification

In the second modification the metal filters were glued on either side of the cylinder, using Tec7 glue, to prevent grains of sand from escaping the cylinder and entering the core permeameter, see Figure 3.4. First, the bottom filter was glued to the bottom part of the cylinder. After the

glue had dried, the sand was added to the cylinder in steps, by adding two table spoons of sand at a time, followed by packing the sample with a polyoxymethylene rod (POM rod), see Figure 3.5. This was done alternately until the cylinder was filled to the top. Then the second filter was glued on top of the cylinder.

a) b)

Figure 3.4: Second modification. a) cylinder and glued bottom filter and b) cross-section of cylinder with no soil sample inside. Photo: Runa A. Solberg.

After the glue had dried, the cylinder was inserted into the core holder of the air permeameter. The sand sample was then flooded with air and the flow rate of the air was measured using a flow meter. The test was successful with regards to no sand grains escaping and flowing into the rest of the system. However, in a core sample one expects the flow rate to increase with increasing pressure. Similarly, one would expect the flow rate to increase with pressure when using unconsolidated samples, if they are packed well enough to keep the grains in the sample in place. However, in this test the flow rate decreased when the inlet and outlet pressures of the core holder were increased. Fines migrating in the sample could be a cause of the drop in flow rate. When finer sediment migrates through the sample they can block pore spaces in the sample and consequently reduce the flow rate. The cause of the fines migrating in the sample could be because the sand sample had not been packed well enough, allowing grains to move within the sample when air was flooded through the sample. The migration of sand could possibly be avoided if a new method of packing the sand was applied.

Figure 3.5: Packed sand sample in cylinder and POM rod. Photo: Runa A. Solberg.

3.1.3 Third modification

To improve the grade of packing, the sand sample was compressed using a bench press. 2 table spoons of sample were added to the cylinder in steps, and the POM rod was placed on top of the sand sample, see Figure 3.6. A weight of 1 ton was applied on top of the POM rod, compressing the sand sample in the cylinder. This procedure was repeated until the cylinder was full. The application of a load using this method is similar to the method using the consolidation-cell seen in Figure 2.7. When releasing the load, one discovered that the pressure on the bottom metal filter had caused it to detach from the cylinder, which meant that the glue was not strong enough to withstand such loads. When applying a load on the sand sample like the one described above, one would also cause the sand grains to push horizontally onto the sidewalls of the cylinder. No flow rate tests were conducted for this modification since the setup was not ideal.

Figure 3.6: Compressing the soil sample using a bench press. Photo: Runa A. Solberg.

3.1.4 Fourth modification

In the fourth modification, the bottom filter was welded to the bottom of the cylinder, which allowed the sand sample to be packed using the bench press without the bottom filter detaching from the cylinder. Next, the sand sample was packed, using the previously mentioned procedure and then compressed with the bench press for every step. The top filter was not welded to the top part of the cylinder because it was desirable to be able to conduct several tests using the same cylinder, but different sand samples. Therefore, the top filter was glued to the top of the cylinder using Tec7 glue. The strength of the glue was believed to be acceptable for the top filter, since it would not need to handle such great loads when using the bench press. The air permeameter was used with this modified setup providing results for flow rate and calculated hydraulic conductivity that were within realistic ranges for the type of sand sample used. See the results of the tests done with the bench press in subchapter 4.5.2 and Table 2.3 for expected hydraulic conductivity of sand. Although the values obtained for flow rate and hydraulic conductivity were within realistic ranges, the load applied to pack the sand sample was not. This is because the bench press puts too much force on the sample and creates an unrealistic, compaction grade compared with “in-situ” compaction grade of an undisturbed soil sample. In

reality, the load applied to the sand sample was over 100 times as high as the overlying loads on a sand sample in the field. It was concluded that a better method of packing the sand sample in the cylinder was needed.

3.1.5 Fifth modification

Instead of compressing the sample with the bench press, a vibrator of brand Makita, was used to pack the sample, with the middle part of the vibrator touching the outside of the cylinder wall causing vibrations in the sand sample in the cylinder. The cylinder was packed with small samples of sand, and the vibrator was used to pack the sand sample between the addition of each small sample. The POM rod was used to apply a load on top of the sand sample when the vibrator was used, forcing the grains to pack closely together in the cylinder. An advantage of using the vibrator compared with the bench press was that the grains would pack more evenly with the vibrator as opposed to being packed with a large load from the bench press. This led to the final modified version of the cylinder, with the bottom metal filter welded in place, whilst the top filter was glued on top to make it possible to remove the filter when removing and adding sand samples. Further, the vibrator was used to imitate a compaction grade similar to the one in the field. To make it easier to insert the cylinder in the core holder with the rubber sleeve, the edges of the metal filters were smoothed with sand paper.

3.2 Modifying the Darcy-cell

This subchapter describes the process of modifying the existing Darcy-cell. The purpose of modifying the cell is to try to better estimate hydraulic conductivity of groundwater in unconsolidated sand in the laboratory.

Being able to fully saturate the sand sample in the Darcy-cell is of great importance when estimating the hydraulic conductivity. This is because if there is air present in the sample when conducting the test, the flow rate will be affected, causing an underestimated value of hydraulic conductivity. One can remove air from the sand sample by applying vacuum onto the cell. The presence of vacuum in the cell causes water to easily enter the pore spaces of the sand because no air is present. An attempt at applying vacuum on an existing Darcy-cell in the laboratory of Engineering Geology at the Department of Geoscience and Petroleum was performed by Tømmerdal (2017). The cell wall was not strong enough to withstand vacuum and cracked when this was applied to the cell. In addition, it has been a challenge to imitate the “in-situ” compaction grade of the sample in the cell. The following subchapter describes the

modifications done to the original Darcy-cell and includes amongst others, the modifications done to make it possible to apply vacuum on the cell and other procedures for imitating the "in-situ" compaction grade. It also describes other done modifications to the existing Darcy-cell that are believed to influence the flow rate through the sand sample. The objective of modifying the cell is to try to estimate a value of hydraulic conductivity that better represents the value of an undisturbed sample in the field.

The setup of the existing Darcy-cell was described in subchapter 2.10.2. As described above, the cell-wall in the existing Darcy-cell was not strong enough to withstand vacuum. The existing Darcy-cell is made of Plexiglas, which is a type of acrylic. A decision to use polycarbonate (PC) as the material in the cell wall was made by the author in consultation with Staff Engineer Håkon Myhren. Polycarbonates have high impact strength and low water absorption (Gooch, 2007), making the material ideal as a cell wall able to withstand vacuum. The material will also have a long life span compared to acrylic, because it has a higher impact strength (Creative Mechanisms, 2016), see Figure 3.7.

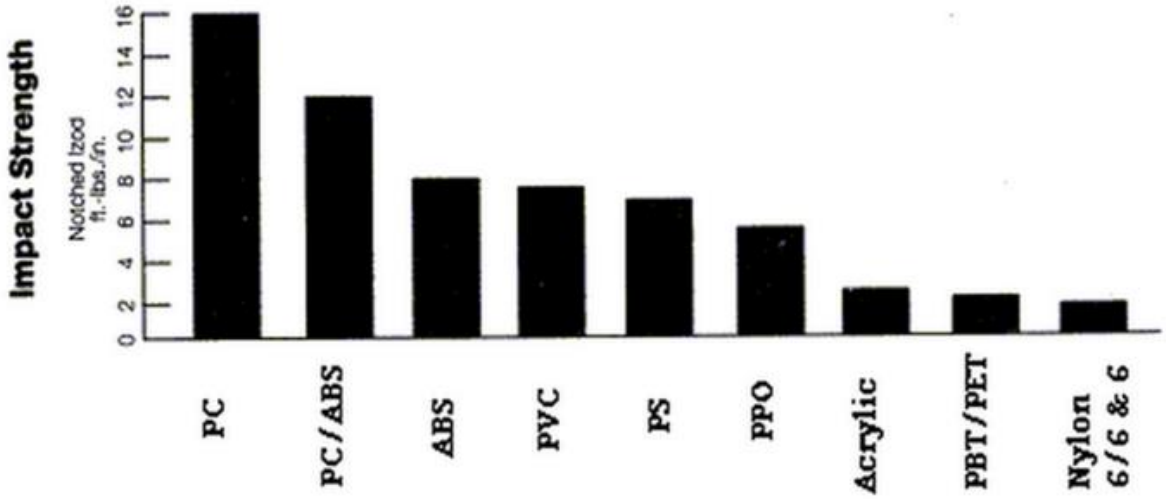

Figure 3.7: Graph displaying impact strength of polycarbonate and acrylic (Polymer Technology and Services, 2015).

The manometers in the existing Darcy-cell were connected with nozzles that extended a certain distance into the cell. The presence of these nozzles was a challenge when trying to imitate the "in-situ" compaction grade of the sand because some sand close to the nozzles was left untouched in the packing process. The circular weight used to pack the sand samples in the original setup was made with "tracks" to make it possible for the weight to pass the nozzles in

the cell. These “tracks” caused the sample material close to the nozzles to be untouched by the force of the circular weight, hence the sample close to the nozzle would not be compacted. The uncompressed material could in practice affect the flow path of water in the area around the nozzles and further affect the final head and flow rate measured during the test.

The fixed-cylinder permeameter described by (D. Daniel et al., 1985), in subchapter 2.4.1, is not connected to manometers and gave rise to the idea of excluding the manometers in the modified cell, to try to better imitate the “in-situ” compaction grade. This would make it easier to compact the whole sand sample, since no nozzles would be present in the cell and one would not need a circular weight with “tracks” to pass any nozzles. Therefore, a rod with a circular end piece with a diameter equal to the inner diameter of the cell was developed to pack the sand samples in the modified cell, see Figure 3.8.

Figure 3.8: Rod used to compact sand samples in the modified Darcy-cell setup. Photo: Runa A. Solberg.

The dimensions of the existing cell were also considered in the modification process. Table 3.1 presents the dimensions of the existing Darcy – cell. As mentioned in subchapter 2.2.2, the inner diameter of the cylinder should be minimum 10 times the largest grain diameter in the soil sample to prevent the “wall-effect”. The existing Darcy – cell had an inner diameter of 114 mm and thus allowed for quite coarse samples of soil to be tested. However, the nozzles extended into the cell of the existing apparatus and would affect how the grains packed in the nearby areas. If one imagines the nozzles creating a circle inside the cell, then the diameter of this circle has to be 10 times the largest grain diameter in the soil sample.

Table 3.1: Dimensions of existing Darcy-cell.

Description	Symbol	Unit	Value
Outer diameter of cylinder	OD	mm	121
Inner diameter of cylinder	ID	mm	114
Thickness of cylinder	T	mm	7
Cylinder length	L	mm	450

By excluding manometers from the setup in the modified Darcy-cell one could use a cell with a smaller inner diameter than the diameter of the existing cell. An advantage of a smaller inner diameter is that less sample material is needed for each measurement. The largest grain diameter in the sand sample used in this master thesis is between 2 to 4 mm, see subchapter 3.3. If the requirement described in subchapter 2.2.2 is applied, the minimum dimension of the inner diameter can be 40 mm. To allow for coarser sand samples to be tested in the cell as well at a later time, an inner diameter of 64 mm and outer diameter 70 mm was chosen for the modified cell. The length of the cell in the existing Darcy-cell was kept unchanged making it possible to test a larger sample if needed.

Removing the manometers meant that one had to use another method for determining whether the pressure difference along the flow line was kept constant. A pressure sensor, brand Aplisens Type PCE-28 with range -1 – 1,5 bar, was installed in the top and bottom part of the cell and the values were logged in a program called LabView on a computer. The range of the pressure sensor was chosen from -1 to 1,5 bar to be able to record the pressure value once vacuum was applied on the cell, -1 bar being the value of complete vacuum. Similarly, temperature sensors, brand Aplisens Type APT-28 with range 0-120 °C, were placed in the top and bottom of the cell and recorded the temperature of the saltwater when it flowed through the cell and then logging it in LabView. The hypothesis of using pressure- and temperature sensors to measure the two parameters in the cell is that the sensors will give more accurate values for the parameters, and one also removes the chance of human error that can occur when recording the readings manually. The top- and bottom lid of the Darcy-cell was based on the lids in the existing Darcy-cell, but with other dimensions. The already existing lids were built of metal, but the new lids were built of polyvinyl chloride (PVC), which is a type of plastic. This material was chosen because it is easier to machine than metal lids and also cheaper. A disk to be placed at the top of the sand sample to keep it in place was made from the same material. The design

of the top- and bottom lid as well as the disk were done by the author, however further designs in a programme called AutoCAD was done by Senior Engineer Noralf Vedvik. The blueprints of the lids and the disks made in AutoCAD are seen in Figure 3.9, Figure 3.10 and Figure 3.11. The lids and disk were built by Staff Engineer Håkon Myhren.

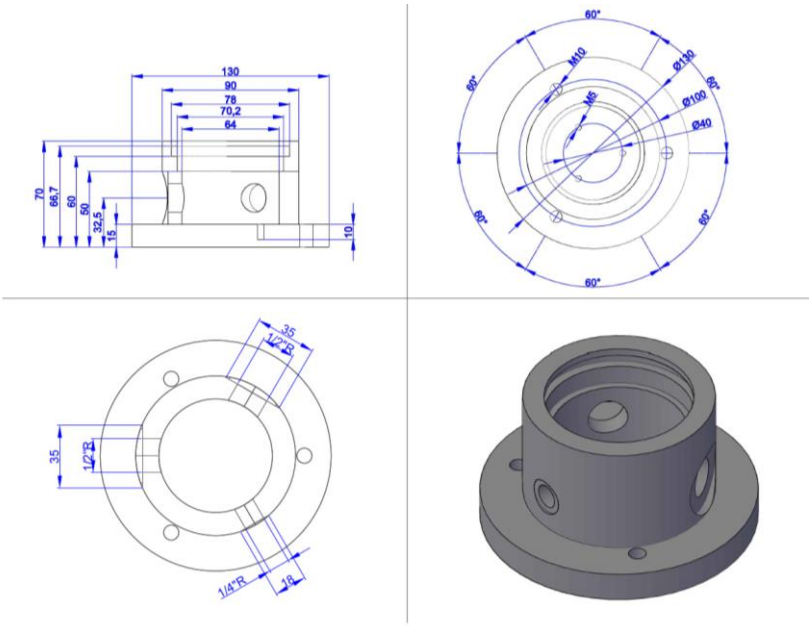

Figure 3.9: Blueprint from AutoCAD showing the design of the bottom lid for the modified Darcy-cell. Design in AutoCAD created by Senior Engineer Noralf Vedvik.

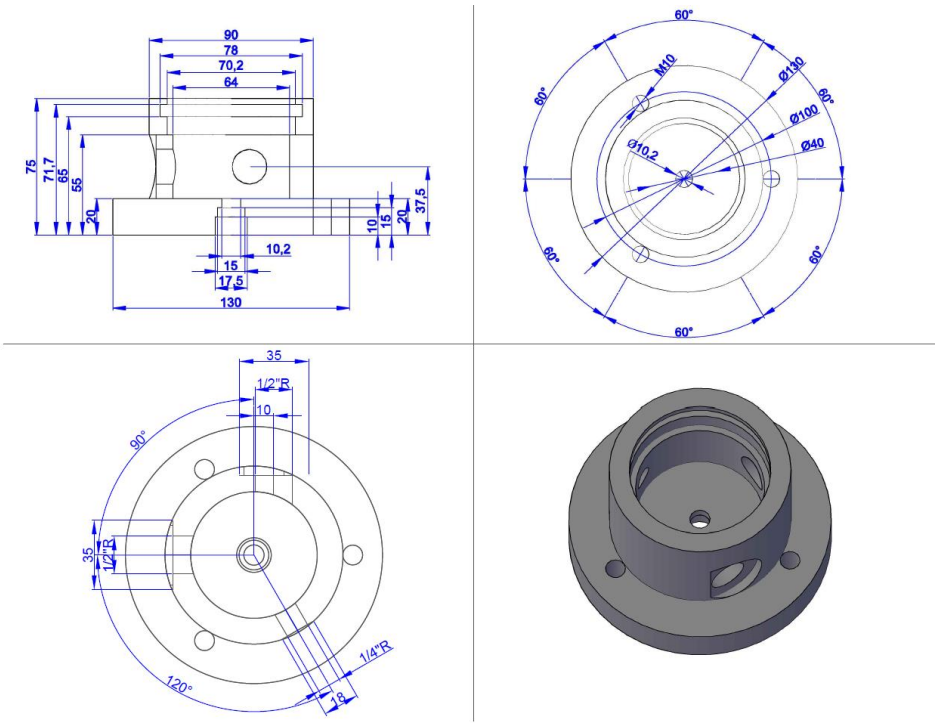

Figure 3.10: Blueprint from AutoCAD showing the design of the top lid for the modified Darcy-cell. Design in AutoCAD created by Senior Engineer Noralf Vedvik.

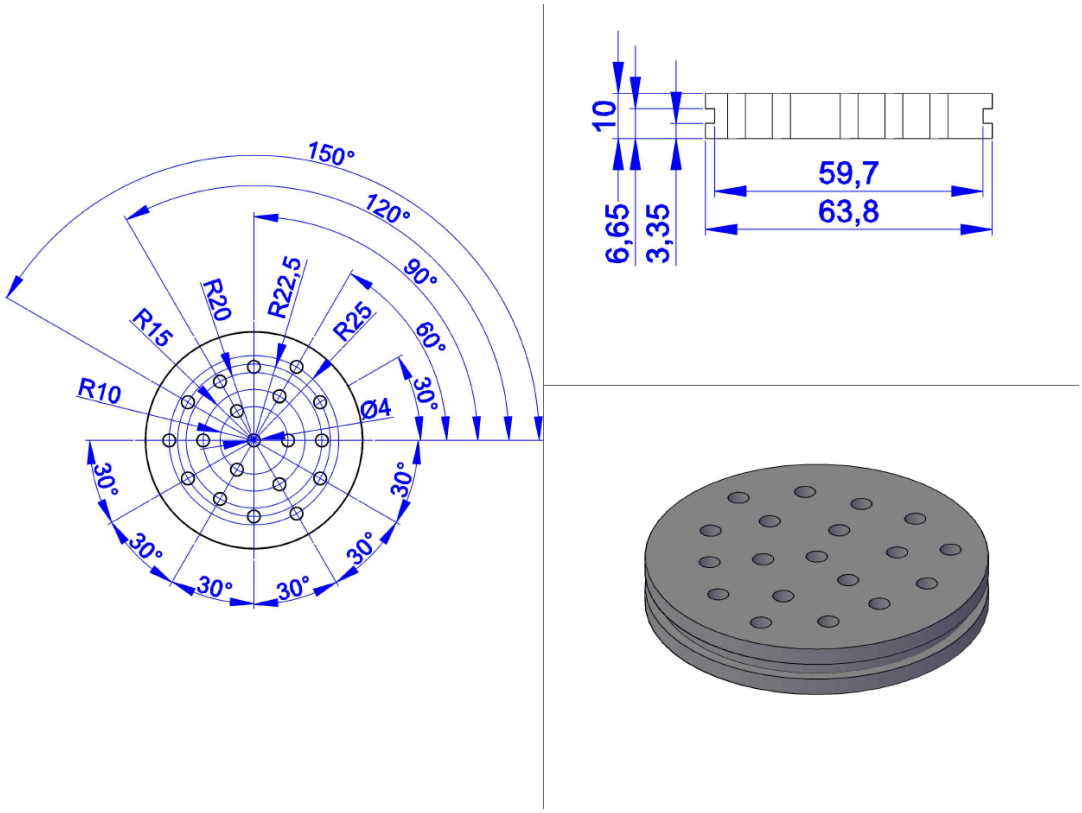

Figure 3.11: Blueprint from AutoCAD showing the design of the disk for the modified Darcy-cell. Design in AutoCAD created by Senior Engineer Noralf Vedvik.

The remaining components in the existing Darcy-cell were used in combination with the modified components. The method used to calculate the hydraulic conductivity with this new setup is described in subchapter 3.6.

3.3 Sieve analysis

As mentioned in subchapter 2.2.2, the diameter of the grains in a sample are important when conducting a Darcy-cell experiment because the largest grain diameter in the sample determines the minimum inner diameter of the cylinder in the Darcy-cell. A sieve analysis of the sand sample is conducted to determine the grain size distribution and determine the maximum grain diameter present in the sand sample.

The sieve analysis was conducted according to International Organization for Standardization (2004). Before conducting the sieve-analysis, the sand sample needs to be separated into equal parts using a splitter, see Figure 3.12. The splitting is conducted to make sure that the sand used for the sieve analysis contains grains that that represent the whole sand sample. The splitter is open below and consists of numerous slides that are oriented in two different directions. Adding the sand sample causes the sand to separate into two containers located on either side of the

splitter. By switching out one of the full containers with an empty container and adding the sand sample from the full container to the splitter, one can split the sample into the desired quantity. This desired quantity is used for the sieve analysis. One could observe some fine material escaping when pouring the material into the splitter.

Figure 3.12: Splitter with sand sample. Photo: Runa A. Solberg.

During the sieving, standardized sieves with mesh sizes 2 mm, 1 mm, 0,5 mm, 0,25 mm, 0,125 mm and 0,063 mm were used. The sand sample was sieved in a sieving machine for 15 minutes. The weight of the sand sample before and after sieving was measured to determine sample loss during the sieving process. Then, the weight of sand sample on each sieve was measured. Following this, the grain size distribution of the sand sample was presented by plotting the grain sizes in a logarithmic scale on the x-axis and the cumulative percent finer by weight on an arithmetic scale on the y-axis. See subchapter 4.1 for sieving results and the grain size distribution curve.

Figure 3.13: Sieving machine. Photo: Runa A. Solberg.

3.4 Calculating effective porosity

The effective porosity of the sand sample was calculated using a helium porosimeter by applying the principle of gas expansion, described by Boyle's law, see equation 2.10. The sand sample was packed into a matrix cup, see Figure 3.14. To reach what was assumed to be a sufficient compaction grade, equal amounts of sand sample was packed in 5 steps. The POM rod was used to pack the sand in between each added layer by pushing it into the matrix cup 3 times, between the addition of each new layer. This procedure was repeated until the sand had reached a certain level below the top of the matrix cup. To prevent small grains from escaping into the helium porosimeter system, a paper filter was added on top of the sand sample, see Figure 3.14.

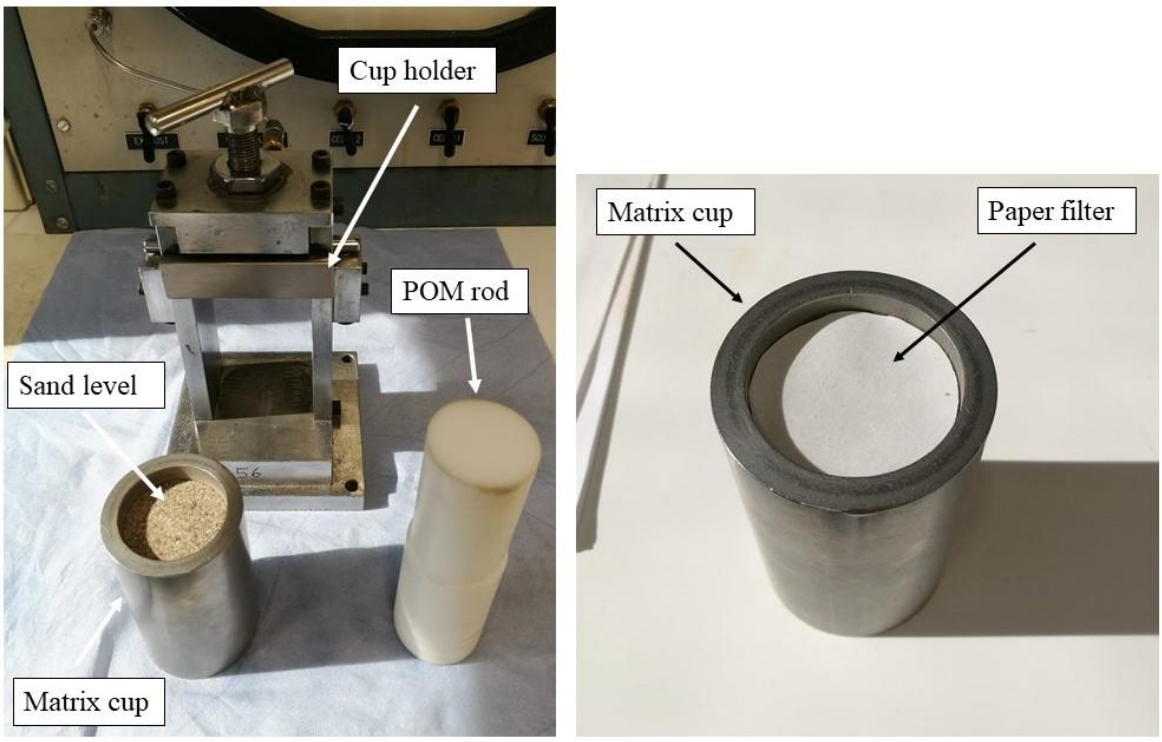

Figure 3.14: Helium porosimeter method. a) Some components of the helium porosimeter setup and b) the matrix cup filled with sand and a paper filter on top. Photo: Runa A. Solberg.

The inner diameter, the total height of the inner part of the matrix cup and the height from the sand sample and the top of the matrix cup was measured using a calliper. From this, it was possible to measure the bulk volume of the sand sample, V_b [cm^3], see equation 2.14. Then the matrix cup, with the sand sample and filter, was mounted in the cup holder. Helium gas with a pressure of 10 bars is then applied to the cup holder with the matrix cup. Following this, switches named "source", "supply" and "cell 1" are opened. The needle is regulated at 100 psi before closing the "source" and "supply" switches and opening the "core holder" switch causing the gas to flow from the reference chamber to the sample chamber, or in this case the matrix cup, similar to the description in subchapter 2.6. The volume read from the porosimeter, see Figure 3.15, is V_2 [cm^3] and is the volume of the sand sample and an unknown volume. To finish the reading, the "exhaust" switch was opened, "cell 1" and "core holder" closed and lastly the "exhaust" switch was closed. By repeating the same procedure, but with an empty matrix cup, the volume of the matrix cup V_1 [cm^3] was measured. By applying equations 2.15, 2.13 and 2.16 it is possible to calculate the effective porosity of the sand sample.

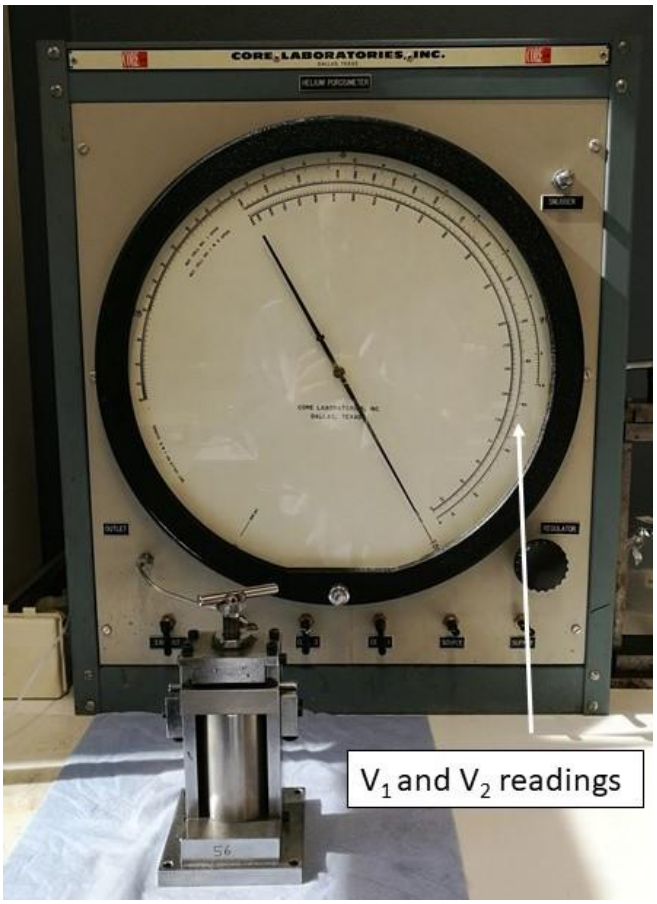

Figure 3.15: Helium porosimeter showing where V_1 and V_2 are recorded. Photo: Runa A. Solberg.

3.5 Calculating hydraulic conductivity using modified core permeameter

The following subchapter describes the method for measuring the permeability of the metal filters. Then the method used to calculate the hydraulic conductivity using an air permeameter and a liquid permeameter is described.

3.5.1 Measuring permeability of metal filters

As described in subchapter 3.1, it is possible to estimate the permeability of the sand sample in the cylinder if the permeability of the metal filters is known. Measuring the permeability of the metal filters was conducted using a Top Industrie 2969 air permeameter, see Figure 3.16. The tests done with sand samples were not conducted using this permeameter because there was a chance of sand grains escaping the cylinder and flowing into the rest of the apparatus. It was therefore decided, in consultation with Staff Engineer Roger Overå, to test the sand samples using two other permeameters, one using air and one using liquid as the permeating fluid. See subchapters 3.5.2 and 3.5.3 for further explanation on these methods.

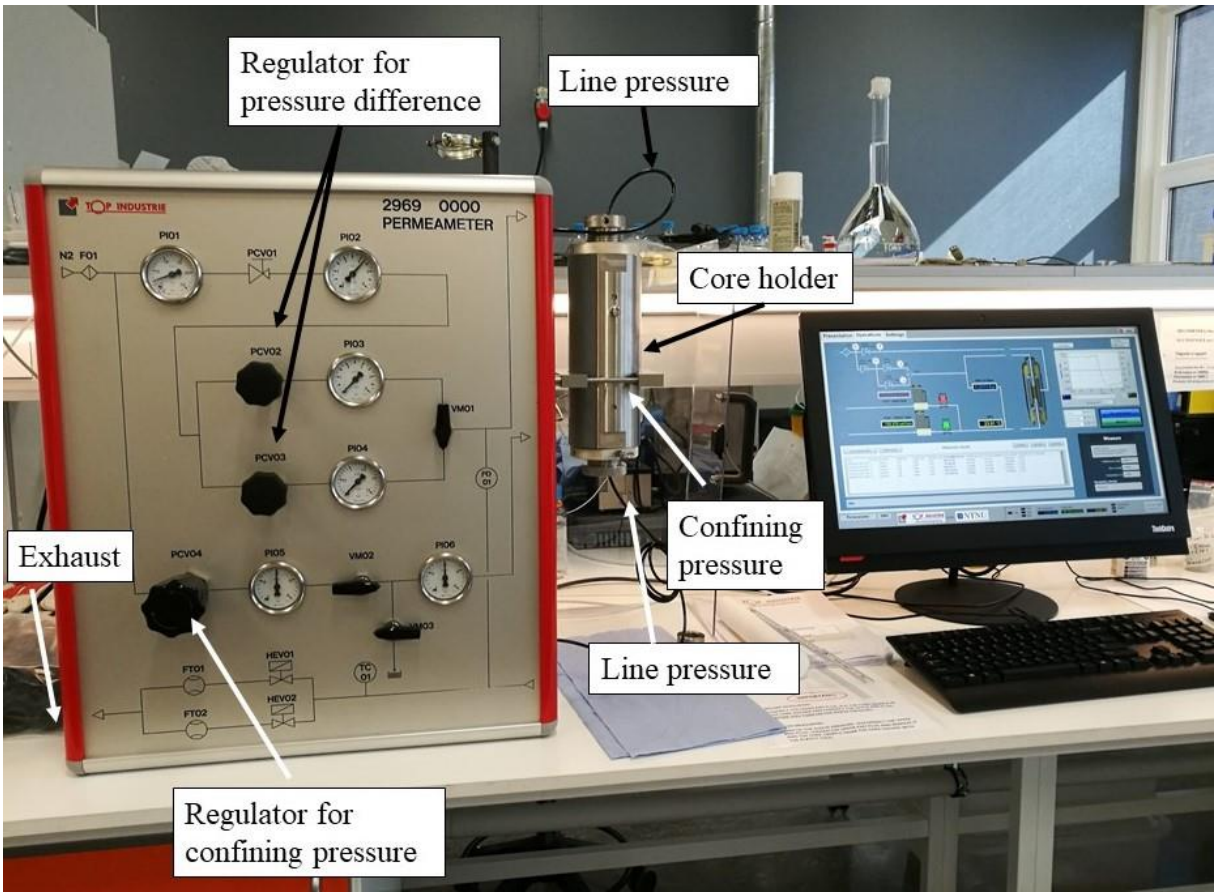

Figure 3.16: Apparatus used to measure permeability of metal filters. Photo: Runa A. Solberg.

The three cylinders were left empty, instead of packing them with sand samples, and the top filters were glued onto the cylinders. The three cylinders with the glued filters were left to dry in room temperature for three hours before the experiment was conducted. In this test the empty space in the cylinder was assumed to not influence the permeability measurements. The empty space was assumed to have an infinite permeability. If one inserts an infinite permeability for the empty space into equation 3.9, the part containing the infinite permeability becomes zero.

The Top Industrie 2969 permeameter functions much in the same manner as the permeameter described in subchapter 2.7. At the start of the experiment, one cylinder was placed in the core holder, and the top piece of the core holder was screwed in place. Confining pressure of 20 bars was applied, followed by the line pressure. It was possible to regulate the pressure difference of the line pressure, see Figure 3.16. The permeameter was connected to a PC programme that displayed different relevant parameters, like pressure difference in the core holder, the flow rate and a graph of the two versus time, see Figure 3.17. A flow rate was set for each measurement by adjusting the pressure difference to correspond with the desired value for flow rate. Once the pressure difference and flow rate had stabilized, a light below the two parameters appeared

on the graph. A measurement of permeability could be conducted once both the pressure difference and the flow rate were stable. The programme uses an equation based on Darcy's law to calculate the permeability of the filters, and by entering the diameter and length of the cylinder, the programme could calculate the permeability of the filters. This procedure was repeated for the two remaining cylinders.

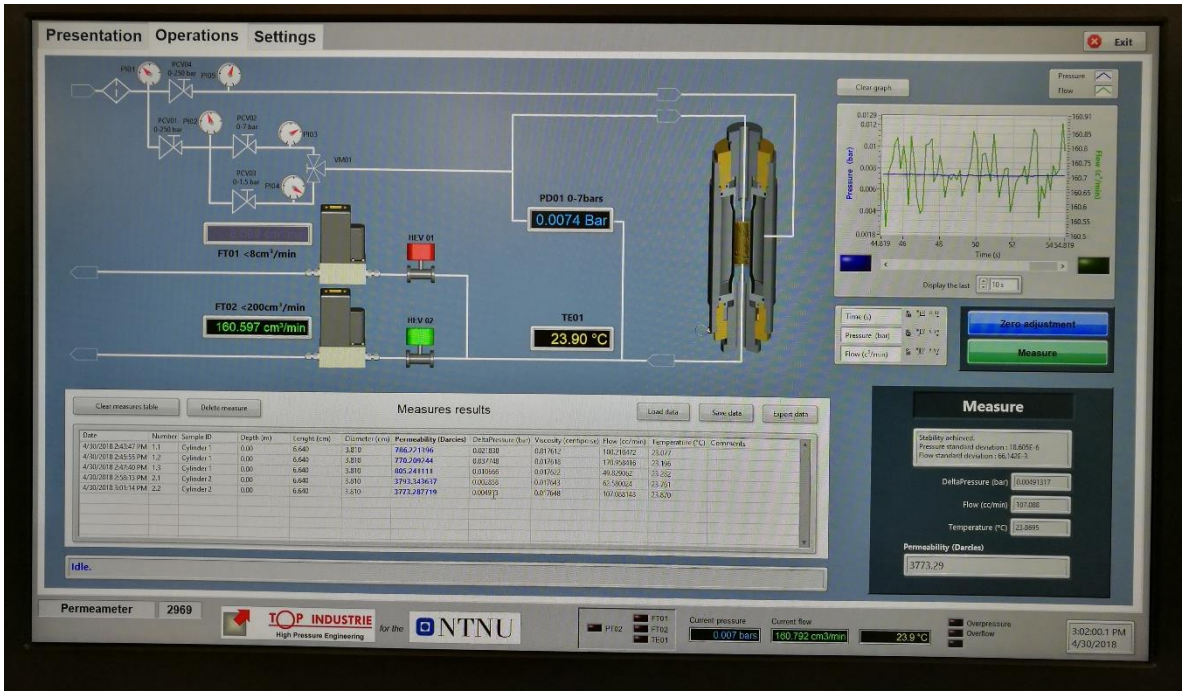

Figure 3.17: PC programme connected to Top Industrie permeameter. Photo: Runa A. Solberg.

Equal permeabilities for the filters was assumed. However, one could observe that the 6 different filters used for the 3 cylinders looked different. The filters used for cylinder 1 seemed to have quite a compact form, while the filters used for the other 2 cylinders looked more porous.

3.5.2 Air permeameter

The tests with the air permeameter were done with cylinder 1 and 2 because metal filters for a third cylinder were not at hand at that time. Prior to every air permeameter test, the two cylinders were packed with sand as described in subchapter 3.1.5, except for Cylinder 1 in test 1. This cylinder was packed with the bench press, but a force of 1 ton applied onto the sand sample was unrealistic when compared to the force on soil in the field. In an attempt to better simulate how the sample packs in the field, the remaining tests both in the air- and the liquid permeameter were conducted by packing the sand sample with a vibrator. After the test, the top filter was removed by separating the glued filter from the cylinder with force. The used sand sample is

removed from the cylinder and the glue on the cylinder and filters were removed. The remaining sand grains on the surface of the filters and the cylinder are cleaned using an air gun. The procedure of packing the sand in the cylinder prior to the test, and removing the filters and glue was repeated for every measurement.

The air permeameter used to calculate the hydraulic conductivity is similar to the schematic in Figure 2.16 and Figure 2.17. The setup of the apparatus is shown in Figure 3.18. Before the start of the experiment, the end piece was loosened from the core holder. The vacuum valve was opened and vacuum applied to the core holder, causing the rubber sleeve to get sucked to its sidewalls. This made it possible to insert the cylinder with the metal filters into the core holder. Then, the end piece was tightened. The vacuum was turned off and the vacuum valve closed. First, confining pressure of 20 bar was applied to the core holder. This was done by checking that the regulator on the gas flask was in top position. The top position of the regulator means that no gas is able to escape from the gas flask to the rest of the system. Gas was then allowed to flow from the gas cylinder to the regulator by opening the valve on the gas cylinder. Then, the gas valve located on the tubes in the system was opened and the pressure was adjusted to 20 bar by turning the regulator downwards until reaching the desired confining pressure. Lastly, the valves to the air pressure were opened causing the sand sample to be flooded with air. It is possible to adjust the pressure at both pressure sensors, making it possible to apply higher line pressure and vary the pressure difference. Finally, the flow rate was read from the flow meter at different pressures. Removing the cylinder from the core holder was done using the same procedure as described above, but in the opposite order. The only exception is that the gas in the system had to be released from the system by opening the exhaust valve.

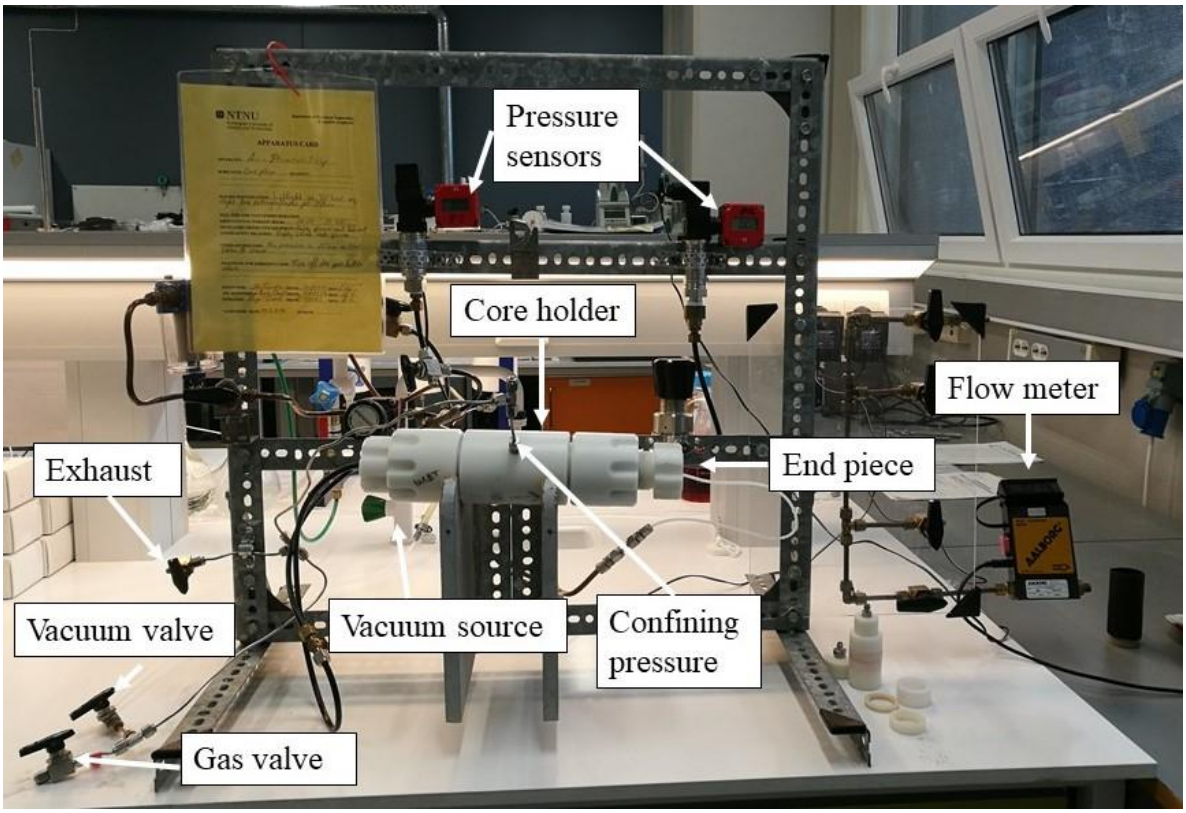

Figure 3.18: Air permeameter setup. Photo: Runa A. Solberg.

As described in subchapter 3.1, the flow rate recorded using the method above, measures both the rate through the two metal filters and the sand sample. This means that the flow rate, and therefore also the calculated permeability, is an average value of the filters and sample. The average permeability is calculated using equation 2.30. The permeability of the sand sample can be calculated using equation 3.10, since both the permeability of the filters, see subchapter 3.5.1, and the average permeability is known. Lastly, the hydraulic conductivity of the sand sample can be calculated using equation 2.7.

After conducting the air permeameter method, the filter at the outlet was removed to empty the cylinder. There was observed some fine material collecting at the surface of the cylinder. As was mentioned in subchapter 3.1.2, one expects the flow rate to increase with increasing pressure. Although the method used to pack the sand sample was changed from using a bench press to using a vibrator one could still observe a decrease in flow rate at some of the higher pressures, see appendix F for flow rate data. The decrease in flow rate at higher pressures could indicate a migration of fines in the sample during the air flooding.

3.5.3 Liquid permeameter

Calculating the permeability of the sand sample using a liquid permeameter was conducted to compare the values of hydraulic conductivity calculated using the air permeameter with the values calculated using the liquid permeameter.

The setup of the liquid permeameter is shown in Figure 3.19. The method works by flooding a 0,1 % salt solution through the core holder containing the cylinder with the sand sample inside. The reason why salt solution was used to flood the sample, and not pure distilled water was because the soil sample could contain traces of clay. Saltwater counteracts some of the surface properties in the clay because the saltwater does not stick as well to the clay minerals. This means that if clay is present in the sample affecting the flow rate, then the salt is added to the distilled water in an attempt at counteracting the properties of the clay minerals.

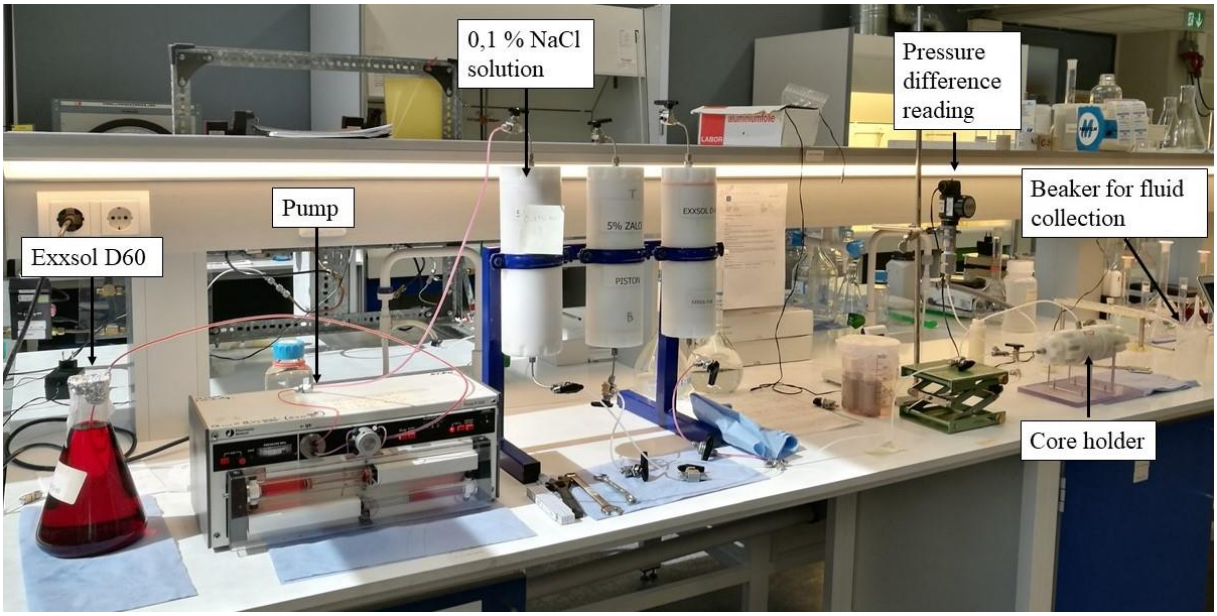

Figure 3.19: Liquid permeameter setup. Photo: Runa A. Solberg.

The salt solution was mixed using the ratio: 1L distilled water at room temperature to 1g sodium chloride (NaCl). The distilled water was added to the salt solution and mixed in a glass beaker using a magnet that spins in the beaker, thus dissolving the salt in the distilled water, see Figure 3.20. Once the salt had dissolved in the water, the solution was added to the tank in Figure 3.19.

Figure 3.20: Mixing of salt solution used as the permeating fluid in liquid permeameter method. Photo: Runa A. Solberg.

One must fully saturate the sand sample before performing the liquid permeameter test. The fluid used to saturate the samples was the same as the salt solution used for the flooding process. Before the saturation process began, the sand sample was packed in the cylinder in the same manner as described in subchapter 3.1.5. It is easier to saturate the sand if the sample is de-aired prior to saturation. This is because the salt solution is easily sucked into the pore spaces of the sand sample when no air is present. The de-airing of the sample was done using a Varian SD-90 vacuum pump. The three packed cylinders were placed in a plastic beaker inside a glass bowl called an exicator, see Figure 3.21. This is an apparatus designed to withstand vacuum, and is airtight. The vacuum pump sucked out the air in the exicator through the lower tubing and once the pressure inside the exicator reached 100 mbar, the saturation process began. The cylinders were left to saturate for 1 hour before they were taken out of the exicator and the beaker was covered with Parafilm, a type of laboratory film. This was used to prevent air from entering the salt solution in the beaker and samples.

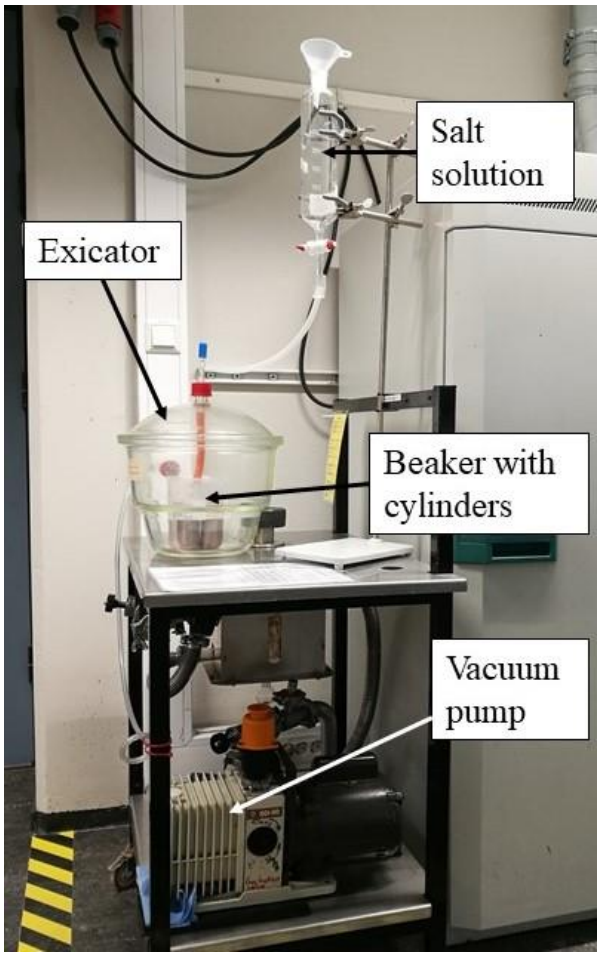

Figure 3.21: Exicator used to apply vacuum on sand sample. Photo: Runa A. Solberg.

To validate whether the sand sample was fully saturated with saltwater after the saturation process, the saturation of saltwater present in the sample was calculated. The density of saltwater had to be estimated to be able to calculate the saltwater saturation in the sand sample. This was done using a pycnometer, see Figure 3.22. The empty pycnometer was placed on a scale and its weight was recorded. Then, the saltwater solution was added to the pycnometer and the total weight was recorded. The weight of saltwater was calculated by subtracting the weight of the empty pycnometer from the total weight. Since the volume of the pycnometer was known, the density of saltwater could be calculated using equation 2.17. It was expected that the density of the salt solution would be approximately equal to the density of water. This was confirmed when the density of the salt water solution was calculated using the pycnometer, see subchapter 4.2 for density results. It was therefore decided to use the density of water in all further calculations related to the liquid permeameter method and also the Darcy-cell method.

Figure 3.22: Apparatus used to calculate density of saltwater. Photo: Runa A. Solberg.

After calculating the density of saltwater, the saturation could be determined. The mass of saltwater and the pore volume was needed in order to calculate the saltwater saturation in the sand sample, see equation 2.19. First, the mass of dry sand sample and the cylinder was recorded. After the saturation process in the exicator was finished, the wet mass of the sand sample and cylinder was recorded. From this, the mass of saltwater present in the sand sample could be calculated:

$$m_{sw} = m_{cws} - m_{cds} \tag{3.11}$$

Where m_{sw} is the mass of saltwater present in the sand sample [g], m_{cws} is the mass of the cylinder and saturated sand sample [g] and m_{cds} is the mass of the cylinder and dry sand sample [g]. The volume of water could be calculated by solving equation 2.17 with respect to volume:

$$V_{sw} = \frac{m_{sw}}{\rho_w} \tag{3.12}$$

Where V_{sw} is the volume of salt water present in the sand sample [cm^3] and ρ_w is the density of water [g/cm^3]. Lastly, the saltwater saturation in the sample was calculated using equation 2.19. The pore volume was assumed to be the same in all test because the packing procedure was kept the same for all tests. This means that the value needed for pore volume in equation 2.19 is the pore volume estimated in the packed sand of the 3 cylinders when using the helium porosimeter. One did however need to estimate the pore volume by finding the ratio of the pore volume from the helium porosimeter to the total volume of the sample. By multiplying this ratio

with the length of the sand sample in the cylinder, one obtained an estimate for the pore volume of the sand sample used in the liquid permeameter test.

It is also possible to calculate the effective porosity of the sand sample by saturating the sand sample in the cylinder using and exicator. The effective porosity was calculated using the following equation:

$$n = \frac{m_{wet} - m_{dry}}{\rho_w V_B} \tag{3.13}$$

The dry weight of the sand sample and cylinder in test 1 was not recorded because the author did not consider determining the porosity and saturation of the samples before having saturated the sand sample in the first test. This decision was made after the saturation process in test 1. So, a decision to use the recorded dry weight for test 2 in test 1 was made, see subchapter 4.3.2 and 4.4 for results. It was a reasonable assumption that the dry weight of sand in the cylinders was approximately equal for test 1 and 2 because the sand was packed using the same packing procedure every time. Calculating porosity by saturation is useful because it can be used to determine if any air is left in the pore spaces of the saturated sand sample. If the calculated porosity by saturation is less than the effective porosity calculated using the helium porosimeter, then this indicates that some of the pore spaces in the saturated sample have not been filled with water, and are left with air.

In test 2 the cylinders were left to saturate in the exicator two times. First, the cylinders were left to saturate for 1 hour and taken out of the exicator so the wet weight of the sand sample could be recorded. As a test to see if the saturation of the sand sample changed if the cylinders were left in the exicator for a longer period of time was done. The cylinders were left in the exicator for 2 more hours and then removed from the exicator and the wet weight of the sand sample was recorded again. The results showed that leaving the cylinders in the exicator for a longer period of time did not change the saturation of the sand and thus not the porosity of the sand sample either, see subchapter 4.3.2 and 4.4 for results.

After having saturated the sand samples, calculated the saltwater saturation and the effective porosity, the first cylinder was inserted into the core holder and the end piece was tightened. The pump was set to a flow rate of 3 mL/min and worked by pumping exxsol D60, a hydrocarbon fluid, through it. The pump was connected by tubes to the salt solution tank. The exxsol D60 solution has a very low solubility in water and will therefore not mix with the saltwater once it comes into contact with it. This means that when the exxsol D60 was pumped

through the tubes it pushed the saltwater from the tank into the core holder and flooded the sand sample. The saltwater flowed through the sand sample and through a tube and lastly into a plastic beaker. Since the tube at the outlet of the core holder was open to the atmosphere, the pressure difference was the pressure recorded at the first pressure sensor. By recording the pressure difference at different times, it was possible to estimate the time at which the pressure difference became stable. The time at which the pressure difference becomes stable is in theory the pressure value one should use in further calculations of permeability if core samples are used. However, in this test one observed fine material collecting at the filter at the outlet after testing. It was therefore assumed that the unconsolidated sand could move inside the cylinder with time, causing the grains to pack more closely at the end of the cylinder closest to the outlet and this is described further below. Because of this, it was decided to use the pressure difference reading at the time when the first fluid entered the plastic beaker. The permeability was calculated using equation 2.23. Lastly, the hydraulic conductivity was calculated using equation 2.7.

After having conducted the liquid permeameter test, the metal filter at the outlet was removed. As mentioned above, fines were observed at the surface of the filter. There were a larger number of fines observed on the surface of the filter after using this method compared with the air permeameter method. The fines could potentially block the pore spaces in the filter and affect the measured flow rate, so it was decided to do a scanning electron microscopy (SEM) to determine if finer grains of soil were present in the pore spaces of the filter. An in-depth description of the SEM method will not be given in this thesis, but a brief description of the procedure used will be covered. The brand of apparatus used was Hitachi SU6600. The SEM analysis was conducted by the author while the handling of the apparatus and the associated program was done by Staff Engineer Kjetil Eriksen and Postdoctoral Fellow Haili Long-Sanouiller. First a secondary electron (SE) analysis was conducted to see the charges on the metal filter. Normally the sample one wants to test is coated with a coating that neutralizes the charges. However, this was not done in this case, allowing one to see the charges on any sand present in the pore spaces of the filter. Charges on the filter was observed, however the charges did not necessarily mean that the charged surface was sand. An energy-dispersive X-ray spectroscopy (EDS) was performed on the metal filter to determine the composition present on the surface of the filter. Using the EDS made it possible to determine whether the charged areas on the filter were composed of minerals common in sand or if they consisted of minerals

common to the metal in the filter itself. From this one was able to conclude if sand was present in the pores of the metal filter.

Another observation made during the liquid permeameter test was the presence of a gap between the cylinder wall and the sand sample. This gap was exposed when removing the metal filter at the outlet of the cylinder. A photo of the gap is seen in Figure 3.23.

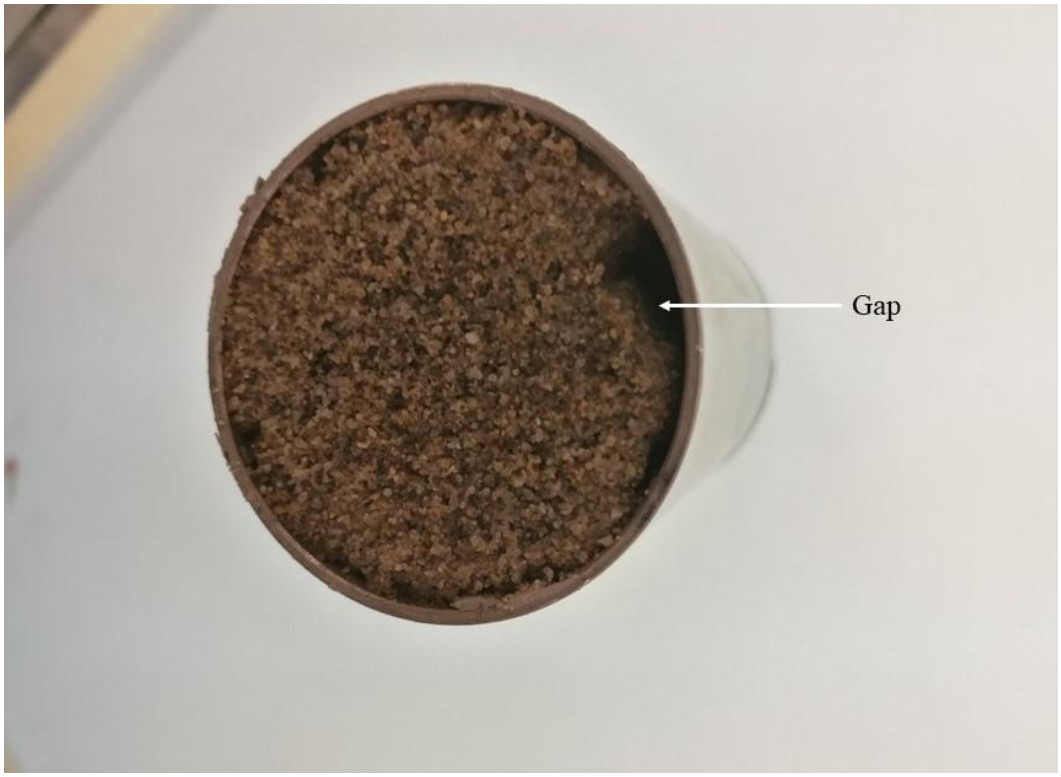

Figure 3.23: Gap observed between the cylinder wall and the sand sample. Photo: Runa A. Solberg.

3.6 Calculating hydraulic conductivity using modified Darcy – cell

The following subchapter describes the method used to calculate the hydraulic conductivity in an unconsolidated sand sample using the modified Darcy – cell. A picture of the setup is shown in Figure 3.24. The top and bottom of the cell was connected to an upper- and lower tank and the pressure- and temperature sensors were connected by a data acquisition unit (DAC) to a computer. The water inlet of the upper tank was connected to another plastic tank at a higher level. This allowed the water to flow from the tank at the higher lever to the upper tank. The inlet of the lower tank was connected to the bottom outlet of the cell, while the outlet of the lower tank was open allowing water to flow from the tank to a beaker where volume of water was recorded.

Prior to the test, water was de-aired using the Varian SD-90 vacuum pump and exicator. The method used to de-air water was the same as the method used to saturate the sand samples in the cylinder in subchapter 3.5.3. Similarly, a 0,1% salt solution was also used in this method. The exicator was filled with salt solution until the solution reached a level close to the lower valve in the exicator. The vacuum pump will suck salt solution into the pump if the solution passes the lower valve, causing it to mix with the oil in the pump system and this is not preferable. The solution was left to de-air for 1 hour before it was added to plastic tanks. The de-airing of saltwater was time-consuming. So, because of a lack of time, the de-airing of water was excluded during measurements 13-43. It was concluded that de-airing the salt solution was unnecessary since the water used was distilled water, and not water from the tap. The fraction of air in distilled water is small, and it was therefore assumed that the presence of air could be neglected.

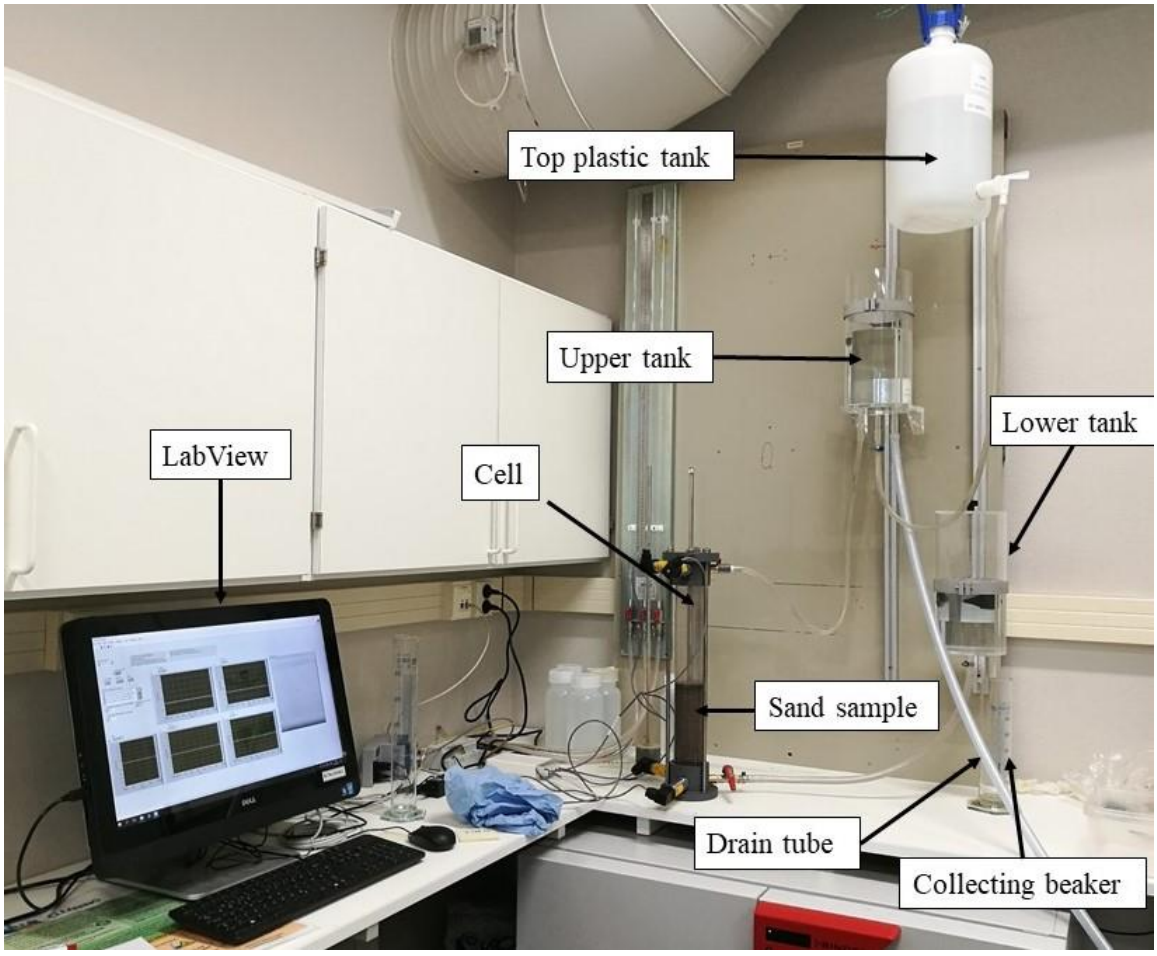

Figure 3.24: Setup of the modified Darcy-cell apparatus. Photo: Runa A. Solberg.

The sand sample was packed in 7 steps. A volume of 100 mL was added in each step, resulting in a volume of 700 mL sand in the cell. Between the addition of each sample, the rod with the

circular end piece was used to pack the sand. To try to imitate a compaction grade similar to how a sample is compacted in the field, the rod was pushed onto the sample by force five times before the addition of a new layer of sand. During this packing process one could observe some fine sand escaping from the cell. Some fines also collected on the rod itself, ass seen in Figure 3.25.

Figure 3.25: Fine material that has collected on the packing rod during the packing process in the Darcy-cell method. Photo: Runa A. Solberg.

Vacuum was applied after the sand was packed in the cell. This was executed by connecting the Varian SD-90 vacuum pump with a tube to the top inlet of the Darcy-cell. The valve at the top inlet was open, whilst the valve at the bottom outlet of the cell was closed. The bottom outlet was connected to a plastic tank containing salt solution using a tube. A photo of the setup can be seen in Figure 3.26. The vacuum pump was turned on and left to suck out the air in the sand sample, applying vacuum to the cell. Normally, if the vacuum pump had been connected to the exicator, as was the case when applying vacuum to the cylinders with sand in subchapter 3.5.3, then the display on the vacuum pump would show a pressure of between 80-100mbar. However, since the vacuum pump in this case was connected to the Darcy-cell, one was not able to reach such a low pressure as 100 mbar. The pressure display showed 120 mbar, which was a reasonable value since the Darcy-cell did not have the same construction as an exicator, where the purpose of the latter is to achieve as close to vacuum as possible. The top valve was

closed and the vacuum pump turned off once a pressure of 120mbar was reached. The valve on the plastic tank with salt solution and the bottom valve of the Darcy-cell was opened, allowing saltwater to flow from the tank and saturate the sample from the bottom of the cell to the top. One could observe some fines escaping from the sand sample and mixing with the saltwater above the sand sample. Once the whole cell had been filled with salt solution, the bottom valve to the cell and the valve to the tank was closed. Then the sand sample was left to saturate for 1 hour.

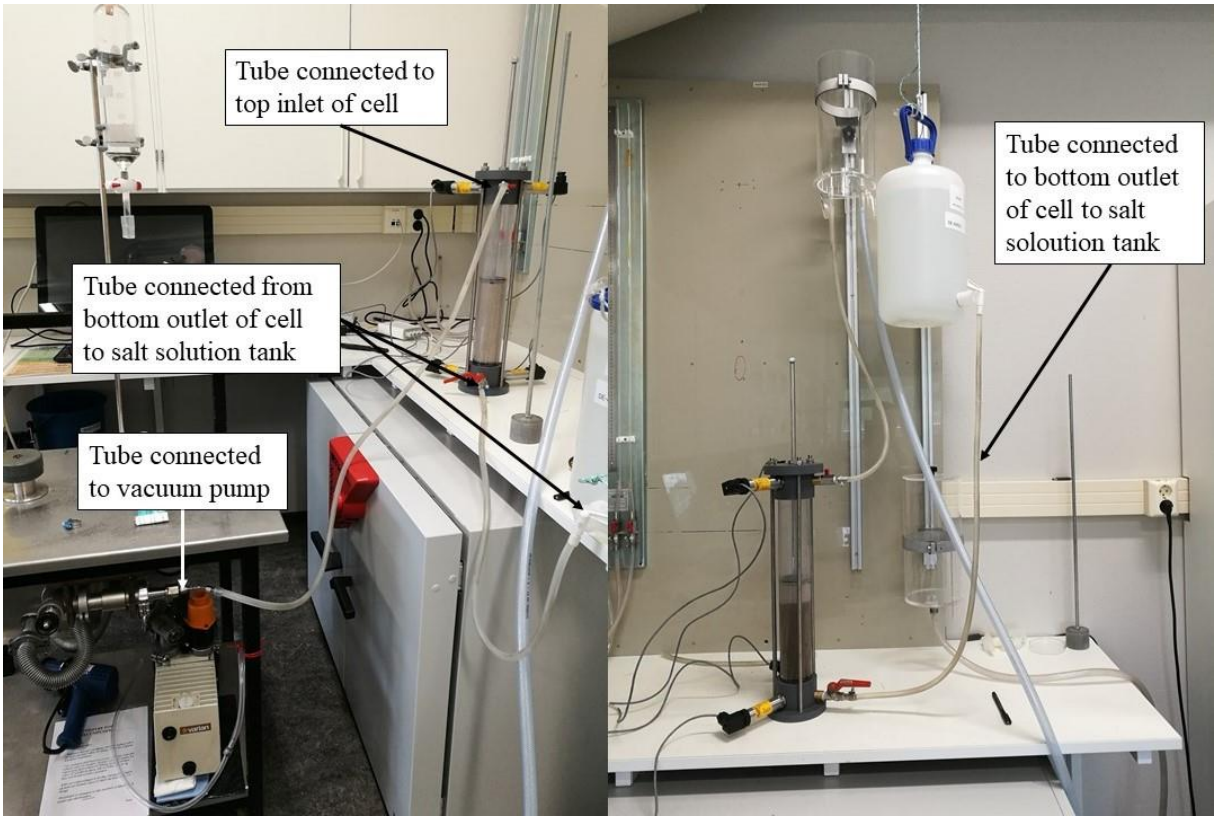

Figure 3.26: Saturation process – Darcy-cell. Applying vacuum on Darcy-cell on the left and saturating the sand sample on the right. Photo: Runa A. Solberg.

By applying vacuum on the cell, one assumes that the saturation process of the sample will leave the cell fully saturated with saltwater. To check if this was the case, the cell with the dry sand sample was weighed prior to saturation. After saturation, the saltwater filled cell with the wet sample was weighed. The mass of salt water present in the whole cell was calculated using equation 3.11. Then the total volume of salt water present in the whole cell was calculated using:

$$V_{sw} = A_{cell}L_{cell} + A_{cell}L_{Bottom} + A_{cell}L_{Top} \tag{3.14}$$

Where L_{Bottom} was the length from the end of the cell wall to the bottom of the lid [cm] and L_{Top} the length of the saltwater column spanning from the end of the top part of the cell wall to the top of the water column [cm]. These last two parts of the equation represent the volume of saltwater present in the top and bottom lid. The bottom lid was fully filled with saltwater during the saturation process, but the top lid was not. This is because some air was present in the cylinder when saturating the sample, and this air was pushed upwards when saltwater was added. Since the valves in the cell were closed, then the air could not escape, and it was left in the top lid. To be able to determine the total volume of sand sample in the cell the following expression was used:

$$V_s = A_{cell} L_s \tag{3.15}$$

Where V_s is the total volume of sand present in the cell [cm^3] and L_s is the length of the sand sample in the cell [cm]. Further, the weight of the saltwater column above the sand sample was calculated using the following expression:

$$V_{swc} = A_{cell} L_{swc} \tag{3.16}$$

Where V_{swc} is the volume of the saltwater column above the sand sample [cm^3] and L_{swc} is the length of the saltwater column above the sand sample [cm]. To determine the volume of salt water present in the sand sample the following expression was used:

$$V_{sws} = V_{sw} - V_{swc} \tag{3.17}$$

Where V_{sws} is the volume of salt water in the sand sample [cm^3]. Lastly the saturation of salt water present in the sample was calculated using equation 2.19, where V_w is in this case V_{sws}. Similar to the liquid permeameter method, one had to estimate the pore volume. This was done in the same manner as explained when calculating the saturation in the liquid permeameter, but the length of the sand sample was different. Then, saltwater saturation was calculated using equation 2.19 and the air saturation can be calculated by rearranging equation 2.21 with respect to S_g.

After having saturated the sand sample, the salt solution tank was disconnected from the bottom outlet of the Darcy-cell. The upper tank consisted of 3 inlets; saltwater-inlet, saltwater-outlet and an overflow drain. The saltwater inlet was connected with tubes to the salt solution tank, the saltwater-outlet was connected with tubes to the Darcy-cell inlet and the overflow drain was connected to a tube that was connected to a drain, allowing the excess saltwater to be channelled there.

Before starting the test, the upper and lower tanks were filled with salt solution until the solution reached the overflow tube (connected to the drain) in the upper tank, and until it reached the overflow tube in the lower tank, that channelled water into a beaker that measured volume of saltwater. LabView was opened and ran simultaneously when starting the test. Then, the valve in the salt solution tank was opened, the valve at the Darcy-cell inlet and outlet was opened and saltwater could flow from the upper tank, through the cell, and to the lower tank. Since the upper and lower water tank was continuously filled with saltwater, it was reasonable to assume that a constant hydraulic head was maintained in the system. This could be checked using the pressure sensors in the cell. The pressure difference from the bottom to the top of the cell was recorded in LabView and if the pressure difference was constant then it was reasonable to assume that the whole system was maintaining a constant hydraulic head. LabView also recorded the temperature versus time. The time it took to fill 200 mL in a measuring cup was recorded and from this it was possible to calculate the flow rate of the salt solution using equation 2.31. It is common to calculate the hydraulic conductivity using equation 2.32. However, in this setup, one did not use the head h_1 and h_2, but pressure sensors that calculated the pressure difference in the cell. So instead, the permeability of the sand sample was calculated using equation 2.23. Lastly, the hydraulic conductivity was calculated using equation 2.7.

3.6.1 LabView

The following subchapter gives an insight into how the pressure- and temperature sensors are connected to LabView. To be able to use LabView one must first let the program know what you want it to do. This is done by coding. The coding was performed by Senior Engineer Steffen Wærnes Moen while the logging of data was done by the author.

The pressure- and temperature sensors measure the pressure and temperature and convert this to 4-20mA signals that are scaled linearly with the range of the sensors. What is called a data acquisition unit (DAQ) from National Instruments, then measures the 4-20mA signal, and sends it to LabView. In LabView, the 4-20mA signal is calculated to actual pressure and temperature and writes the received data along with measured time into a text-file. LabView is in addition used to show real-time data.

4 Results

This chapter presents the results of this thesis. All symbols used in tables and figures are listed in the nomenclature.

4.1 Sieve analysis

The following subchapter presents the results gathered from the sieve analysis. The grain size distribution curve is presented in Figure 4.1. An overview of the parameters extracted from the grain size distribution curve are shown in Table 4.1. A complete overview of the raw data from the sieve analysis can be found in appendix A.

Table 4.1: Recorded values from the grain-size distribution curve.

Parameter	Value
d_{60} [µm]	330
d_{10} [µm]	140
Cu [-]	2,36

Figure 4.1 shows that most of the sand sample lies within the fraction medium sand. A cumulative percent finer by weight of 4 % lies within the fraction coarse silt, 27 % within the fraction fine sand, 62 % within the fraction medium sand and 7 % within the fraction coarse sand. Recorded values from the grain-size distribution curve shows that the uniformity coefficient for the sand sample is less than five, and is therefore categorized as “unified” sand.

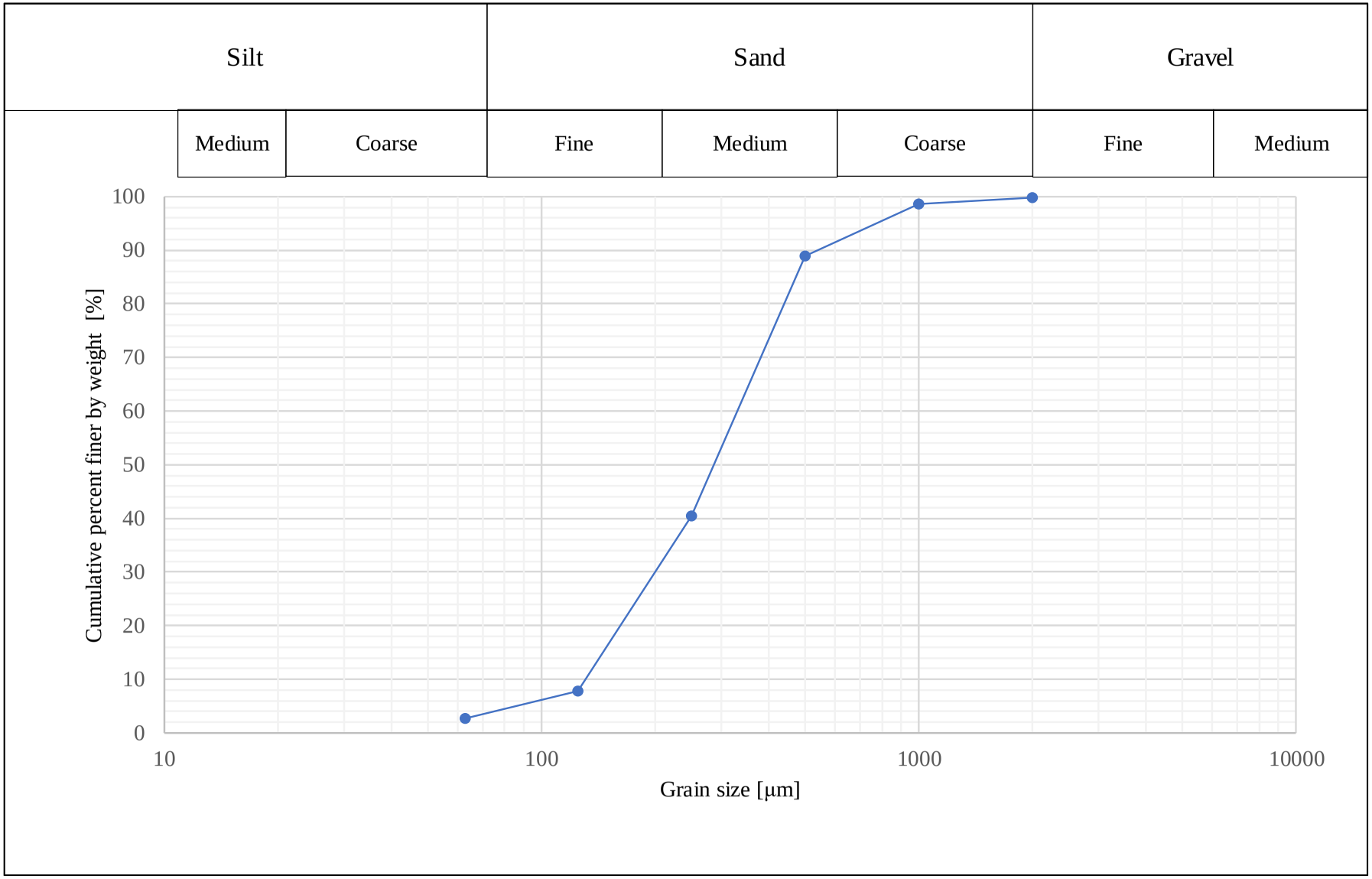

Figure 4.1: Grain-size distribution chart.

4.2 Density of salt solution

Table 4.2 shows the results from the density determination of the salt solution using a pycnometer. This salt solution was used in both the liquid permeameter test and the Darcy-cell test. The density of the salt solution is 0,99 g/cm^3 which is approximately equal to the density of water, 1,00 g/cm^3.

Table 4.2: Results from density determination of salt solution using a pycnometer.

Parameter	Value
V [cm^3]	50,38
m [g]	49,88
ρ [g/cm^3]	0,99

4.3 Effective porosity

The following subchapter presents the results from calculating the porosity of the sand sample using a helium porosimeter and by saturation. A complete overview of the raw data from the calculation of effective porosity can be found in appendix B.

4.3.1 Helium porosimeter

The results from calculating the porosity of the sand sample using a helium porosimeter is shown in Table 4.3.

Table 4.3:Results from calculation of effective porosity using helium porosimeter. V_1 is the volume of the empty matrix cup, V_2 is the volume of the matrix cup and sand sample, V_g is the volume of solid material, V_b is bulk volume, V_p is pore volume, $L_{cyl.\text{-}sample}$ is the length from the top of the sample inside the matrix cup to the top of the matrix cup. Further descriptions of symbols can be found in the nomenclature.

Sample	V_1 [cm^3]	V_2 [cm^3]	$V_g = V_1 - V_2$ [cm^3]	$L_{cyl.\text{-}sample}$ [mm]	L_S [mm]	L_S [cm]	V_b [cm^3]	V_p [cm^3]	n [%]
1,00	93,50	43,50	50,00	7,65	68,54	6,85	80,29	30,29	37,73
2,00	93,50	44,00	49,50	8,39	67,80	6,78	79,42	29,92	37,68
3,00	93,50	44,50	49,00	7,98	68,21	6,82	79,90	30,90	38,68
Avg.			49,5				79,87	30,37	38,03

An average grain volume of 49,5 cm^3 was obtained. Further, an average bulk volume of 79,87 cm^3 and average pore volume 30,37 cm^3 was obtained. The average effective porosity of the sand sample was estimated to 38,03 %.

4.3.2 Porosity by saturation

The results from calculation of effective porosity by saturation is shown in Table 4.4. A complete overview of the raw data from the calculation of porosity by saturation can be found in appendix C.

Table 4.4: Results from calculation of effective porosity by saturation. m_{cds} is the mass of the cylinder with dry sand, m_{cws} is the mass of the cylinder with wet sand.

Test	Cylinder	m_{cds} [g]	m_{cws} [g]	n [%]
1	1	194,71	219,34	41,71
	2	194,56	218,65	40,80
	3	194,29	217,63	39,53
Average				40,68
2	1	194,71	220,26	43,26
	2	194,56	219,93	42,96
	3	194,29	219,19	42,17
Average				42,80
2	1	194,71	220,23	43,21
	2	194,56	219,92	42,95
	3	194,29	219,25	42,27
Average				42,81
Total average				42,09

In test 1 an average porosity of 40,68 % is calculated. As mentioned in subchapter 3.5.3, the cylinders in test 2 were left to saturate in the exicator 2 times. After 1 hour in the exicator, the calculated average porosity of the sand sample was 42,17 %. After 3 hours in the exicator, the calculated average porosity of the sand sample was 42,81 %. This shows an increase in effective porosity of 0,64 % after 3 hours as opposed to 2 hours. The total average porosity is 42,09 %.

4.4 Saturation

The results from determination of saltwater- and air saturation in the liquid permeameter method is shown in Table 4.5. A complete overview of the raw data from the calculation of saturation can be found in appendix D.

Table 4.5: Results from saturation determination for the liquid permeameter method. m_{cds} is the mass of cylinder with dry sand, m_{cws} is the mass of cylinder with wet sand, m_{sw} is the mass of saltwater present in the sand sample, V_{sw} the volume of saltwater present in the sand sample, V_p the pore volume and S_{sw} and S_g are the saltwater- and air saturations respectively.

Test	Cylinder	m_{cds} [g]	m_{cws} [g]	m_{sw} [g]	V_{sw} [cm^3]	V_p [cm^3]	S_{sw} [%]	S_g [%]
1	1	194,71	219,34	24,63	24,63	26,52	92,90	7,10
	2	194,56	218,65	24,09	24,09	26,48	90,98	9,02
	3	194,29	217,63	23,35	23,35	27,18	85,88	14,12
Average							89,92	10,08
2	1	194,71	220,26	25,55	25,55	26,52	96,35	3,65
	2	194,56	219,93	25,37	25,37	26,48	95,81	4,19
	3	194,29	219,19	24,90	24,90	27,18	91,60	8,40
Average							94,59	5,41
2	1	194,71	220,23	25,52	25,52	26,52	96,23	3,77
	2	194,56	219,92	25,36	25,36	26,48	95,78	4,22
	3	194,29	219,25	24,96	24,96	27,18	91,83	8,17
Average							94,61	5,39
Total average							93,04	6,96

Test 1 gives a calculated average saltwater saturation of 89,92 %, and a calculated average air saturation of 10,08 %. Test 2, with cylinders saturated in the exicator for 1 hour, gives a calculated average saltwater saturation of 94,59 %, and a calculated average air saturation of 5,41 %. After 3 hours in the exicator, test 2 gives a calculated average saltwater saturation of 94,61 % and a calculated average air saturation of 5,39 %. The total average of all three measurements gives an average saltwater saturation of 93,04 % and an estimated air saturation of 6,96 %.

The results from saturation determination in the Darcy-cell method is shown in Table 4.6. For raw data, see appendix D.3 and D.4. Because of a lack of time, only one saturation measurement was made. The saltwater saturation is estimated to 91,98 % and the air saturation to 8,02 %.

Table 4.6: Results from saturation determination for the Darcy-cell method.

Parameter	Value
m_{cds} [g]	5114,83
m_{cws} [g]	6300,00
m_{sw} [g]	1185,17
V_{sw} [cm^3]	1185,17
V_s [cm^3]	537,24
V_{swc} [cm^3]	997,27
V_{sws} [cm^3]	187,90
V_p [cm^3]	204,29
S_{sw} [%]	91,98
S_g [%]	8,02

4.5 Core permeameter

The following subchapter presents the results for permeability using the core permeameter. First, the permeability of the metal filters is presented followed by the permeability results using the air permeameter. Lastly, the permeability results using the liquid permeameter is presented.

4.5.1 Filter permeability

The results for filter permeability is shown in Table 4.7. A complete overview of the raw data from the filter permeability tests can be found in appendix E.

Table 4.7: Results for metal filter permeability.

Cylinder	k [D]
1	0,79
2	3,78
3	5,55

The average permeability of the two metal filters in cylinder 1 is 0,79 D. For cylinder 2, the average permeability of the two metal filters is 3,78 D. Lastly, the average permeability of the two metal filters in cylinder 3 is 5,55 D.

4.5.2 Air permeameter

A summary of the results from the air permeameter test is shown in Table 4.8. This table shows the average value of total permeability and total hydraulic conductivity for cylinder 1 and 2, as well as the average values of permeability- and hydraulic conductivity in sand for cylinder 1

and 2. In test 1, cylinder 1 was packed with the bench press. In test 2 and 3 the cylinders were packed with a vibrator. A complete overview of the raw data from the air permeameter test can be found in appendix F.

The results show that, when packed with a bench press, the total hydraulic conductivity in cylinder 1 varies between $9{,}87 \times 10^{-6}$ m/s and $1{,}28 \times 10^{-5}$ m/s, and the hydraulic conductivity in sand varies between $9{,}99 \times 10^{-6}$ m/s and $1{,}33 \times 10^{-5}$ m/s. The average total hydraulic conductivity in cylinder 1 is $1{,}15 \times 10^{-5}$ m/s and the average hydraulic conductivity in sand is $1{,}18 \times 10^{-5}$ m/s.

When packed with a vibrator, the total hydraulic conductivity in cylinder 1 varies between $1{,}14 \times 10^{-5}$ m/s and $1{,}79 \times 10^{-5}$ m/s, the hydraulic conductivity in sand varies between $1{,}17 \times 10^{-5}$ m/s and $1{,}97 \times 10^{-5}$ m/s. In cylinder 2, the total hydraulic conductivity varies between $2{,}57 \times 10^{-5}$ m/s and $3{,}51 \times 10^{-5}$ m/s, and the hydraulic conductivity in sand varies between $2{,}49 \times 10^{-5}$ m/s and $3{,}47 \times 10^{-5}$ m/s. The average total hydraulic conductivity and the average hydraulic conductivity in sand for test 2 and 2 can be seen in Table 4.8.

Table 4.8: Average results from the air permeameter test. k_T is average total permeability, K_T is average total hydraulic conductivity, k_s is average sand permeability and K_s is average hydraulic conductivity of sand.

Test	Cylinder	Packing	k_T [D]	k_T [m^2]	K_T [m/s]	k_S [D]	k_S [m^2]	K_S [m/s]
1	1	Bench press	1,04	1,04E-12	1,15E-05	1,07	1,07E-12	1,18E-05
2	1	Vibrator	1,49	1,49E-12	1,64E-05	1,61	1,61E-12	1,78E-05
2	2	Vibrator	2,82	2,82E-12	3,11E-05	2,76	2,76E-12	3,05E-05
3	1	Vibrator	1,23	1,23E-12	1,35E-05	1,29	1,29E-12	1,42E-05
3	2	Vibrator	2,56	2,56E-12	2,82E-05	2,49	2,49E-12	2,75E-05

The percentage difference in total hydraulic conductivity and for the hydraulic conductivity in sand is shown in Table 4.9 and Table 4.10 and is based on all values for hydraulic conductivity in the raw data. When packed with the bench press, the percentage difference of the total hydraulic conductivity of the cylinder with sand is 25,64 % whilst it is 28,45 % for the hydraulic conductivity in sand. When packed with the vibrator, the percentage difference of the total hydraulic conductivity of cylinder 1 with sand is 44,91 %. For cylinder 2 the percentage difference is 31,14 %. The percentage difference for the hydraulic conductivity in sand is 51,22 % in cylinder 1 and 32,94 % in cylinder 2.

Table 4.9: Percentage difference in total hydraulic conductivity using air permeameter. Max. K_T is the maximum value of total hydraulic conductivity and min. K_T is the minimum value of total hydraulic conductivity from measurements.

Cylinder	Packing	Max. K_T [m/s]	Min. K_T [m/s]	Percentage difference [%]
1	Bench press	1,28E-05	9,87E-06	25,64
1	Vibrator	1,79E-05	1,14E-05	44,91
2	Vibrator	3,51E-05	2,57E-05	31,14

Table 4.10: Percentage difference in hydraulic conductivity in sand using air permeameter. Max. K_s is the maximum average value of hydraulic conductivity of groundwater in sand and Min. K_s is the minimum average hydraulic conductivity of groundwater in sand from measurements.

Cylinder	Packing	Max. K_S [m/s]	Min. K_S [m/s]	Percentage difference [%]
1	Bench press	1,33E-05	9,99E-06	28,45
1	Vibrator	1,97E-05	1,17E-05	51,22
2	Vibrator	3,47E-05	2,49E-05	32,94

4.5.3 Liquid permeameter

The graphical presentation of pressure difference versus time for cylinder 1-3 is shown in Figure 4.2, Figure 4.3, Figure 4.4 and Figure 4.5. The time it takes for the pressure difference to stabilise is longer for cylinder 1 than for cylinder 2 and 3. The value for pressure difference used to calculate the hydraulic conductivity of sand is chosen from the graphs. A value for each cylinder in measurement 1 and 2 is chosen when the pressure difference has stabilised. The values for pressure difference and the calculated total hydraulic conductivity and hydraulic conductivity in sand is shown in Table 4.11. A complete overview of the raw data from the liquid permeameter test can be found in appendix G.

The results show that the hydraulic conductivity in sand in cylinder 1 varies from $4{,}22 \times 10^{-7}$ m/s to $6{,}03 \times 10^{-7}$ m/s. For both measurement 1 and 2, the calculated hydraulic conductivity in sand in cylinder 2 is $2{,}41 \times 10^{-6}$ m/s. For cylinder 3, the value varies from $3{,}07 \times 10^{-6}$ m/s to $4{,}22 \times 10^{-6}$ m/s.

The percentage difference for the hydraulic conductivity in sand using the liquid permeameter is shown in Table 4.12. The percentage difference of the hydraulic conductivity in sand in cylinders 1-3 is 35,46 %, 0,00 % and 31,73 % respectively.

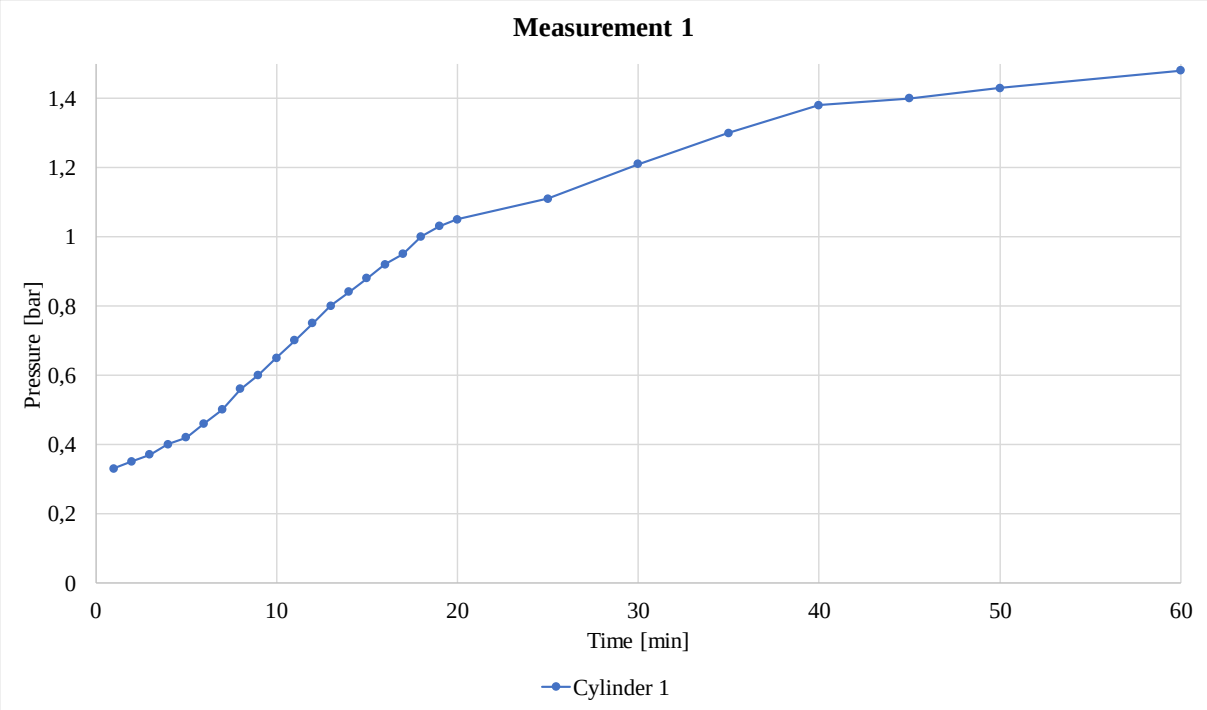

Figure 4.2: Pressure versus time for cylinder 1, measurement 1.

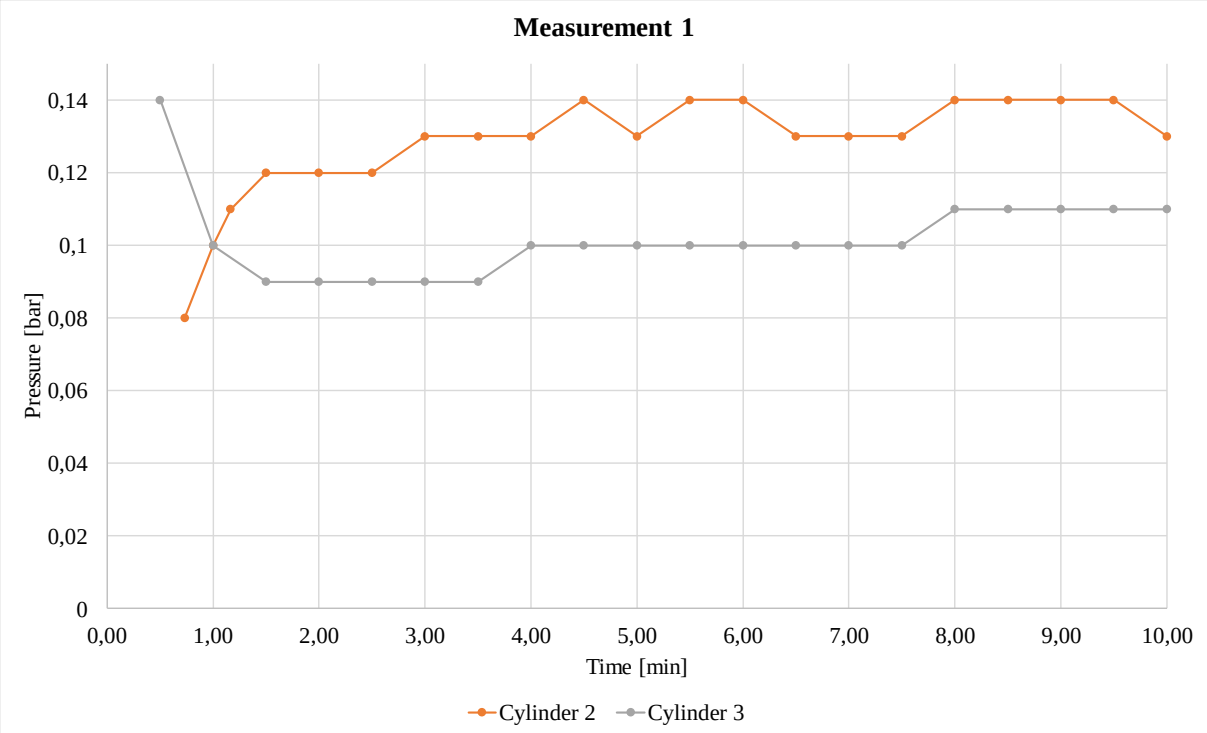

Figure 4.3: Pressure versus time for cylinder 2 and 3, measurement 1.

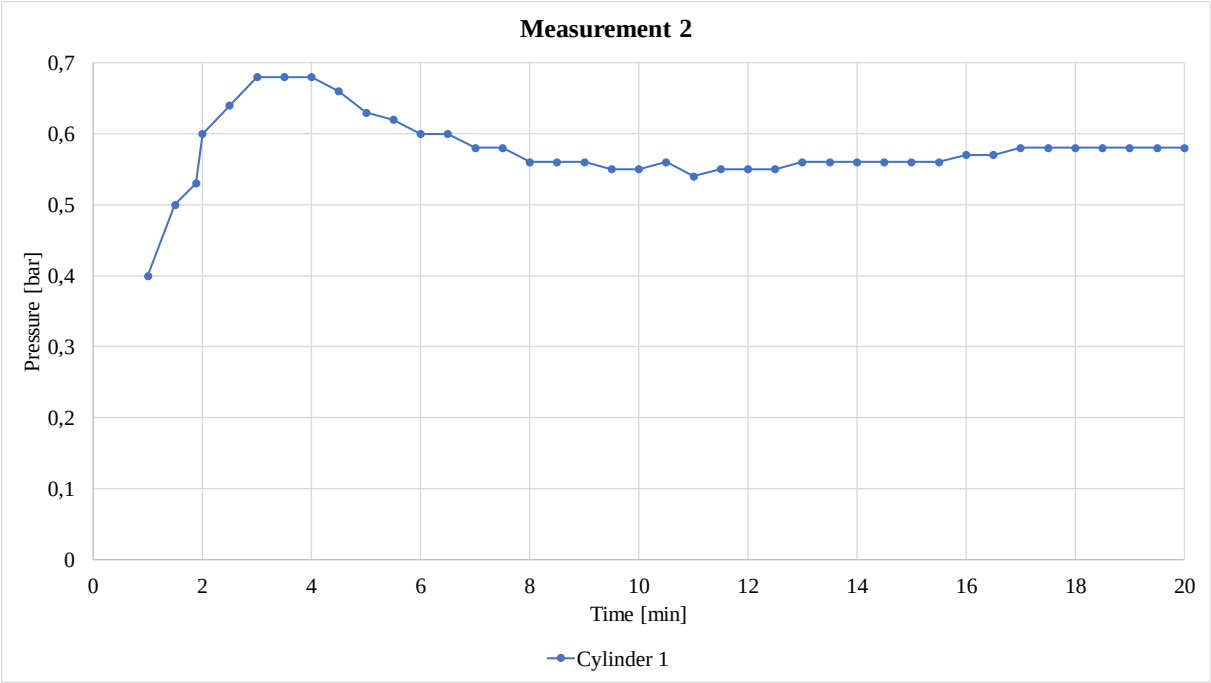

Figure 4.4: Pressure versus time for cylinder 1, measurement 2.

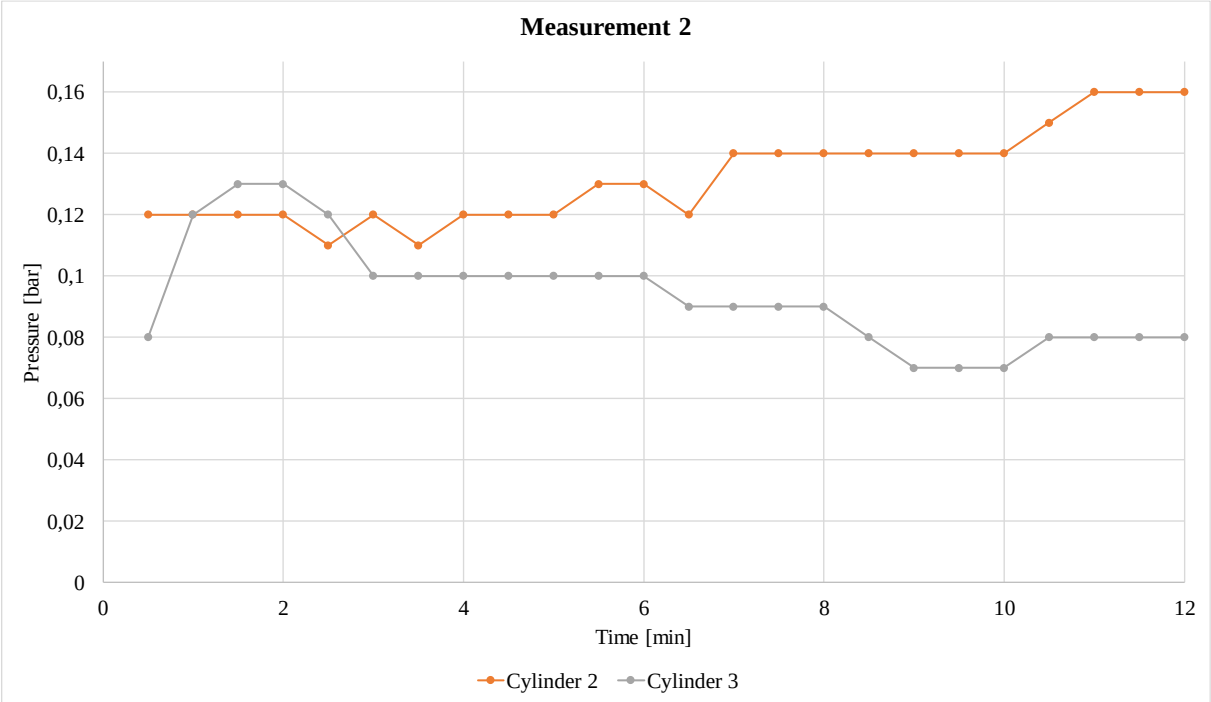

Figure 4.5: Pressure versus time for cylinder 2 and 3, measurement 2.

Table 4.11: Results for hydraulic conductivity in sand from the liquid permeameter method. Explanation of symbols is found in nomenclature.

Parameter	**Measurement 1**			**Measurement 2**		
	Cyl. 1	**Cyl. 2**	**Cyl. 3**	**Cyl. 1**	**Cyl. 2**	**Cyl. 3**
Δ_p [bar]	0,80	0,14	0,11	0,56	0,14	0,08
k_T [D]	0,04	0,24	0,30	0,06	0,24	0,41
k_T[m^2]	4,13E-14	2,36E-13	3,00E-13	5,90E-14	2,36E-13	4,13E-13
k_f [D]	0,79	3,78	5,55	0,79	3,78	5,55
k_f [m^2]	7,87E-13	3,78E-12	5,55E-12	7,87E-13	3,78E-12	5,55E-12
k_s [m^2]	3,83E-14	2,19E-13	2,78E-13	5,47E-14	2,19E-13	3,83E-13
K_s [m/s]	4,22E-07	2,41E-06	3,07E-06	6,03E-07	2,41E-06	4,22E-06

Table 4.12: Percentage difference in hydraulic conductivity in sand from liquid permeameter method. Explanation of symbols is found in nomenclature.

Parameter	**Cylinder 1**	**Cylinder 2**	**Cylinder 3**
Max. K_s [m/s]	6,03E-07	2,41E-06	4,22E-06
Min. K_s [m/s]	4,22E-07	2,41E-06	3,07E-06
Percentage difference [%]	35,46	0,00	31,73

4.6 SEM analysis

This subchapter presents the results from the SEM analysis. Figure 4.6 shows the photo generated during the secondary electron analysis (SE) method. The white areas are the charged particles while the grey areas are not charged. The darker grey areas represent pores in the filter.

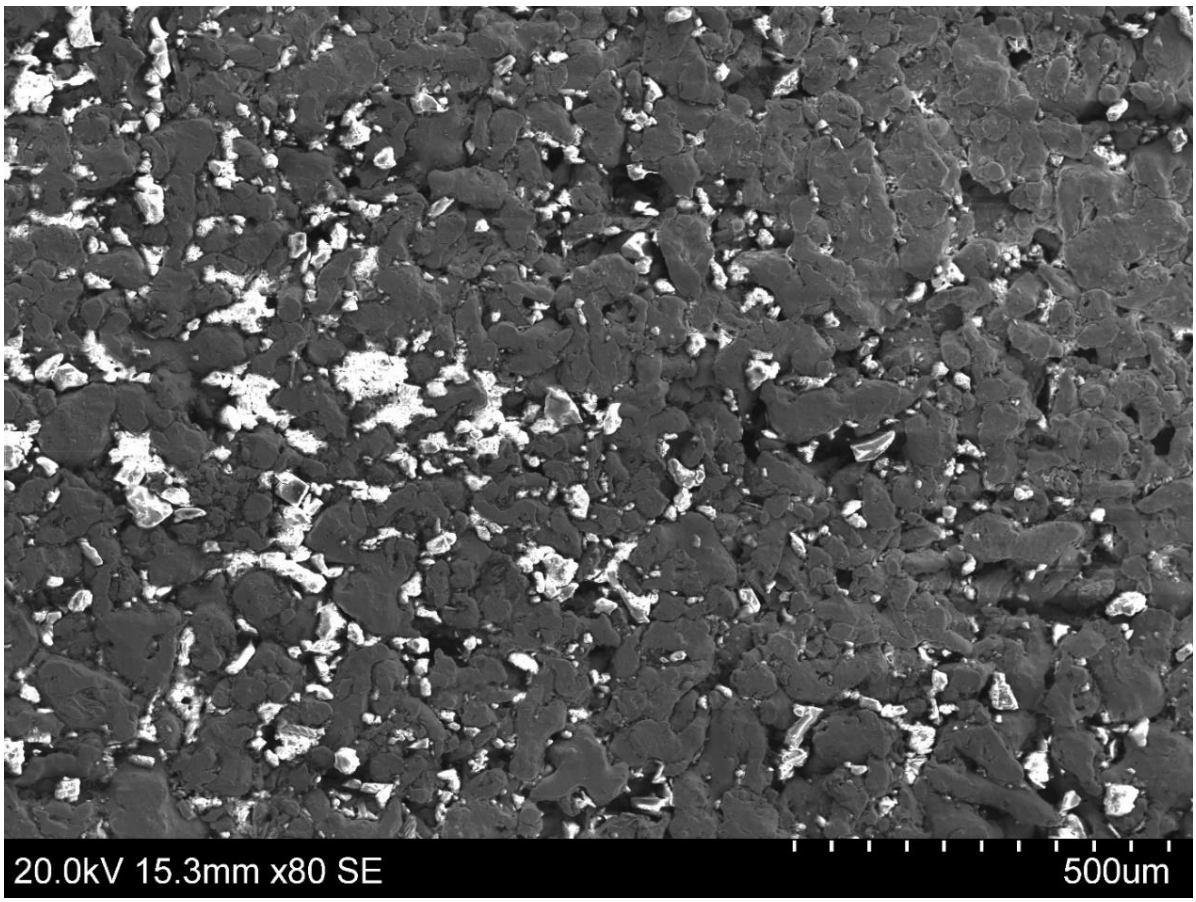

Figure 4.6: Photo generated using the secondary electron method during the scanning electron microscopy (SEM) analysis. The white areas are charged particles.

Figure 4.8 shows the generated photo from the energy-dispersive X-ray spectroscopy (EDS) analysis. The photo shows six marked points where each point gives the composition in that location. The composition of point 1 is shown in Figure 4.7. The graphs for points 2-6 can be found in Appendix H. A summary of the elemental composition of the 6 points is shown in Table 4.13. and Table 4.14. In general, points 1, 4 and 5 show an abundance of oxygen, silicon and aluminium, while points 2,3 and 6 show an abundance of iron, chromium and nickel.

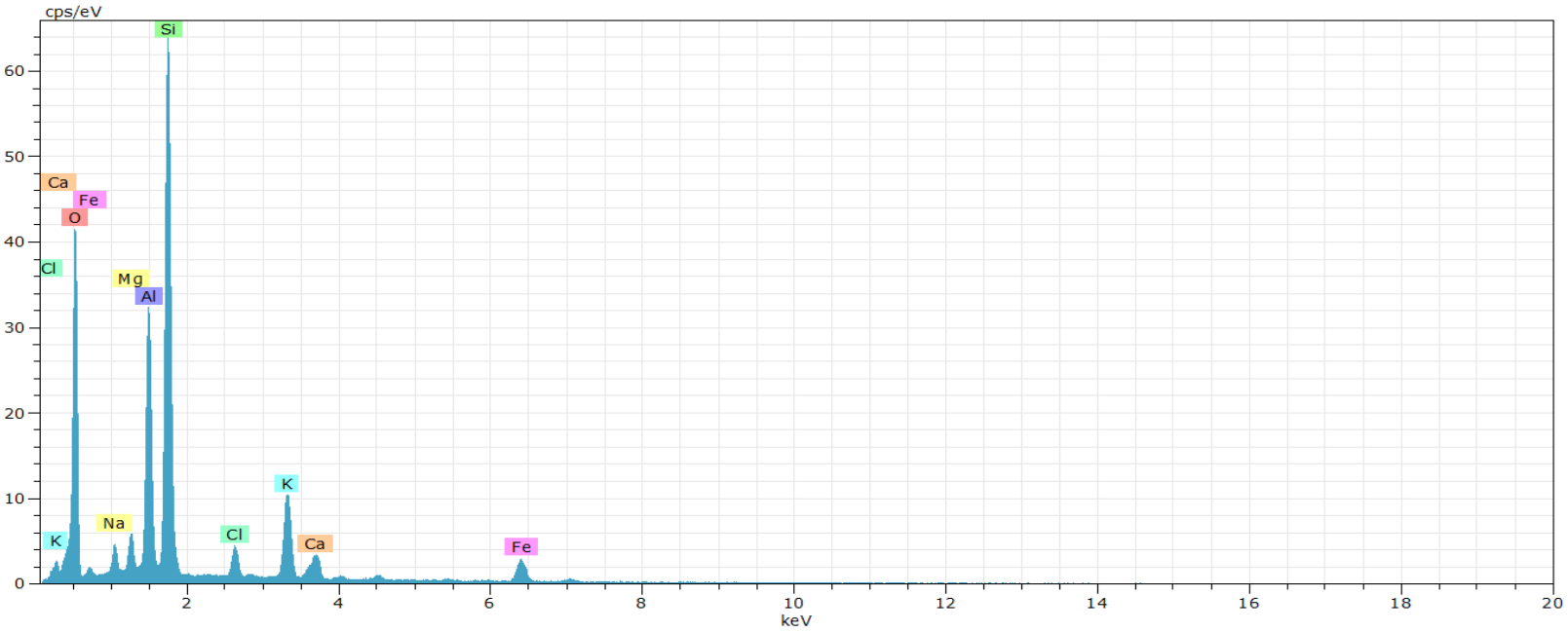

1 Date:29.05.2018 09:47:17 HV:20,0kV Puls th.:22,07kcps

El	AN	Series	unn. C [wt.%]	norm. C [wt.%]	Atom. C [at.%]	Error (1 Sigma) [wt.%]
O	8	K-series	42,47	48,74	64,52	5,38
Si	14	K-series	17,70	20,31	15,32	0,79
Al	13	K-series	9,81	11,26	8,84	0,50
K	19	K-series	5,22	5,99	3,25	0,19
Fe	26	K-series	4,78	5,48	2,08	0,18
Na	11	K-series	1,88	2,15	1,98	0,16
Mg	12	K-series	1,73	1,98	1,73	0,13
Ca	20	K-series	1,89	2,17	1,15	0,09
Cl	17	K-series	1,67	1,91	1,14	0,09
		Total:	87,14	100,00	100,00	

Figure 4.7: EDS composition results for point 1.

Table 4.13: Results from SEM analysis. Points 1-3.

Point	El	Unn. C [wt.%]	Norm. C [wt.%]	Atom. C [at.%]	Error (1 sigma) [wt.%]
1	O	42,47	48,74	64,52	5,38
	Si	17,70	20,31	15,32	0,79
	Al	9,81	11,26	8,84	0,50
	K	5,22	5,99	3,25	0,19
	Fe	4,78	5,48	2,08	0,18
	Na	1,88	2,15	1,98	0,16
	Mg	1,73	1,98	1,73	0,13
	Ca	1,89	2,17	1,15	0,09
	Cl	1,67	1,91	1,14	0,09
	Total	87,14	100,00	100,00	
2	Fe	59,61	66,74	58,21	1,62
	Cr	14,05	15,73	14,74	0,42
	Ni	10,22	11,44	9,49	0,33
	C	1,81	2,02	8,20	0,56
	O	1,72	1,92	5,85	0,38
	Si	1,02	1,14	1,98	0,08
	S	0,89	1,00	1,52	0,07
	Total	89,31	100,00	100,00	
3	Fe	56,28	63,38	51,57	1,53
	Cr	13,48	15,18	13,27	0,40
	O	3,01	3,39	9,62	0,57
	C	2,19	2,47	9,35	0,62
	Ni	9,73	10,96	8,49	0,31
	Si	1,34	1,51	2,45	0,09
	Al	1,18	1,32	2,23	0,09
	Na	0,78	0,88	1,74	0,10
	S	0,80	0,90	1,28	0,06
	Total	88,79	100,00	100,00	

Table 4.14: Results from SEM analysis. Points 4-6.

Point	El	Unn. C [wt.%]	Norm. C [wt.%]	Atom. C [at.%]	Error (1 sigma) [wt.%]
4	O	22,77	33,97	49,99	4,66
	Si	19,83	29,58	24,80	0,95
	Al	8,54	12,75	11,12	0,52
	K	10,62	15,85	9,54	0,40
	Fe	3,39	5,06	2,14	0,15
	Mg	0,64	0,96	0,93	0,11
	Na	0,50	0,74	0,76	0,11
	Cl	0,73	1,09	0,73	0,09
	Total	67,03	100,00	100,00	
5	O	30,35	39,63	54,44	4,22
	Si	21,84	28,51	22,31	0,97
	Al	11,85	15,47	12,61	0,60
	K	6,20	8,10	4,55	0,23
	C	0,70	0,92	1,67	0,44
	Fe	2,61	3,41	1,34	0,12
	Cl	1,50	1,96	1,22	0,09
	Mg	0,83	1,08	0,98	0,08
	Na	0,71	0,92	0,88	0,09
	Total	76,60	100,00	100,00	
6	Fe	61,48	65,89	58,78	1,67
	Cr	14,49	15,52	14,87	0,43
	Ni	11,56	12,38	10,51	0,37
	C	1,87	2,00	8,30	0,57
	O	1,46	1,57	4,88	0,35
	Si	0,95	1,02	1,81	0,08
	Mo	1,51	1,62	0,84	0,09
	Total	93,32	100,00	100,00	

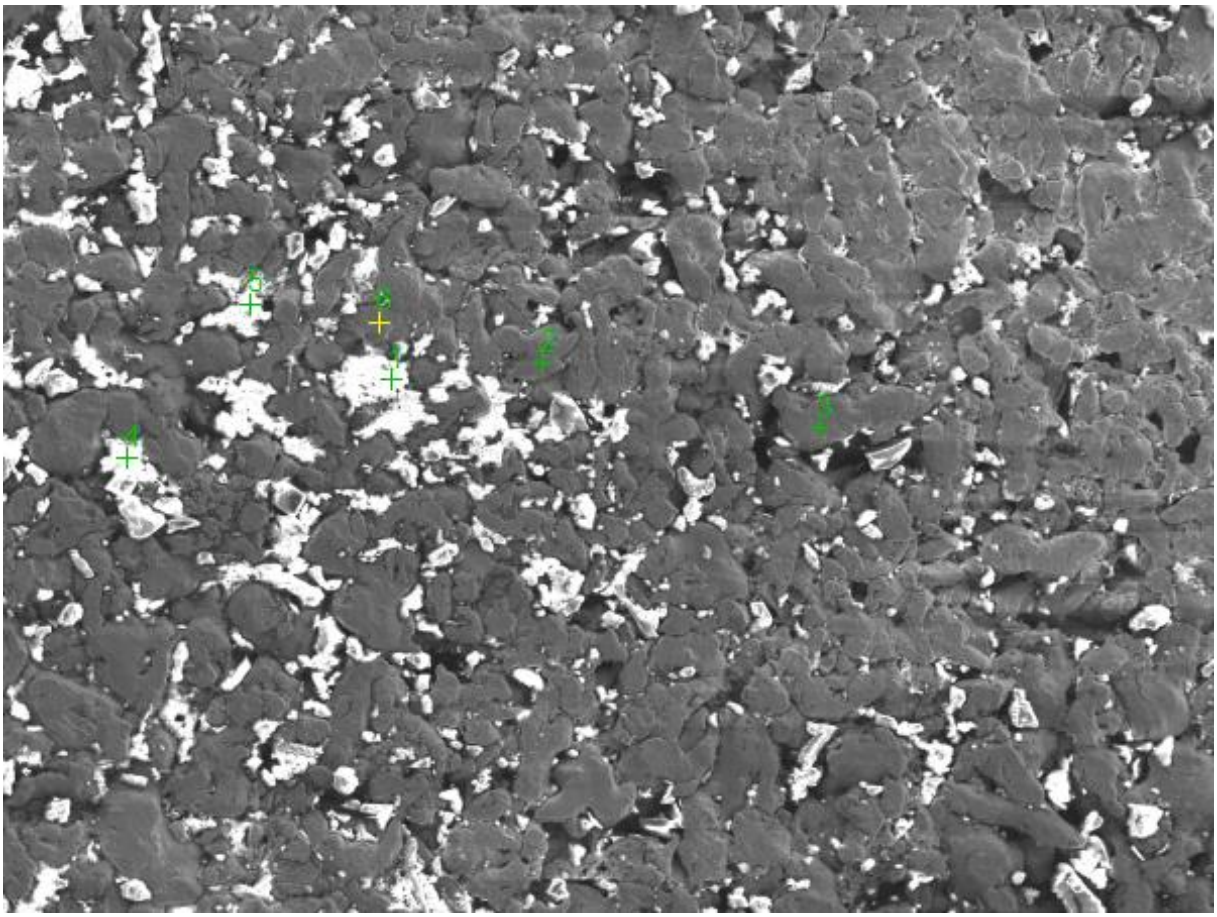

Figure 4.8: Result from the energy-dispersive X-ray spectroscopy (EDS) during the scanning electron microscopy (SEM) analysis. The composition is determined by placing 6 points on different areas of the metal filter.

4.7 Darcy-cell

The results for hydraulic conductivity in sand is shown in Table 4.15. Measurement 1-12 are not included in the results because LabView had a fault in the programming which led to these measurements displaying the wrong time. The estimated value of hydraulic conductivity in sand spans from $1{,}08 \times 10^{-3}$ m/s to $1{,}33 \times 10^{-3}$ m/s, where the average estimated value of hydraulic conductivity for all measurements is $1{,}26 \times 10^{-3}$ m/s. A complete overview of the raw data from the Darcy-cell method can be found in appendix I.

Table 4.15: Results from the Darcy-cell method. Explanation of symbols is found in nomenclature.

Measurement	t [s]	Δp [Pa]	Q [m^3/s]	K_{smin} [m/s]	K_S [m/s]	K_{smax} [m/s]	Uncer-tainty [%]
13	138,21	1800,00	1,45E-06	9,36E-04	1,08E-03	1,27E-03	30,17
14	130,41	1700,00	1,53E-06	1,04E-03	1,21E-03	1,44E-03	31,89
15	128,02	1700,00	1,56E-06	1,06E-03	1,23E-03	1,46E-03	31,91
16	127,12	1700,00	1,57E-06	1,07E-03	1,24E-03	1,47E-03	31,92
17	127,82	1800,00	1,56E-06	1,01E-03	1,17E-03	1,37E-03	30,29
18	123,61	1700,00	1,62E-06	1,10E-03	1,28E-03	1,52E-03	31,97
19	124,12	1700,00	1,61E-06	1,09E-03	1,27E-03	1,51E-03	31,96
20	123,51	1700,00	1,62E-06	1,10E-03	1,28E-03	1,52E-03	31,97
21	123,61	1800,00	1,62E-06	1,05E-03	1,21E-03	1,42E-03	30,34
22	122,21	1700,00	1,64E-06	1,11E-03	1,29E-03	1,53E-03	31,99
23	124,82	1800,00	1,60E-06	1,04E-03	1,19E-03	1,41E-03	30,33
24	124,53	1700,00	1,61E-06	1,09E-03	1,27E-03	1,51E-03	31,96
25	123,63	1800,00	1,62E-06	1,05E-03	1,21E-03	1,42E-03	30,34
26	121,34	1700,00	1,65E-06	1,12E-03	1,30E-03	1,55E-03	32,00
27	120,53	1700,00	1,66E-06	1,13E-03	1,31E-03	1,56E-03	32,01
28	122,71	1800,00	1,63E-06	1,05E-03	1,21E-03	1,43E-03	30,35
29	121,12	1700,00	1,65E-06	1,12E-03	1,30E-03	1,55E-03	32,00
30	120,72	1700,00	1,66E-06	1,12E-03	1,31E-03	1,55E-03	32,01
31	121,22	1800,00	1,65E-06	1,07E-03	1,23E-03	1,45E-03	30,37
32	120,33	1800,00	1,66E-06	1,07E-03	1,24E-03	1,46E-03	30,38
33	119,92	1800,00	1,67E-06	1,08E-03	1,24E-03	1,46E-03	30,39
34	120,12	1700,00	1,66E-06	1,13E-03	1,31E-03	1,56E-03	32,01
35	119,72	1700,00	1,67E-06	1,13E-03	1,32E-03	1,57E-03	32,02
36	120,33	1700,00	1,66E-06	1,13E-03	1,31E-03	1,56E-03	32,01
37	122,73	1700,00	1,63E-06	1,11E-03	1,29E-03	1,53E-03	31,98
38	119,02	1700,00	1,68E-06	1,14E-03	1,33E-03	1,58E-03	32,03
39	119,53	1700,00	1,67E-06	1,14E-03	1,32E-03	1,57E-03	32,02
40	119,92	1800,00	1,67E-06	1,08E-03	1,24E-03	1,46E-03	30,39

Measurement	t [s]	Δp [Pa]	Q [m^3/s]	K_{smin} [m/s]	K_S [m/s]	K_{smax} [m/s]	Uncer-tainty [%]
41	120,01	1700,00	1,67E-06	1,13E-03	1,32E-03	1,56E-03	32,02
42	120,53	1700,00	1,66E-06	1,13E-03	1,31E-03	1,56E-03	32,01
43	120,82	1700,00	1,66E-06	1,12E-03	1,31E-03	1,55E-03	32,00
Average	122,97	1732,26	1,63E-06	1,09E-03	1,26E-03	1,49E-03	31,45

K_{smin} and K_{smax} refer to the maximal and minimal hydraulic conductivity of sand that can be expected based on uncertainty in measurements. The calculations are based on the uncertainties shown in Table 4.16. The uncertainty of time and volume are estimates chosen by the author. The pressure and temperature uncertainties are given by the company Aplisens, that make the sensors. To calculate the maximum uncertainty, the uncertainties yielding the largest flow rate are inserted into equation 2.31. Similarly, the uncertainties yielding the largest value for permeability of sand is inserted into equation 2.23 and the values yielding the larges value for hydraulic conductivity of groundwater in sand is inserted into equation 2.7. A graphical presentation of the calculated hydraulic conductivity using the Darcy-cell, including the maximum and minimum values is shown in Figure 4.9.

Table 4.16: Uncertainty in measurements for the Darcy-cell method.

Measured parameter	Uncertainty [±]
Time [s]	1,00
V_{sw} [mL]	1,00
V_{sw} [m^3]	1,00E-06
Pressure [Pa]	250,00
Temperature [°C]	0,192

The percentage difference in the calculated hydraulic conductivity of sand is shown in Table 4.17. This calculation is based on the maximum and minimum calculated value of hydraulic conductivity in the results of Table 4.15.

Table 4.17: Percentage difference in Darcy-cell measurements.

Parameter	Value
Max. K_S [m/s]	1,33E-03
Min. K_S [m/s]	1,08E-03
Percentage difference [%]	20,59

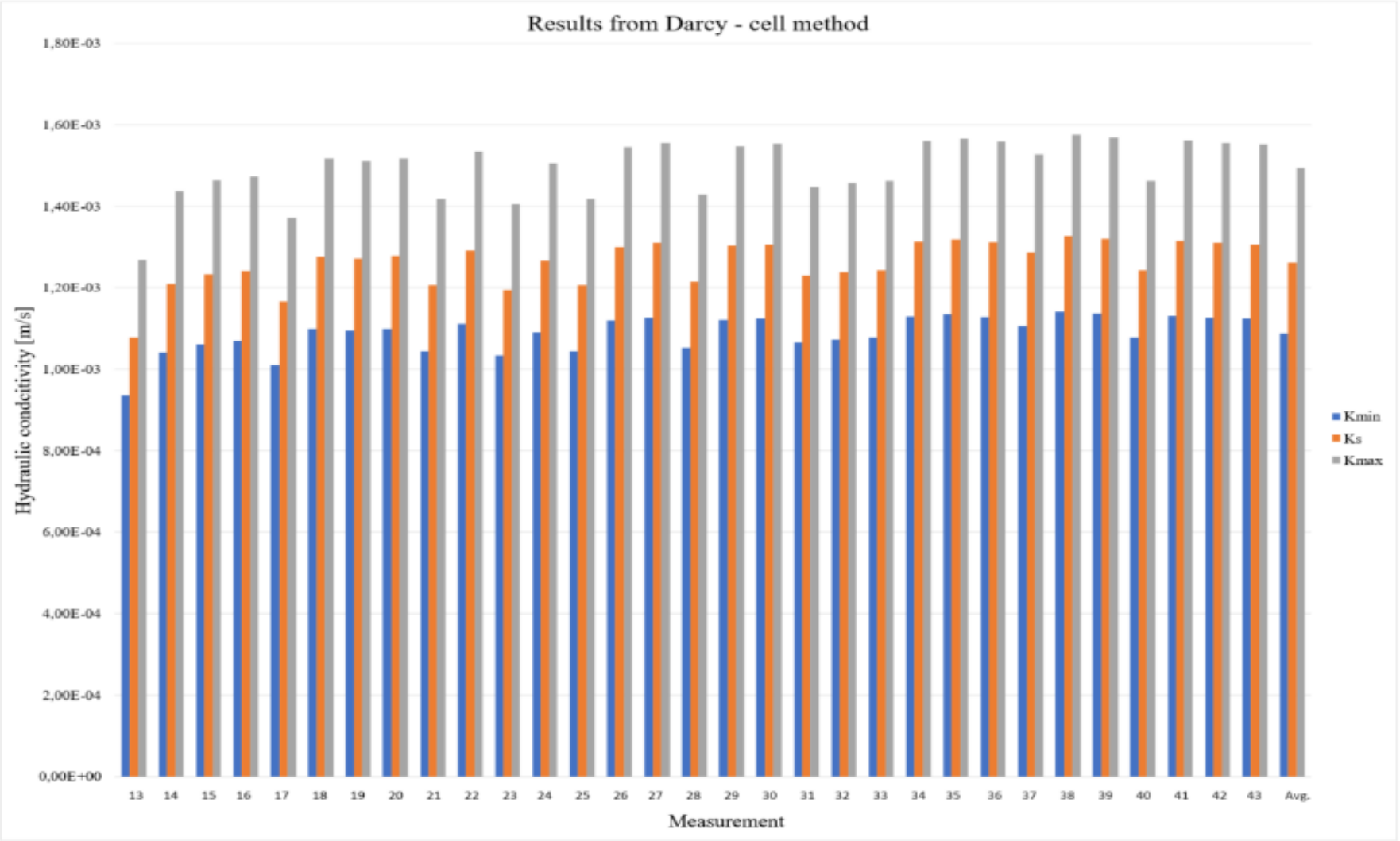

Figure 4.9: Results from Darcy-cell method. K_{min} and K_{max} refer to the minimum and maximum estimated value of hydraulic conductivity based on uncertainty in measurements.

4.8 Hydraulic conductivity results from all tests

Table 4.18 presents the estimated hydraulic conductivity from all permeameter tests.

Table 4.18: Comparison of hydraulic conductivity values for the 3 permeameters.

Permeameter type	**Cylinder**	**Packing**	**$K_{s\ water}$ [m/s]**
Air	1	Bench press	1,18E-05
Air	1	Vibrator	1,78E-05
Air	1	Vibrator	1,42E-05
Air	2	Vibrator	3,05E-05
Air	2	Vibrator	2,75E-05
Average		Vibrator	2,25E-05
Liquid	1	Vibrator	4,22E-07
Liquid	1	Vibrator	6,03E-07
Liquid	2	Vibrator	2,41E-06
Liquid	2	Vibrator	2,41E-06
Liquid	3	Vibrator	3,07E-06
Liquid	3	Vibrator	4,22E-06
Average			2,19E-06
Darcy – cell avg.	-	-	1,26E-03

5 Discussion

The results for the 3 methods is shown in Table 4.18. The smallest average value of hydraulic conductivity is calculated using the liquid permeameter with a value of $2{,}19 \times 10^{-6}$ m/s, followed by the air permeameter with a value of $2{,}25 \times 10^{-5}$ m/s. The largest value was calculated using the Darcy-cell with an average value of $1{,}26 \times 10^{-3}$ m/s. What is apparent from these results is that they give large variations of hydraulic conductivity. The hydraulic conductivity calculated using the air permeameter is 100 times lower than when using the Darcy-cell and, what is more, the hydraulic conductivity calculated using the liquid permeameter is 1000 times smaller than the values calculated using the Darcy-cell. It is difficult to explain why these values are so different and the most apparent conclusion is that it is not possible to use the modified core permeameter to estimate the hydraulic conductivity of groundwater in unconsolidated sand.

The calculated hydraulic conductivity using the air- and liquid permeameters both show significantly lower values compared to the Darcy-cell. There is little purpose in trying ty compare the hydraulic conductivity obtained using the core permeameters with the Darcy-cell when the values are 1000 times apart from the lowest to the highest calculated hydraulic conductivity. It is however, useful to compare and discuss the calculated values obtained from the core permeameters and discuss the Darcy-cell results separately.

The Darcy-cell method is a commonly used method for estimation of hydraulic conductivity of groundwater in unconsolidated sand. This method is also the one that has been modified the least in this thesis. The modifications done to the existing Darcy-cell are not drastic and should in theory not produce large errors to the calculated hydraulic conductivity. The conclusion is therefore that the Darcy-cell method produces results that are reliable and could be used as an estimation of what the "in-situ" hydraulic conductivity of groundwater in an undisturbed unconsolidated sand in the field could be.

The results from the sieve analysis, see Figure 4.1 for the grain-size distribution chart, show that most of the sand sample lies within the fraction medium sand. A cumulative percent finer by weight of 4 % lies within the fraction coarse silt, 27 % within the fraction fine sand, 62 % within the fraction medium sand and 7 % within the fraction coarse sand. Medium sand has an expected hydraulic conductivity between 10^{-3}-10^{-5} m/s, see Table 2.3. The calculated hydraulic conductivity obtained using the air permeameter and the Darcy-cell lie within this range, but

not the values calculated using the liquid permeameter. The calculated hydraulic conductivity obtained using the liquid permeameter is in the order 10^{-6} m/s, which is within the range fine sand, and is 10 times lower than the lowest expected value for medium sand.

The values calculated using the air permeameter show that the average hydraulic conductivity when using the bench press to pack the sand sample is $1{,}18 \times 10^{-5}$ m/s as opposed to $2{,}25 \times 10^{-5}$ m/s when using the vibrator. When using the bench press, a weight of 1 ton is applied onto each layer of sand when it is added to the cylinder. This weight can have forced the grains to pack close together and thus have reduced the pore space in the sample. It is possible to test this theory by measuring the weight of the cylinder with the sand sample after packing it with the bench press and compare this weight with the weight of the cylinder and sand sample after packing it with the vibrator. If the weight of the sample using the bench press is higher than the weight of the sand sample when packing it with the vibrator, it means that one has been able to pack more sand into the cylinder with the bench press. If more sand is present in the cylinder after using the bench press, then this results in smaller pore spaces in the sand and causes water to flow slower through the sample. This consequently leads to a lower calculated hydraulic conductivity. The weight of the sand sample packed with a bench press was not recorded because the author thought of doing this after the tests had been conducted. As explained in subchapter 3.5.2, all subsequent tests with the cylinders were packed using a vibrator.

5.1 Sedimentary dispersion

Prior to the core permeameter tests, a vibrator is used to pack the sand sample in the cylinders. From observations made during the packing process, it seems that the vibrator causes the grains to pack closely together. It was assumed that this method of packing simulated the compaction grade in the field quite well. One issue that could arise by using the vibrator is that sediments can move during the packing process. Whether sedimentary dispersion occurs in the sample is hard to determine because one is not able to see the sand sample when it is in the core holder, which means one is not able to determine if any sediment is moving in the sample. When applying vibrations onto the sample, the finer sediments could potentially migrate through the pore system of the sample and therefore not represent the grade of packing one would expect in the field. The fines that migrate could potentially block some pore spaces, and when fluid is flooded through the sand sample, block the fluid flow. This in turn could affect the calculated hydraulic conductivity.

Sedimentary dispersion can also have occurred during the flooding process, both when using air and saltwater. The sieve analysis shows that a fraction of 27 % fine sand is present in the sample. When flooding the sand sample with air, one can cause this finer material to move with the flow of air through the sample. Similar to when using the vibrator, finer material can get stuck in pore throats that are too small for the fines to pass. Some material may even move all the way to the metal filter at the outlet. If finer material blocks some of the pore throats, then air or saltwater will not be able to flow through these, and this will ultimately lead to a lower flow rate and give an underestimation of hydraulic conductivity.

During the air permeameter test, some fines were observed collecting on the metal filter at the outlet. It is however unsure if fines had collected in the pores of the filter, since this observation was based on the naked eye. When fines collect on the surface of the filter, it is possible that some of the sediments also travel into the pores of the filter and block some of the pore throats in the same manner as in the sample. No attempt was made at finding a method to determine if fines had collected in the pores of the filter when using the air permeameter. However, an even more apparent collection of fines was observed at the filter at the outlet when using the liquid permeameter and in this case, it was decided to use scanning electron microscopy (SEM) to determine if the fines had travelled into the pore system of the filter. A hypothesis is that the charged areas on the metal filter during the SEM analysis are sand grains blocking the pores of the metal filter. The energy-dispersive X-ray spectroscopy (EDS) determines the composition of the charged areas and the grey areas, as seen in Figure 4.7, Figure H.1, Figure H.2, Figure H.3, Figure H.4 and Figure H.5. From this, one can determine that the charged areas, points 1, 4 and 5 contains an abundance of oxygen, silicon and aluminium in general, while the grey areas, points 2, 3 and 6 show an abundance of iron and chromium and nickel. As is explained by Sepp S. (2013), sand is known to contain a lot of oxygen and silicon in the form of quartz minerals and it is natural to assume that the charged areas are indeed sand grains. It is unknown what type of metal is present in the filters but one can assume that the points 2, 3 and 6 are parts of the metal filter, since the metals iron and nickel are most prominent in the areas marked by the points. With these results, one can conclude that finer material does migrate through the sand sample and that some fine material reaches the metal filter at the outlet, blocking some pores in the metal filter. The blockage of these pores directly affects the flow rate of the saltwater and this could contribute to the lower calculated hydraulic conductivity using the liquid permeameter as opposed to the air permeameter.

The migrated grains are likely a cause of insufficient packing of sample when using the vibrator in both the air and liquid permeameter. In addition to this, during the liquid permeameter test, some of the sediments are more prone to reacting with liquid than with air. As explained by Zolotukhin & Ursin (2000), one assumes no reactions between the fluid and the porous medium when performing the liquid permeameter test. However, as Zolotukhin & Ursin (2000) also points out, liquid can sometimes interact with the porous rock and give other calculated values of permeability and thus also hydraulic conductivity. This fluid rock interaction could be a potential cause of the difference in calculated hydraulic conductivity when using the liquid permeameter as opposed to the air permeameter. Clay minerals can have interacted with saltwater during the liquid permeameter test, and this is a fluid rock type interaction. As explained in subchapter 2.3, the sand sample used in this thesis does not have any swelling clay minerals in it, however it is known to contain some non-swelling clay minerals. The non-swelling clay minerals can interact with the salt water and flow through the sand sample and get attracted to the grain surfaces as they travel through the sample. This can cause the pore throats to get thinner, restricting the flow of saltwater, or in some cases totally block the pore throats, not allowing any salt water to pass.

It should be noted that sedimentary dispersion alone cannot cause the results from the liquid permeameter to be 1000 times lower than those of the Darcy-cell. The sedimentary dispersion along with the clay interaction during the liquid permeameter test could however, explain why the calculated hydraulic conductivity using the liquid permeameter is 10 times lower than when using the air permeameter.

To try and prevent sedimentary dispersion and sufficiently pack the sample, it is suggested to create a device that allows for packing of the sample in the cylinder in a similar manner to the method used in this thesis, but it should be possible to screw the top filter onto the cylinder and at the same time push the sand in the cylinder and thus keeping it in place. This could prevent gaps in the sample from forming during the test. One could draw inspiration from the consolidation-cell described in subchapter 2.4.1.

Sedimentary dispersion could also be an issue when performing the Darcy-cell experiment. The cell wall is see-through so it is, to a larger extent, possible to determine if sediments move within the sample during the test. No observations of fines migrating in the sand sample were made during the tests. Although no migration of sediments was observed, fines could have migrated in the middle of the sample, and this would not be possible to see from the outside of

the cell. However, one did observe some fine sediments escaping through the metal filter on the top of the sand sample when saturating it with saltwater. In addition, the salt solution used in the Darcy-cell method is the same as for the liquid permeameter. This means clay minerals interacting with the grains is a possibility in this method as well.

5.2 Saturation

In the liquid permeameter test, Zolotukhin & Ursin (2000) explains that one assumes a fully saturated sample with fluid before the start of the test. In theory, if the sand sample in the liquid permeameter test is fully saturated with saltwater, the two values obtained from the air- and liquid permeameters would be similar. The difference in hydraulic conductivity in the 2 methods could be because the sand sample in the liquid permeameter test is not fully saturated with saltwater, see the results from the saturation determination in Table 4.5. The average saltwater saturation in the sand sample is 93,04 %, meaning that the remaining pore spaces in the sand sample is filled with air, with an average air saturation of 6,96 %. Hillel (2008) explains that encapsulated air can block pore passages. If the trapped air in the saltwater saturated sand sample is in pore spaces that blocks water flow, then the presence of air in the sample can reduce the flow rate of saltwater. However, it should be noted that one does not know where in the pore system of the sample the air is situated. If the air is in pores that do not affect the flow of water thorough the sample, then the estimated hydraulic conductivity does not necessarily have to be affected by the presence of air. However, since the percentage of air present in the sample is quite high, at an average of 6,96 % of total pore volume, it is reasonable to assume that some air will be in pores that do affect the flow of water. In a dry sand sample, as is the case in the air permeameter, air will flow freely through these pores. If the air in the sand sample does block the saltwater flow through the sample, one would expect the hydraulic conductivity values estimated using the liquid permeameter to be lower than the values of hydraulic conductivity using the air permeameter. The calculated hydraulic conductivity is around 10 times less when using the liquid permeameter, and the air present in the sand sample cannot alone explain this large difference. However, in combination with the discussed sedimentary dispersion in subchapter 5.1, it could explain the difference in values between the liquid and the air permeameter.

An air pocket at the end of the sample can also affect the calculated hydraulic conductivity using the liquid permeameter. This pocket can arise when the sample is saturated with salt water in the exicator. When salt water enters the pore system of the sand sample, the grains that are

held in place only by each other can collapse causing the whole sample to compact further. This can cause an air pocket to develop in the top of the cylinder when it is in the exicator. If the sample is packed further, then the effective volume in the sample can be reduced. The saltwater has less flow lines to follow so the flow rate is reduced. This ultimately leads to an underestimation of the hydraulic conductivity. It is not possible to determine whether the grains change places during the saturation of the sample since the cylinder is not see-through. However, the Darcy-cell is packed using the same procedure as when packing the sand sample in the cylinders. The cell-wall in the Darcy-cell is see-through and one is therefore able to determine if the sand level is reduced in the cell after having saturated the sand sample. The level at which the sand was packed was marked on the cylinder, prior to the saturation of the sample. Once the sample had been left to saturate for 1 hour, the sand level was recorded again. The results showed that the levels before and after saturation were the same. If one assumes that the same occurs during the liquid permeameter test, then it is reasonable to think that the level of sand will stay unchanged also here. However, after the liquid permeameter test was performed, one did observe a small air pocket at the side of the sand sample inside the cylinder during one of the measurements. It is uncertain whether this air pocket was caused during the saturation process and the flooding or if it was caused by removing the filter from the cylinder after the test was finished. Also, air pockets were not looked for in the other liquid permeameter measurements and one cannot say for sure if air pockets were present in more than one measurement.

One argument that supports the existence of air pockets during the saturation process is the estimated porosity by saturation. If the calculated effective porosity determined using the helium porosimeter is compared with the porosity determined using the porosity by saturation method, one sees that the porosity is 38,03 % and 42,09 % for the two methods respectively, see Table 4.3 and Table 4.4. If an air pocket is present at the end of the sample in the cylinder, then it will be filled with salt water when the sample is saturated in the exicator. The difference in the dry and wet weight of the sample will therefore be an overestimation. This in turn causes an overestimation of porosity by saturation and could explain why the porosity using the helium porosimeter and the porosity by saturation is different. If air pockets are present during the liquid permeameter test, then this can explain why the calculated hydraulic conductivity is 10 times lower for the liquid permeameter than for the air permeameter. The air pocket can totally dominate the flow line and greatly affect the flow rate. If this is the case, then the underestimation of hydraulic conductivity is within reason for the liquid permeameter method.

When performing the Darcy-cell test one assumes the sand sample in the cell to be fully saturated with saltwater. To better the chances of a fully saturated sample one applies vacuum onto the cell prior to the saturation process. Because of the vacuum in the cell, the pore spaces more easily pull on the water, allowing for the whole sample to be saturate in both a quicker and more reliable manner than saturating the sample with no vacuum. As mentioned in subchapter 3.6, the pressure display on the vacuum pump showed a pressure of 120 mbar as opposed to a pressure of 90-100 mbar which is common in the exicator. This meant that it was not possible to reach the same level of vacuum as one normally reaches in the exicator. This is because the Darcy-cell is not specifically designed for vacuum and accordingly contains some leakage points. Thus, the pressure achieved in the cell is higher than for the exicator. Not being able to apply a complete vacuum on the cell could lead to one not being able to saturate the sand sample fully. If air is present in the pore spaces of the sample, then the flow could be affected in a similar manner as for the sand in the liquid permeameter. The results for the saturation of the Darcy-cell is shown in Table 4.6. The estimated saltwater in the sample is 91,98 % while the amount of air present in the sample is estimated to 8,02 %. The air present in the sand sample is higher in the Darcy-cell method than for the liquid permeameter method but the calculated hydraulic conductivity is 1000 times higher in the Darcy-cell method than for the liquid permeameter. One can therefore conclude that the presence of air alone cannot be the cause of such a difference in hydraulic conductivity. Air pockets were not observed in the Darcy-cell and it is more likely that these air pockets in combination with sedimentary dispersion can result in the large difference in hydraulic conductivity between the liquid permeameter and the Darcy-cell.

According to Chapuis (2012) the hydraulic conductivity will increase by a factor of 4 if the sample increases from a water saturation of 80 % to 100 %. Therefore, methods of fully saturating the sand sample needs to be further investigated in both the liquid permeameter- and the Darcy-cell method.

5.3 Boundary effects

Boundary effects can affect the calculated hydraulic conductivity of sand. As described in subchapter 2.2.2, Chapuis (2012) explains that the inner diameter of the permeameter must be eight to ten times the largest grain diameter in the sample. If one applies the requirement set in this thesis, then the inner diameter of the cylinder or cell, must be ten times the largest grain diameter of the sample. In the core permeameter methods, the inner diameter of the cylinder is

35,5 mm and the largest grain diameter is between 2 mm to 4 mm. Because of a lack of time, one was not able to determine if the largest grain diameter was closer to 2 mm or 4 mm. If one assumes the grain diameter to be the largest of the two, 4 mm, then the inner diameter of the cylinder has to be 40 mm. The inner diameter of the cylinder is as mentioned, 35,5 mm and is less than the minimum diameter in the requirement. This means that if the largest grain diameter is 4 mm in the sand sample, then grains in the sample are affected by the "wall effect" further into the sample than is recommended by the requirement. The "wall effect" is caused by the wall of the cylinder pushing on the grains close to the wall. These grains will in turn apply a force on the neighbouring grains. This exchange of forces continue until one reaches a certain point in the sample. As long as one has a large enough inner diameter, then the grains and subsequently the flow of air, will not be affected in the middle of the sand sample. However, with the inner diameter being smaller than 40 mm, then the flow in the middle of the sample could be affected by the "wall effect". Although, one does not know if the largest grain diameter is 2 mm or 4 mm and therefore does not know for sure if the grains in the middle of the sand are affected by the "wall effect" or not. One can therefore not say with certainty that boundary effects cause the underestimation of hydraulic conductivity in the core permeameters. Even if there are boundary effects in the samples, these effects alone do not explain the large difference in calculated hydraulic conductivity between the core permeameters and the Darcy-cell.

The reason why the inner diameter of the cylinder was chosen to be 35,5 mm is because the largest outer diameter possible for the cylinder is 38,1 mm. The core holder which the cylinder is inserted into, has an inner diameter of 38,1 mm and does not allow for cores, or in this case, a cylinder of outer diameters exceeding this value. It is suggested to increase the inner diameter of the cylinder to meet this requirement. However, an increase in inner diameter will make it impossible to place the cylinder in the existing core holder. One would therefore have to increase the dimensions of the core holder to make it possible to place the cylinder inside it. Increasing the dimensions of the core holder is not very realistic, since it is originally made to test cores with a standard outer diameter of 38,1 mm. An increase in inner diameter of the core holder will therefore not make it possible to test standard core samples in the modified apparatus. Changing the soil type one wants to test is a more realistic approach. If one chooses a soil that contains a maximum grain diameter of 3 mm then the minimum inner diameter of the cylinder can be 30 mm. The existing cylinder has an inner diameter of 35,5 mm and by changing the soil type one thus meets the requirement. The existing inner diameter of the

cylinder will therefore create a restriction as to what type of soil type can be tested using the modified core permeameter, with 3 mm being the maximum allowed grain size in the sample

If one applies the requirement to the Darcy-cell, then the minimum inner diameter of the Darcy-cell can be 40 mm. The chosen inner diameter of the Darcy-cell is 64 mm and is thus larger than the minimum given by the requirement. It is therefore reasonable to assume that the "wall-effect" will not affect the grains in the middle of the sand sample. Further, the flow rate of saltwater in the sample should not be significantly affected by the "side-wall" effect and the same applies for the estimated hydraulic conductivity of sand.

5.4 Filter permeabilities

The metal filter permeabilities are different for the 3 cylinders used in the air permeameter method. As shown in Table 4.7, the metal filters in cylinder 1, 2 and 3 have an average permeability of 0,79 darcy, 3,78 darcy and 5,55 darcy respectively. The reason why filters of different permeabilities were used was because there were no equal filters at hand at the institute. An attempt at ordering new metal filters with equal permeabilities was made, but the delivery time was too long so the order was not sent.

The metal filters used for the core permeameters do in general provide a high uncertainty in the calculated hydraulic conductivity values. The permeability of the filters was not known prior to the core permeameter tests. This meant that the permeability had to be estimated using the TopIndustrie permeameter. As mentioned in subchapter 3.5.1, it was assumed that the permeability of the filters was all equal, and one was therefore able to calculate the permeability of the filters belonging to the 3 cylinders using the theory of flow in series, as described in subchapter 3.1. However, the calculations showed that the permeability of the metal filters in the cylinders were not equal, ranging from 0,79 darcy, 3,78 darcy and 5,55 darcy for cylinder 1-3 respectively. As was mentioned in subchapter 5.3, fine sediment was found clogging the pores of the metal filter in the air- and liquid permeameter methods. Sedimentary dispersion is likely a large cause of this, but it is also very likely that the metal filters used in the modified core permeameters were not adequate.

5.5 Pressure- and temperature sensors in the modified Darcy-cell

The following paragraph discusses the use of pressure sensors in the modified setup of the Darcy-cell as opposed to the manometers used in the original setup. One of the reasons for choosing pressure sensors instead of manometers is to make it easier to pack the sand sample in the cell. When no manometers are present, then no nozzles extend into the cell and one is able to pack the sample equally. This contributes to a higher compaction grade and also makes it less likely for sand grains to migrate through the sample. Further, since the pressure readings are logged automatically in LabView, the addition of pressure sensors make recording the pressure in the cell easier than if one has to read the head from the manometers manually. In addition, LabView in itself makes it easier to record pressure, plots the pressure versus time directly into a text-file, and allows for the user to see the real-time data on the PC screen. Also, the text-file can be easily exported to Excel or Matlab for analysis. The pressure sensors do have an uncertainty of ±250 Pa which needs to be discussed. Although this range is quite small, it can affect the estimated hydraulic conductivity significantly. The manometers on the other hand, allows for one to measure the head quite exact because on read the height of the water column by the millimetre. The downside here is that human error when recording the height of the water column could lead to recorded values that are incorrect. In addition, one is able to determine when the system has stabilized, because the levels in the manometer becomes constant once stabilization is reached. Since the manometers do provide accurate readings of head when measured correctly, a suggestion to further modification is to use a T-connection where the pressure sensor is located in the modified setup. The T-connection will allow measurements of the pressure with the sensor as well as measurements of the head using the manometers. This makes it possible to compare the values obtained from the pressure sensor with the manometer and also makes it possible to see when the system has stabilized and is ready for testing. One should however, consider if the more exact readings using the manometer is worth the time and effort, since the aim of the manometers is only to check if the head remains constant over time.

The following paragraph discusses the use of temperature sensors in the modified setup of the Darcy-cell as opposed to the thermometer used in the original setup. The purpose of the temperature measurement is to determine the temperature in the cell. The old thermometers were placed in the upper and lower tank and adds some uncertainty to the temperature measurements in the test. This is because the temperature of the saltwater can change from the

top tank to when it reaches the bottom tank and may not be representative of the temperature in the cell. It should be noted that the Darcy-cell test is performed with room tempered saltwater and the hydraulic conductivity is not largely affected by a small change in temperature at temperatures in the ranges of room temperature. Larger variations are common at lower temperatures. It was however decided to place the sensors in the top and bottom of the lid in the cell to reduce uncertainty in measurements.

5.6 Percentage difference

It should be noted that there is a large variation in the estimated values for hydraulic conductivity in sand when using the core permeameter. This can be seen when looking at the percentage difference in Table 4.9, Table 4.10 and Table 4.12. For the air permeameter, the calculated total hydraulic conductivity has a percentage difference of 25,64 %, 44,91 % and 31,14 % for cylinder 1-3 respectively. The percentage difference in the calculated hydraulic conductivity in sand using the air permeameter is 28,45 %, 51,22 % and 32,94 % for cylinder 1-3 respectively. This shows that there is large variety in the calculated values for total hydraulic conductivity and the hydraulic conductivity in sand using the air permeameter. For the liquid permeameter, the percentage difference for the calculated hydraulic conductivity in sand is 35,46 %, 0,00 % and 31,73 % for cylinder 1-3 respectively. There is also here, a large variety in the estimated values for hydraulic conductivity of sand using the liquid permeameter. These differences make it clear that the estimated value for hydraulic conductivity of sand using the air permeameter are not reliable. The percentage difference for the calculated hydraulic conductivity using the Darcy-cell is 20,59 %, see Table 4.17. This value is much lower when compared with the percentage difference calculated from the core permeameters. This further supports the argument of the modified Darcy-cell being a more reliable method to estimate hydraulic conductivity. It should be noted that in the Darcy-cell method, the calculated maximum and minimum values of hydraulic conductivity based on uncertainty in measurements provide an average uncertainty of 31,45 % in the readings. However, the uncertainties in volume and time were chosen by the author and are not necessarily correct and could produce a higher average uncertainty than what is actually realistic.

5.7 Sources of error

5.7.1 Splitting process

The splitting process was conducted under an exhaust to prevent inhaling the finer fractions of soil. One could observe some fine material being pulled into the exhaust during the splitting process. Based on visual observations the quantity of fines escaping seemed like a significant amount. A lower fine fraction in the sample can result in an overestimation of hydraulic conductivity. However, there are not very large amounts of fines present in the sample so the loss of fines is not assumed to influence the calculated hydraulic conductivity to a large extent.

5.7.2 Packing the sample

The sample was packed using the same procedure for every measurement in all 3 methods. The aim of the packing process was to imitate the “in-situ” compaction grade of an undisturbed sample in the field to better estimate a value for hydraulic conductivity. In all 3 methods one could observe fine material escaping when the sample was packed with the packing rod. A lower fraction of fines could lead to an overestimation of the hydraulic conductivity.

In all methods, it was assumed that the packing process caused the sand sample to be compressed as much as is possible when compared to its natural state. However, the packing process did not compress the sample well enough, then this can have caused sediments to migrate through the sample. The migration can cause grains to block pores in the sample and finer material to migrate to the outlet and block the pores at the surface of the metal filter. This will lead to a lower recorded flow rate and result in an underestimation of hydraulic conductivity. It is suggested to create a device that makes it possible to screw in the top piece and at the same time compressing the sample in the cylinder.

5.7.3 Boundary effects

Boundary effects can cause error in the air- and liquid permeameter methods. The dimeter of the cylinder used in these methods did not meet the requirement of the inner diameter being at least 10 times the largest grain diameter in the sample. The effect the wall has on the grains in the sample can influence the flow rate, which in turn, affects the estimated hydraulic conductivity.

5.7.4 Metal filters used in modified core permeameters

The SEM analysis showed that finer material blocked some pores on the surface of the metal filter. It is assumed that fines collected at the filter at the outlet in both the air permeameter test and in the liquid permeameter test. The blockage of the pores on the surface of the metal filter will lead to a lower recorded flow rate and cause an underestimation of hydraulic conductivity. It is very likely that the metal filters used in the modified core permeameters were not adequate.

5.7.5 Clay interaction with saltwater

During the liquid permeameter method and the Darcy-cell method, the clay can interact with the saltwater causing the water molecules to stick to the clay particles. If clay interacts with the saltwater it could have great effect on the recorded flow rate and cause an underestimated hydraulic conductivity. It could be interesting to determine whether clay particles do interact with the saltwater during the test and further investigations on this is suggested.

5.7.6 Saturation process

A fully saltwater saturated sample is of great importance when conducting the liquid permeameter test and the Darcy-cell test. When estimating the saltwater saturation in the two methods it is apparent that the samples are not fully saturated with saltwater. According to Chapuis (2012) the hydraulic conductivity will increase by a factor of 4 if the sample increases from a water saturation of 80 % to 100 %. This means that the air present in the pores of the sand sample can cause an underestimated hydraulic conductivity. To achieve a higher saltwater saturation, one could have allowed the saltwater to circulate though the cell for a longer period of time. However, Chapuis (2012) explains that the pore volume had to be replaced 60 to 100 times to achieve a water saturation of 100 %. He points out that this could take days or weeks. Since the setup of the modified Darcy-cell consist of a plastic tank filled with saltwater which emptied within an hour and not a large reservoir that can feed the Darcy-cell for a longer amount of time, it made leaving the cell to saturate for days not possible.

5.7.7 Lack of data

Aside from the factors affecting the estimated hydraulic conductivity when using the air- and liquid permeameter, the validity and representability of the gathered results depend on the number of measurements made during the testing. It took a long time to land on a final modification for the core permeameters and this meant that there was less time for measurements.

Similarly, it took a long time for all the ordered parts of the Darcy-cell to arrive and it took a long time to build. There were also leakage problems in the cell that meant a lot of measurements had to be rejected. Further, LabView recorded wrong time measurements, so the data collected during those measurements had to be rejected as well. Once the setup for the Darcy-cell worked, the author was left with a limited amount of time to collect measurements.

With a larger amount of data, one would more easily see trends in the measurements and one would be able to do probability analysis on the results. This would help in the conclusion of what factors largely affect the flow rate and the estimated hydraulic conductivity.

6 Conclusion

The following conclusions can be drawn based on the work in this thesis:

- The smallest average hydraulic conductivity is $2{,}19 \times 10^{-6}$ m/s, and is calculated using the liquid permeameter, followed by $2{,}25 \times 10^{-5}$ m/s calculated using the air permeameter. The largest value was calculated using the Darcy-cell with an average value of $1{,}26 \times 10^{-3}$ m/s.
- The sieve-analysis shows that the majority of the sand fraction is a medium sand.
- The estimated hydraulic conductivity using the air permeameter and the Darcy – cell is within the expected range for a medium sorted sand, while the estimated value is not within the expected range for a medium sand, but a fine sand.
- The packing process causes fine material to escape from the cylinder and cell in the 3 methods.
- Occurrence of sedimentary dispersion in the core permeameters is likely. Sedimentary dispersion is believed to be a result of insufficient grade of packing. The sedimentary dispersion along with clay interaction and boundary effects can explain why the calculated hydraulic conductivity using the liquid permeameter is 10 times lower than when using the air permeameter.
- Presence of air pocket during the liquid permeameter test is likely. Air pockets can totally dominate the flow line and greatly affect the flow rate. This can cause underestimated hydraulic conductivity.
- The metal filters used during the air- and liquid permeability tests provide high uncertainty in the results and are not adequate to use as filters for these methods.
- The diameter of the cylinders used in the air- and liquid permeameter methods are smaller than what is recommended causing uncertainty in the validity of the estimated hydraulic conductivity using these methods. The diameter of the Darcy – cell is within what is required.
- The Darcy-cell method seems to be most fitted for estimating hydraulic conductivity in the laboratory.

To further conclude, there is little purpose in trying to compare the calculated hydraulic conductivity from the core permeameter with the Darcy-cell because the values are in totally different ranges. It is difficult to explain why these values are so different and the most apparent

conclusion is that it is not possible to use the modified core permeameters to estimate the hydraulic conductivity of groundwater in unconsolidated sand. The test procedures and the discussed uncertainties must be significantly improved in the air- and liquid permeameter methods to enable testing of unconsolidated sand in core permeameters. Further modifications of the setup and collection of more data is needed. The modified Darcy-cell provides the most reliable values for hydraulic conductivity, but methods of fully saturating the sample needs to be further investigated to obtain results for hydraulic conductivity of groundwater that can be used as an estimate of the "in-situ" hydraulic conductivity of unconsolidated sand in the field.

7 Further work

The following chapter gives suggestions to further work:

- Further modify the setup for the core permeameters to enable testing of unconsolidated sand in the laboratory.
- For the core permeameters, create a device that makes it possible to screw in the top piece and at the same time compress the sample in the cylinder to obtain a better grade of packing.
- Investigate other methods of fully saturating the sample in the Darcy-cell.
- Add T-connections to Darcy-cell to enable measurement of pressure and head at the same time.

References

ASTM International. (2006). *Standard Test Method for Permeability of Granular Soils (Constant Head) (ASTM D2434 - 68 (2006))*. https://doi.org/10.1520/D2434-68R06

ASTM International. (2015). *Standard Test Method for Measurement of Hydraulic Conductivity of Porous Material Using a Rigid-Wall, Compaction-Mold Permeameter (ASTM D5856-15)*. https://doi.org/10.1520/D5856-15

ASTM International. (2016). *Standard Test Methods for Measurement of Hydraulic Conductivity of Saturated Porous Materials Using a Flexible Wall Permeameter (ASTM D5084 − 16a)*. https://doi.org/10.1520/D5084-16A

Bear, J. (1972). *Dynamics of fluids in porous media*. New York: Dover Publications.

Bear, J., & Bachmat, Y. (1967). A Generalized Theory on Hydrodynamic Dispersion in Porous Media. *Int. Union Geod. Geophys. Publ.*, *72*, 16.

Bear, J., Zaslavsky, D., & Irmay, S. (1968). *Physical principles of water percolation and seepage* (Vol. 29). Paris: United Nations Educational, Scientific and Cultural Organization.

Brattli, B. (2009). *Fysisk og Kjemisk Hydrogeologi* (3rd ed.). Trondheim: Norwegian University of Science and Technology.

Brattli, B. (2015). *Ingeniørgeologi Løsmasser* (2nd ed.). Trondheim: Norwegian University of Science and Technology, Department of Geoscience and Petroleum.

Carman, P. C. (1997). Fluid flow through granular beds. *Chemical Engineering Research and Design*, *75*, 32–48. https://doi.org/10.1016/S0263-8762(97)80003-2

Chapuis, R. P. (2012). Predicting the saturated hydraulic conductivity of soils: a review. *Bulletin of Engineering Geology and the Environment*, *71*(3), 401–434. https://doi.org/10.1007/s10064-012-0418-7

Creative Mechanisms. (2016). Everything You Need To Know About Polycarbonate (PC). Retrieved May 10, 2018, from https://www.creativemechanisms.com/blog/everything-you-need-to-know-about-polycarbonate-pc

Dake, L. P. (1983). *Fundamentals of Reservoir Engineering* (8th ed.). Amsterdam: Elsevier.

Daniel, D., Anderson, D., & Boynton, S. (1985). Fixed-Wall Versus Flexible-Wall Permeameters. In *STP34573S Hydraulic Barriers in Soil and Rock* (pp. 107–126). 100 Barr Harbor Drive, PO Box C700, West Conshohocken, PA 19428-2959: ASTM International. https://doi.org/10.1520/STP34573S

Daniel, D. E., Trautwein, S. J., Boynton, S. S., & Foreman, D. E. (1984). Permeability Testing with Flexible-Wall Permeameters. *Geotechnical Testing Journal*, *GTJODJ*, *7*(3), 113–122.

Fetter, C. W. (2001). *Applied hydrogeology* (4th ed.). New Jersey: Prentice-Hall.

Freeze, R. A., & Cherry, J. A. (1979). *Groundwater*. Prentice-Hall.

Geological Survey of Norway. (2015). Grunnvarme. Retrieved November 22, 2017, from http://www.ngu.no/fagomrade/grunnvarme

Geotechdata.info. (2010). Constant head permeability test. Retrieved from http://www.geotechdata.info/geotest/constant-head-permeability-test.html

Gooch, J. W. (Ed.). (2007). *Encyclopedic Dictionary of Polymers*. New York: Springer New York. https://doi.org/10.1007/978-0-387-30160-0

Hawley, J. G., & Northey, R. D. (1981). Laboratory Permeability Tests with Annular Seals. In P. C. of X.ICSMFE (Ed.), *Soil Mechanics and Foundation Engineering Tenth International Conference* (pp. 617–620). Rotterdam: A. A. Balkema.

Hillel, D. (2008). SOIL-WATER DYNAMICS. In *Soil in the Environment* (pp. 91–101). New York: Elsevier. https://doi.org/10.1016/B978-0-12-348536-6.50012-5

International Organization for Standardization. (2004). *ISO/TS 17892-4 Geotechnical investigation and testing-Laboratory testing of soil-Part 4: Determination of particle sized distribution*. Geneve: ISO Copyright office.

Katti, D. R., Amarasinghe, P., & Katti, K. S. (2010). *US20100089124A1*. United States of America.

Lindmark, P. (2014). Grundvatten. Retrieved May 29, 2018, from http://slideplayer.se/slide/2827253/

M.T.H Corporation. (2014). Permeability Serial Flow. Retrieved November 25, 2017, from https://www.slideshare.net/MTaherHamdani/permeability

O'Geen, A. T. (2013). Soil Water Dynamics. *Nature Education Knowledge, 4*(5), 9.

PetroWiki. (2016). Formation damage from swelling clays. Retrieved from http://petrowiki.org/Formation_damage_from_swelling_clays

Polymer Technology and Services. (2015). Impact strenght of commonly used plastics. Retrieved May 10, 2018, from http://www.ptsllc.com/Search/MaterialGroupSearch.aspx?GroupID=10

Schwartz, F. W., & Zhang, H. (2003). *Fundamentals of ground water*. John Wiley & Sons.

Sepp, S. (2013). Sand Minerals. Retrieved May 30, 2018, from http://www.sandatlas.org/sand-minerals/

Solberg, R. A. (2017). *Beregning av hydraulisk konduktivitet ved bruk av laboratoriemetoder of simuleringsverktøyet CMG - STARS*. Norwegian University of Science and Technology.

Tømmerdal, H. M. (2017). *En evaluering av emiriske formler som relaterer kornfordeling til hydraulisk konduktivitet og deres egnethet til bruk i fluviale og glasifluviale sedimenter*. Norwegian University of Science and Technology.

Torsæter, O., & Abtahi, M. (2000). *Experimental Reservoir Engineering Laboratory Work Book*. Trondheim: Norwgian University of Science and Technology.

Verruijt, A. (1982). *Theory of groundwater flow* (2nd ed.). Surrey: The Macmillan Press Ltd.

Zolotukhin, A. B., & Ursin, J. . (2000). *Introduction to Petroleum Reservoir Engineering*. Høyskoleforlaget, Norwegian Academic Press.

Appendix

A Sieve analysis

A.1 Weight of sand before and after sieving process

Table A.1: Weight of sand sample before and after sieving.

Parameter	Value
Weight of sample before sieving [g]	416,7
Weight of sample after sieving [g]	416,6

A.2 Sieve analysis raw data

Table A.2: Sieve analysis raw data. m_{sieve} is the mass of the sieve, $m_{sieve+s}$ is the mass of the sieve and the sand sample on the sieve, m_s is the mass of sand sample and m_{cum} is cumulated mass.

Sieve aperture [µm]	Fraction [mm]	m_{sieve} [g]	$m_{sieve + s}$ [g]	m_s [g]	m_{cum} [g]	m_{cum} [%]
2000	2 - 4	423,30	424,30	1,00	1,00	99,76
1000	1 - 2	355,70	360,20	4,50	5,50	98,68
500	0,5 - 1	310,00	350,90	40,90	46,40	88,86
250	0,25 - 0,5	283,20	484,90	201,70	248,10	40,45
125	0,125 - 0,25	296,60	432,50	135,90	384,00	7,83
63	0,063 - 0,125	299,00	320,60	21,60	405,60	2,64
rest	<0,063	346,20	357,10	10,90	416,50	0,02
Sum		2314,00	2730,50	416,50		
Sample loss [%]				0,05		

B Helium porosimeter

B.1 Dimensions of matrix cup

Table B.1: Dimensions of matrix cup.

Parameter	Value
l [mm]	76,19
l [cm]	7,62
d [mm]	38,62
d [cm]	3,86
A [cm^2]	11,71

B.2 Helium porosimeter – raw data and results

Table B.2: Helium porosimeter – raw data and results.

Sample	V_1 [cm^3]	V_2 [cm^3]	V_k [cm^3]	$L_{cyl - sample}$ [mm]	L_{sample} [mm]	L_{sample} [cm]	V_b [cm^3]	V_p [cm^3]	n [%]
1,00	93,50	43,50	50,00	7,65	68,54	6,85	80,29	30,29	37,73
2,00	93,50	44,00	49,50	8,39	67,80	6,78	79,42	29,92	37,68
3,00	93,50	44,50	49,00	7,98	68,21	6,82	79,90	30,90	38,68
Avg.			49,5				79,87	30,37	38,03

C Porosity by saturation

C.1 Input parameters

Table C.1: Parameters used to estimate porosity of sand sample prior to liquid permeameter test.

Parameter	Value
ρ_w [g/cm^3]	1,00
$L_{cyl.}$ [cm]	6,00
$ID_{cyl.}$ [cm]	3,54
A [cm^2]	9,84
V_b [cm^3]	59,05

C.2 Porosity by saturation – raw data and results

Table C.2: Estimation of porosity by saturation - raw data and results

Test	Cylinder	m_{cds} [g]	m_{cws} [g]	n [%]
1	1	194,71	219,34	41,71
1	2	194,56	218,65	40,80
1	3	194,29	217,63	39,53
Average				40,68
2	1	194,71	220,26	43,26
2	2	194,56	219,93	42,96
2	3	194,29	219,19	42,17
Average				42,80
2	1	194,71	220,23	43,21
2	2	194,56	219,92	42,95
2	3	194,29	219,25	42,27
Average				42,81
Total avg.				42,09

D Saturation determination

D.1 Input parameters liquid permeameter method

Table D.1: Input parameters used to estimate saltwater saturation in sand sample during liquid permeameter test.

Parameter	Value
ρ_w [g/cm^3]	1,00

D.2 Saturation determination liquid permeameter method – raw data and results

Table D.2: Saturation determination raw data and results for liquid permeameter test.

Test	Cylinder	m_{cds} [g]	m_{cws} [g]	m_{sw} [g]	V_{sw} [cm^3]	V_p [cm^3]	S_w [%]	S_g [%]
1	1	194,71	219,34	24,63	24,63	26,52	92,90	7,10
	2	194,56	218,65	24,09	24,09	26,48	90,98	9,02
	3	194,29	217,63	23,35	23,35	27,18	85,88	14,12
Avg.							89,92	10,08
2	1	194,71	220,26	25,55	25,55	26,52	96,35	3,65
	2	194,56	219,93	25,37	25,37	26,48	95,81	4,19
	3	194,29	219,19	24,90	24,90	27,18	91,60	8,40
Avg.							94,59	5,41
2	1	194,71	220,23	25,52	25,52	26,52	96,23	3,77
	2	194,56	219,92	25,36	25,36	26,48	95,78	4,22
	3	194,29	219,25	24,96	24,96	27,18	91,83	8,17
Avg.							94,61	5,39
Tot. Avg.							93,04	6,96

D.3 Input parameters Darcy – cell method

Table D.3: Input parameters used for determining saltwater saturation in sand sample during Darcy-cell test.

Parameter	Value
ρ_w [g/cm^3]	1,00
L_{cell} [cm]	44,00
$L_{top\ bottom}$ [cm]	3,70
L_t [cm]	47,70
ID_{cell} [cm]	6,40
A_{cell} [cm^2]	32,17
L_s [cm]	16,70
L_{swc} [cm]	31,00
$V_{p\ ratio}$ [-]	0,38

D.4 Saturation determination Darcy-cell method – raw data and results

Table D.4: Saturation determination Darcy-cell method – raw data and results.

Parameter	Value
$m_{celldry}$ [g]	5114,83
$m_{cellwet}$ [g]	6300,00
m_{sw} [g]	1185,17
V_{sw} [cm^3]	1185,17
V_s [cm^3]	537,24
V_{swc} [cm^3]	997,27
V_{sws} [cm^3]	187,90
V_p [cm^3]	204,29
S_{sw} [%]	91,98
S_g [%]	8,02

E Filter permeability

Table E.1: Estimated permeability of metal filters using the TopIndustrie permeameter - raw data and results.

Cylinder	l [cm]	d [cm]	k [mD]	k [D]	Δp [bar]	μ [cP]	Q [cm3/min]	T [°C]
1	6,64	3,81	786,22	0,79	0,02	0,02	100,21	23,08
1	6,64	3,81	770,21	0,77	0,04	0,02	170,96	23,20
1	6,64	3,81	805,24	0,81	0,01	0,02	49,83	23,28
Average				0,79				
2	6,64	3,81	3793,34	3,79	0,00	0,02	62,58	23,76
2	6,64	3,81	3773,29	3,77	0,00	0,02	107,09	23,87
2	6,64	3,81	3778,49	3,78	0,01	0,02	160,51	23,95
Average				3,78				
3	6,64	3,81	5616,61	5,62	0,00	0,02	46,56	24,26
3	6,64	3,81	5550,88	5,55	0,00	0,02	112,39	24,35
3	6,64	3,81	5488,40	5,49	0,01	0,02	168,42	24,44
Average				5,55				

F Air permeameter

F.1 Input parameters

Table F.1: Input parameters used when estimating hydraulic conductivity using the air permeameter.

Parameter	Value
μ_{air} [cP]	1,79E-02
μ_w [PaS]	8,90E-04
g [m/s^2]	9,81
ρ_w [kg/m^3]	1000,00
L_s [cm]	6,00
L_s[m]	0,06
$ID_{cyl.}$ [cm]	3,54
$ID_{cyl.}$ [m]	0,04
A [cm^2]	9,84
P_a [bar]	1,00
L_{f1} [cm]	0,25
L_{f2} [cm]	0,25
L_{fT} [cm]	0,50
L_t [cm]	6,50

F.2 Calculation of total hydraulic conductivity – raw data and results

Table F.2: Calculation of total hydraulic conductivity – raw data and results. Packing type b.p is short for bench press and vibr. Is short for vibrator.

Test	Cyl.	Packing	p_1 [bar]	p_2 [bar]	Δp [bar]	pm [bar]	Q [l/min]	Q [cm^3/s]	k_T [D]	k_T [m^2]	K_T [m/s]
1	1	B.p.	1,04	1,00	0,04	1,02	0,24	4,00	1,16	1,16E-12	1,28E-05
1	1	B.p.	1,06	1,02	0,04	1,04	0,23	3,83	1,09	1,09E-12	1,20E-05
1	1	B.p.	1,08	1,04	0,04	1,06	0,20	3,33	0,93	9,29E-13	1,02E-05
1	1	B.p.	1,10	1,06	0,04	1,08	0,25	4,17	1,14	1,14E-12	1,26E-05
1	1	B.p.	1,12	1,08	0,04	1,10	0,20	3,33	0,90	8,96E-13	9,87E-06
2	1	Vibr.	1,04	1,00	0,04	1,02	0,33	5,50	1,59	1,59E-12	1,76E-05
2	1	Vibr.	1,06	1,02	0,04	1,04	0,34	5,67	1,61	1,61E-12	1,77E-05
2	1	Vibr.	1,08	1,04	0,04	1,06	0,35	5,83	1,63	1,63E-12	1,79E-05
2	1	Vibr.	1,10	1,06	0,04	1,08	0,30	5,00	1,37	1,37E-12	1,51E-05
2	1	Vibr.	1,12	1,08	0,04	1,10	0,28	4,67	1,25	1,25E-12	1,38E-05
2	2	Vibr.	1,04	1,00	0,04	1,02	0,66	11,00	3,19	3,19E-12	3,51E-05
2	2	Vibr.	1,06	1,02	0,04	1,04	0,61	10,17	2,89	2,89E-12	3,18E-05
2	2	Vibr.	1,08	1,04	0,04	1,06	0,60	10,00	2,79	2,79E-12	3,07E-05
2	2	Vibr.	1,10	1,06	0,04	1,08	0,56	9,33	2,55	2,55E-12	2,82E-05
2	2	Vibr.	1,12	1,08	0,04	1,10	0,60	10,00	2,69	2,69E-12	2,96E-05
3	1	Vibr.	1,04	1,00	0,04	1,02	0,25	4,17	1,21	1,21E-12	1,33E-05
3	1	Vibr.	1,06	1,02	0,04	1,04	0,30	5,00	1,42	1,42E-12	1,57E-05
3	1	Vibr.	1,08	1,04	0,04	1,06	0,25	4,17	1,16	1,16E-12	1,28E-05
3	1	Vibr.	1,10	1,06	0,04	1,08	0,29	4,83	1,32	1,32E-12	1,46E-05
3	1	Vibr.	1,12	1,08	0,04	1,10	0,23	3,83	1,03	1,03E-12	1,14E-05
3	2	Vibr.	1,04	1,00	0,04	1,02	0,55	9,17	2,66	2,66E-12	2,93E-05
3	2	Vibr.	1,06	1,02	0,04	1,04	0,55	9,17	2,60	2,60E-12	2,87E-05
3	2	Vibr.	1,08	1,04	0,04	1,06	0,57	9,50	2,65	2,65E-12	2,92E-05
3	2	Vibr.	1,10	1,06	0,04	1,08	0,56	9,33	2,55	2,55E-12	2,82E-05
3	2	Vibr.	1,12	1,08	0,04	1,10	0,52	8,67	2,33	2,33E-12	2,57E-05

F.3 Estimated sand permeability and hydraulic conductivity in sand – raw data and results

Table F.3:Calculated sand permeability and hydraulic conductivity in sand – raw data and results. Packing type b.p is short for bench press and vibr. Is short for vibrator.

Test	Cylinder	Packing	k_S [D]	k_S [m^2]	K_S water [m/s]
1	1	B.p.	1,21	1,21E-12	1,33E-05
1	1	B.p.	1,13	1,13E-12	1,24E-05
1	1	B.p.	0,94	9,44E-13	1,04E-05
1	1	B.p.	1,18	1,18E-12	1,31E-05
1	1	B.p.	0,91	9,06E-13	9,99E-06
2	1	Vibr.	1,74	1,74E-12	1,92E-05
2	1	Vibr.	1,76	1,76E-12	1,94E-05
2	1	Vibr.	1,78	1,78E-12	1,97E-05
2	1	Vibr.	1,46	1,46E-12	1,61E-05
2	1	Vibr.	1,32	1,32E-12	1,45E-05
2	2	Vibr.	3,15	3,15E-12	3,47E-05
2	2	Vibr.	2,83	2,83E-12	3,12E-05
2	2	Vibr.	2,73	2,73E-12	3,01E-05
2	2	Vibr.	2,49	2,49E-12	2,74E-05
2	2	Vibr.	2,62	2,62E-12	2,89E-05
3	1	Vibr.	1,26	1,26E-12	1,39E-05
3	1	Vibr.	1,52	1,52E-12	1,68E-05
3	1	Vibr.	1,21	1,21E-12	1,33E-05
3	1	Vibr.	1,40	1,40E-12	1,55E-05
3	1	Vibr.	1,06	1,06E-12	1,17E-05
3	2	Vibr.	2,59	2,59E-12	2,86E-05
3	2	Vibr.	2,54	2,54E-12	2,80E-05
3	2	Vibr.	2,58	2,58E-12	2,85E-05
3	2	Vibr.	2,49	2,49E-12	2,74E-05
3	2	Vibr.	2,26	2,26E-12	2,49E-05

G Liquid permeameter

G.1 Pressure and time data – measurement 1

Table G.1:Pressure and time data from liquid permeameter test – measurement 1. A constant pump rate of Q = 0,05 mL/s is used for all measurements. The values marked in blue are where pressure is assumed constant. These are used to further calculate sand permeability and hydraulic conductivity as seen in Table 4.11. BT is short for time of breakthrough.

Cylinder 1		**Cylinder 2**		**Cylinder 3**	
T [°C]	22,20	T [°C]	21,90	T [°C]	22,20
BT [min]	0,75	BT [min]	0,00	BT [min]	0,00
t [min]	**Δ_p [bar]**	**t [min]**	**Δ_p [bar]**	**t [min]**	**Δp [bar]**
1,00	0,33	0,73	0,08	0,50	0,14
2,00	0,35	1,00	0,10	1,00	0,10
3,00	0,37	1,17	0,11	1,50	0,09
4,00	0,40	1,50	0,12	2,00	0,09
5,00	0,42	2,00	0,12	2,50	0,09
6,00	0,46	2,50	0,12	3,00	0,09
7,00	0,50	3,00	0,13	3,50	0,09
8,00	0,56	3,50	0,13	4,00	0,10
9,00	0,60	4,00	0,13	4,50	0,10
10,00	0,65	4,50	0,14	5,00	0,10
11,00	0,70	5,00	0,13	5,50	0,10
12,00	0,75	5,50	0,14	6,00	0,10
13,00	**0,80**	**6,00**	**0,14**	6,50	0,10
14,00	0,84	6,50	0,13	7,00	0,10
15,00	0,88	7,00	0,13	7,50	0,10
16,00	0,92	7,50	0,13	**8,00**	**0,11**
17,00	0,95	8,00	0,14	8,50	0,11
18,00	1,00	8,50	0,14	9,00	0,11
19,00	1,03	9,00	0,14	9,50	0,11
20,00	1,05	9,50	0,14	10,00	0,11
25,00	1,11	10,00	0,13	-	-
30,00	1,21	-	-	-	-
35,00	1,30	-	-	-	-
40,00	1,38	-	-	-	-
45,00	1,40	-	-	-	-
50,00	1,43	-	-	-	-
60,00	1,48	-	-	-	-

G.2 Pressure and time data – measurement 2

Table G.2: Pressure and time data from liquid permeameter test – measurement 2. A constant pump rate of Q = 0,05 mL/s is used for all measurements. The values marked in blue are where pressure is assumed constant. These are used to further calculate sand permeability and hydraulic conductivity as seen in Table 4.11. BT is short for time of breakthrough.

Cylinder 1		**Cylinder 2**		**Cylinder 3**	
T [˚C]	26,30	T [˚C]	26,60	T [˚C]	26,80
BT [min]	1,88	BT [min]	0,00	BT [min]	0,00
t [min]	**Δp [bar]**	**t [min]**	**Δp [bar]**	**t [min]**	**Δp [bar]**
1,00	0,40	0,50	0,12	0,50	0,08
1,50	0,50	1,00	0,12	1,00	0,12
1,88	0,53	1,50	0,12	1,50	0,13
2,00	0,60	2,00	0,12	2,00	0,13
2,50	0,64	2,50	0,11	2,50	0,12
3,00	0,68	3,00	0,12	3,00	0,10
3,50	0,68	3,50	0,11	3,50	0,10
4,00	0,68	4,00	0,12	4,00	0,10
4,50	0,66	4,50	0,12	4,50	0,10
5,00	0,63	5,00	0,12	5,00	0,10
5,50	0,62	5,50	0,13	5,50	0,10
6,00	0,60	6,00	0,13	6,00	0,10
6,50	0,60	6,50	0,12	6,50	0,09
7,00	0,58	7,00	0,14	7,00	0,09
7,50	0,58	7,50	0,14	7,50	0,09
8,00	0,56	8,00	0,14	8,00	0,09
8,50	**0,56**	**8,50**	**0,14**	**8,50**	**0,08**
9,00	0,56	9,00	0,14	9,00	0,07
9,50	0,55	9,50	0,14	9,50	0,07
10,00	0,55	10,00	0,14	10,00	0,07
10,50	0,56	10,50	0,15	10,50	0,08
11,00	0,54	11,00	0,16	11,00	0,08
11,50	0,55	11,50	0,16	11,50	0,08
12,00	0,55	12,00	0,16	12,00	0,08
12,50	0,55	-	-	-	-
13,00	0,56	-	-	-	-
13,50	0,56	-	-	-	-
14,00	0,56	-	-	-	-
14,50	0,56	-	-	-	-
15,00	0,56	-	-	-	-
15,50	0,56	-	-	-	-
16,00	0,57	-	-	-	-
16,50	0,57	-	-	-	-
17,00	0,58	-	-	-	-

Cylinder 1		Cylinder 2		Cylinder 3	
T [°C]	26,30	T [°C]	T [°C]	26,30	T [°C]
BT [min]	1,88	BT [min]	BT [min]	1,88	BT [min]
t [min]	**Δ_p [bar]**	**t [min]**	**Δ_p [bar]**	**t [min]**	**Δ_p [bar]**
17,50	0,58	-	-	-	-
18,00	0,58	-	-	-	-
18,50	0,58	-	-	-	-
19,00	0,58	-	-	-	-
19,50	0,58	-	-	-	-
20,00	0,58	-	-	-	-

G.3 Input parameters

Table G.3: Input parameters used in estimation of sand permeability and hydraulic conductivity in liquid permeameter test.

Parameter	Value
μ_w [PaS]	8,90E-04
μ_w [cP]	1,00
g [m/s^2]	9,81
ρ_w [kg/m^3]	1000,00
L_s [cm]	6,00
L_s [m]	0,06
$ID_{cyl.}$ [cm]	3,54
$ID_{cyl.}$ [m]	0,04
A [cm^2]	9,84
L_{f1} [cm]	0,25
L_{f2} [cm]	0,25
L_{ft}[cm]	0,50
L_t [cm]	6,50
Q [mL/s]	0,05

H SEM analysis

H.1 EDS composition results for point 2.

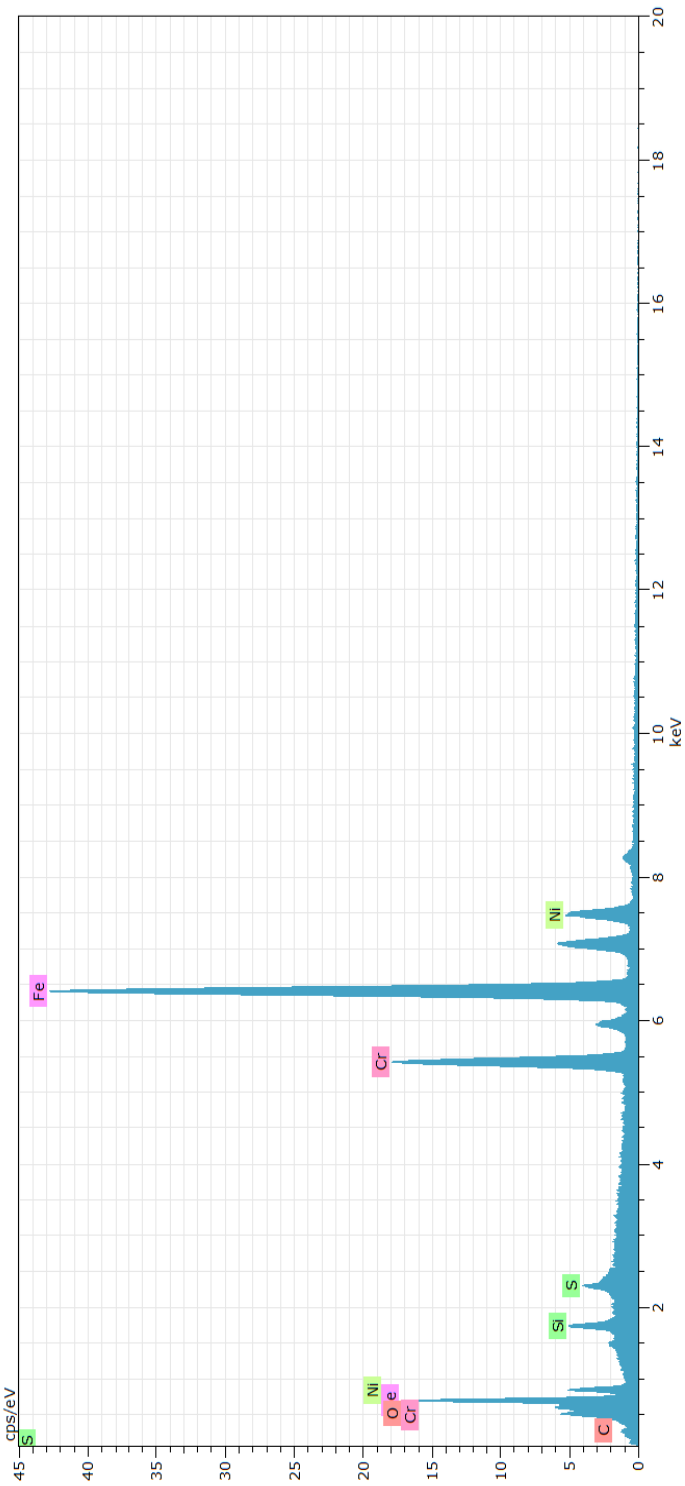

2 Date:29.05.2018 09:47:28 HV:20,0kV Puls th.:26,05kcps

El	AN	Series	unn. C [wt.%]	norm. C [wt.%]	Atom. C [at.%]	Error (1 Sigma) [wt.%]
Fe	26	K-series	59,61	66,74	58,21	1,62
Cr	24	K-series	14,05	15,73	14,74	0,42
Ni	28	K-series	10,22	11,44	9,49	0,33
C	6	K-series	1,81	2,02	8,20	0,56
O	8	K-series	1,72	1,92	5,85	0,38
Si	14	K-series	1,02	1,14	1,98	0,08
S	16	K-series	0,89	1,00	1,52	0,07
		Total:	89,31	100,00	100,00	

Figure H.1: EDS composition results for point 2.

H.2 EDS composition results for point 3

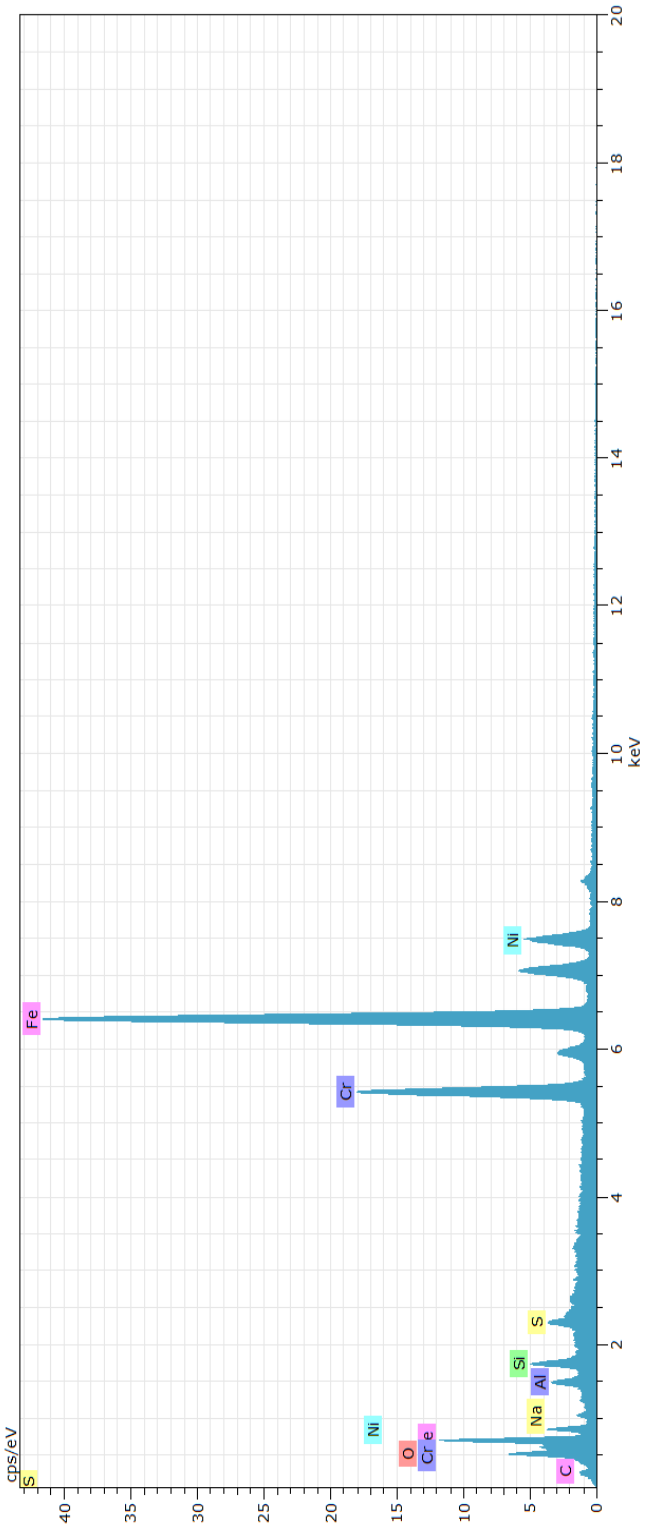

3 Date:29.05.2018 09:47:39 HV:20,0kV Puls th.:24,92kcps

El	AN	Series	unn. C [wt.%]	norm. C [wt.%]	Atom. C [at.%]	Error (1 Sigma) [wt.%]
Fe	26	K-series	56,28	63,38	51,57	1,53
Cr	24	K-series	13,48	15,18	13,27	0,40
O	8	K-series	3,01	3,39	9,62	0,57
C	6	K-series	2,19	2,47	9,35	0,62
Ni	28	K-series	9,73	10,96	8,49	0,31
Si	14	K-series	1,34	1,51	2,45	0,09
Al	13	K-series	1,18	1,32	2,23	0,09
Na	11	K-series	0,78	0,88	1,74	0,10
S	16	K-series	0,80	0,90	1,28	0,06
		Total:	88,79	100,00	100,00	

Figure H.2: EDS composition results for point 3

H.3 EDS composition results for point 4

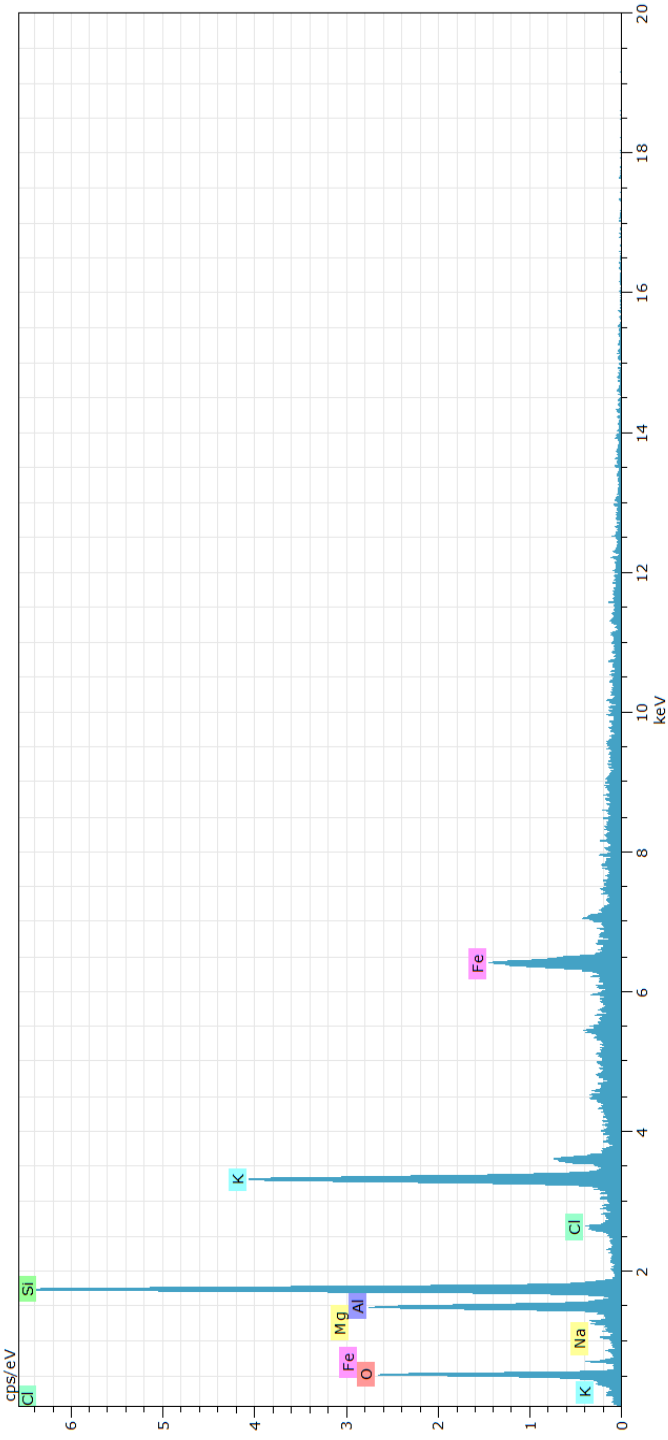

4 Date:29.05.2018 09:47:49 HV:20,0kV Puls th.:6,53kcps

El	AN	Series	unn. C [wt.%]	norm. C [wt.%]	Atom. C [at.%]	Error (1 Sigma) [wt.%]
O	8	K-series	22,77	33,97	49,99	4,66
Si	14	K-series	19,83	29,58	24,80	0,95
Al	13	K-series	8,54	12,75	11,12	0,52
K	19	K-series	10,62	15,85	9,54	0,40
Fe	26	K-series	3,39	5,06	2,14	0,15
Mg	12	K-series	0,64	0,96	0,93	0,11
Na	11	K-series	0,50	0,74	0,76	0,11
Cl	17	K-series	0,73	1,09	0,73	0,09
		Total:	67,03	100,00	100,00	

Figure H.3: EDS composition results for point 4.

H.4 EDS composition results for point 5

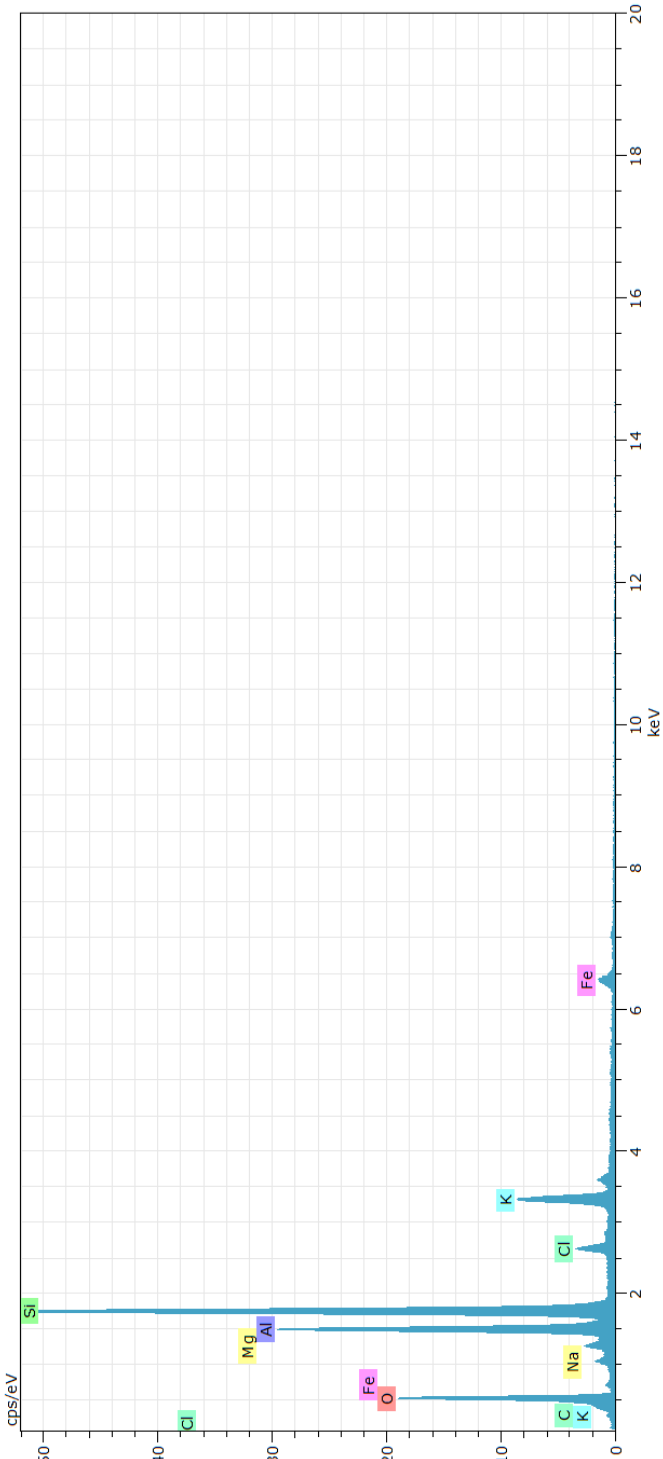

5 Date:29.05.2018 09:48:00 HV:20,0kV Puls th.:16,98kcps

El	AN	Series	unn. C [wt.%]	norm. C [wt.%]	Atom. C [at.%]	Error (1 Sigma) [wt.%]
O	8	K-series	30,35	39,63	54,44	4,22
Si	14	K-series	21,84	28,51	22,31	0,97
Al	13	K-series	11,85	15,47	12,61	0,60
K	19	K-series	6,20	8,10	4,55	0,23
C	6	K-series	0,70	0,92	1,67	0,44
Fe	26	K-series	2,61	3,41	1,34	0,12
Cl	17	K-series	1,50	1,96	1,22	0,09
Mg	12	K-series	0,83	1,08	0,98	0,08
Na	11	K-series	0,71	0,92	0,88	0,09
		Total:	76,60	100,00	100,00	

Figure H.4: EDS composition results for point 5.

H.5 EDS composition results for point 6

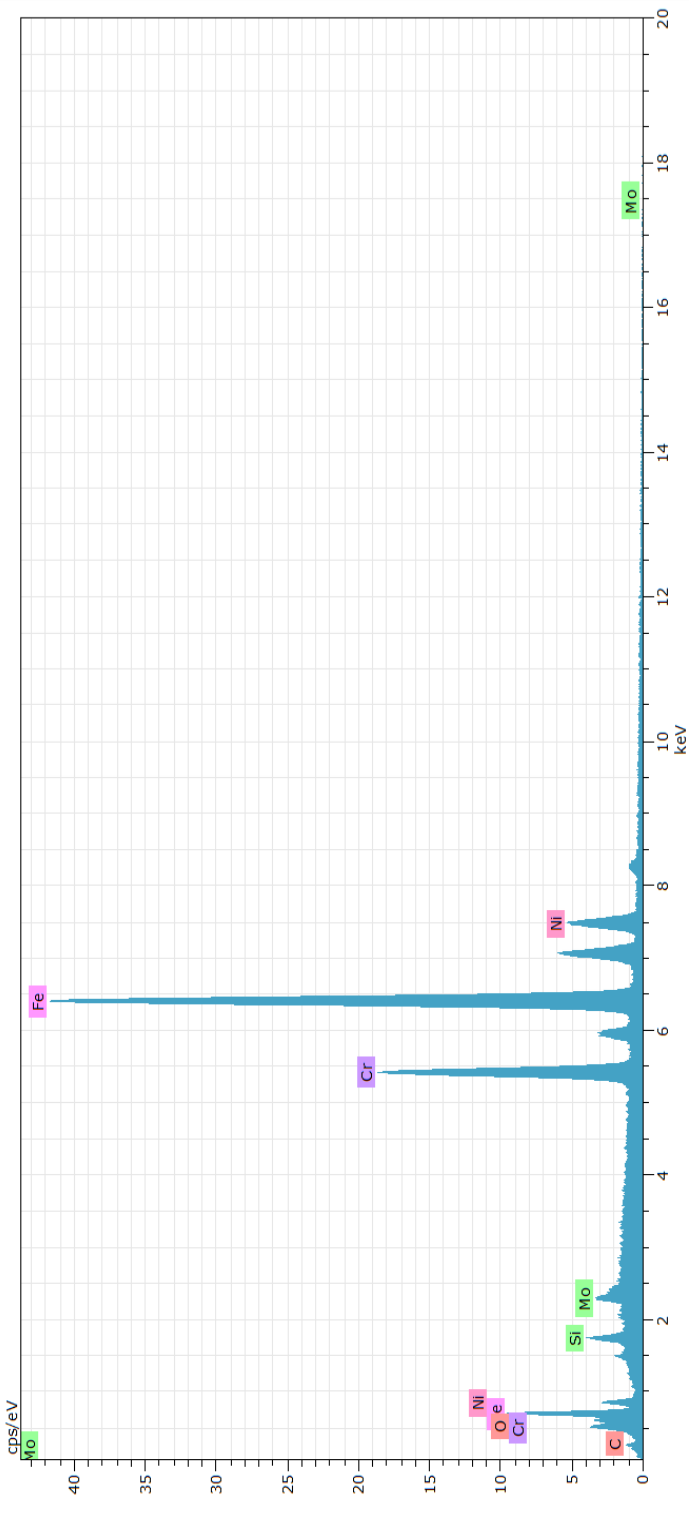

6 Date:29.05.2018 09:48:11 HV:20,0kV Puls th.:23,81kcps

El	AN	Series	unn. C [wt.%]	norm. C [wt.%]	Atom. C [at.%]	Error (1 Sigma) [wt.%]
Fe	26	K-series	61,48	65,89	58,78	1,67
Cr	24	K-series	14,49	15,52	14,87	0,43
Ni	28	K-series	11,56	12,38	10,51	0,37
C	6	K-series	1,87	2,00	8,30	0,57
O	8	K-series	1,46	1,57	4,88	0,35
Si	14	K-series	0,95	1,02	1,81	0,08
Mo	42	L-series	1,51	1,62	0,84	0,09
		Total:	93,32	100,00	100,00	

Figure H.5: EDS composition results for point 6.

I Darcy-cell

I.1 Input parameters

Table I. 1:Input parameters used to estimate hydraulic conductivity using the Darcy-cell method.

Parameter	Value
ρ_w [g/cm^3]	1,00
ρ_w [kg/m^3]	1000,00
μ_w [PaS]	8,90E-04
g [m/s^2]	9,81
L_{cell} [cm]	44,00
L_{cell} [m]	0,44
ID_{cell} [cm]	6,40
ID_{cell} [m]	0,06
A_{cell} [cm^2]	32,17
A_{cell} [m^2]	3,22E-03
V_{sw} [mL]	200,00
V_{sw} [m^3]	2,00E-04

Meas.	t [s]	p1 [bar]	p2 [bar]	T1 [°C]	T2[°C]	Δp [bar]	Δp [Pa]	Q [m³/s]	ks[D]	ks [m²]	Ksmin [m/s]	Ks [m/s]	Ksmax [m/s]
13	138,21	0,05	0,07	21,43	22,44	0,02	1800,00	1,45E-06	97,86	9,79E-11	9,36E-04	1,08E-03	1,27E-03
14	130,41	0,05	0,07	21,55	22,44	0,02	1700,00	1,53E-06	109,81	1,10E-10	1,04E-03	1,21E-03	1,44E-03
15	128,02	0,05	0,07	21,67	22,43	0,02	1700,00	1,56E-06	111,87	1,12E-10	1,06E-03	1,23E-03	1,46E-03
16	127,12	0,05	0,07	21,79	22,44	0,02	1700,00	1,57E-06	112,66	1,13E-10	1,07E-03	1,24E-03	1,47E-03
17	127,82	0,05	0,07	21,79	22,43	0,02	1800,00	1,56E-06	105,82	1,06E-10	1,01E-03	1,17E-03	1,37E-03
18	123,61	0,05	0,07	21,67	22,44	0,02	1700,00	1,62E-06	115,86	1,16E-10	1,10E-03	1,28E-03	1,52E-03
19	124,12	0,05	0,07	21,68	22,44	0,02	1700,00	1,61E-06	115,38	1,15E-10	1,09E-03	1,27E-03	1,51E-03
20	123,51	0,05	0,07	21,55	22,43	0,02	1700,00	1,62E-06	115,95	1,16E-10	1,10E-03	1,28E-03	1,52E-03
21	123,61	0,05	0,07	21,55	22,43	0,02	1800,00	1,62E-06	109,42	1,09E-10	1,05E-03	1,21E-03	1,42E-03
22	122,21	0,05	0,07	21,56	22,43	0,02	1700,00	1,64E-06	117,18	1,17E-10	1,11E-03	1,29E-03	1,53E-03
23	124,82	0,05	0,07	21,55	22,45	0,02	1800,00	1,60E-06	108,36	1,08E-10	1,04E-03	1,19E-03	1,41E-03
24	124,53	0,05	0,07	21,55	22,44	0,02	1700,00	1,61E-06	115,01	1,15E-10	1,09E-03	1,27E-03	1,51E-03
25	123,63	0,05	0,07	21,54	22,44	0,02	1800,00	1,62E-06	109,41	1,09E-10	1,05E-03	1,21E-03	1,42E-03
26	121,34	0,05	0,07	21,54	22,44	0,02	1700,00	1,65E-06	118,03	1,18E-10	1,12E-03	1,30E-03	1,55E-03
27	120,53	0,05	0,07	21,55	22,44	0,02	1700,00	1,66E-06	118,82	1,19E-10	1,13E-03	1,31E-03	1,56E-03
28	122,71	0,05	0,07	21,55	22,44	0,02	1800,00	1,63E-06	110,22	1,10E-10	1,05E-03	1,21E-03	1,43E-03
29	121,12	0,05	0,07	21,55	22,44	0,02	1700,00	1,65E-06	118,24	1,18E-10	1,12E-03	1,30E-03	1,55E-03
30	120,72	0,05	0,07	21,55	22,43	0,02	1700,00	1,66E-06	118,63	1,19E-10	1,12E-03	1,31E-03	1,55E-03
31	121,22	0,05	0,07	21,55	22,44	0,02	1800,00	1,65E-06	111,57	1,12E-10	1,07E-03	1,23E-03	1,45E-03
32	120,33	0,05	0,07	21,55	22,43	0,02	1800,00	1,66E-06	112,40	1,12E-10	1,07E-03	1,24E-03	1,46E-03
33	119,92	0,05	0,07	21,54	22,43	0,02	1800,00	1,67E-06	112,79	1,13E-10	1,08E-03	1,24E-03	1,46E-03
34	120,12	0,05	0,07	21,55	22,45	0,02	1700,00	1,66E-06	119,22	1,19E-10	1,13E-03	1,31E-03	1,56E-03
35	119,72	0,05	0,07	21,54	22,44	0,02	1700,00	1,67E-06	119,62	1,20E-10	1,13E-03	1,32E-03	1,57E-03
36	120,33	0,05	0,07	21,55	22,44	0,02	1700,00	1,66E-06	119,02	1,19E-10	1,13E-03	1,31E-03	1,56E-03
37	122,73	0,05	0,07	21,55	22,43	0,02	1700,00	1,63E-06	116,69	1,17E-10	1,11E-03	1,29E-03	1,53E-03
38	119,02	0,05	0,07	21,55	22,44	0,02	1700,00	1,68E-06	120,32	1,20E-10	1,14E-03	1,33E-03	1,58E-03
39	119,53	0,05	0,07	21,54	22,44	0,02	1700,00	1,67E-06	119,82	1,20E-10	1,14E-03	1,32E-03	1,57E-03
40	119,92	0,05	0,07	21,55	22,43	0,02	1800,00	1,67E-06	112,79	1,13E-10	1,08E-03	1,24E-03	1,46E-03
41	120,01	0,05	0,07	21,55	22,44	0,02	1700,00	1,67E-06	119,33	1,19E-10	1,13E-03	1,32E-03	1,56E-03
42	120,53	0,05	0,07	21,54	22,44	0,02	1700,00	1,66E-06	118,82	1,19E-10	1,13E-03	1,31E-03	1,56E-03
43	120,82	0,05	0,07	21,55	22,44	0,02	1700,00	1,66E-06	118,53	1,19E-10	1,12E-03	1,31E-03	1,55E-03
Avg.	122,97	0,05	0,07	21,57	22,44	0,02	1732,26	1,63E-06	114,50	1,14E-10	1,09E-03	1,26E-03	1,49E-03

Table I. 2: Darcy-cell raw data and results. Meas. is short for measurement.

J Overview of electronic attachments

The Excel file *"Electronic attachment to master thesis"* contains the raw data logged in LabView during the Darcy – cell test. This data was used to calculate the hydraulic conductivity. The Excel file contains the following sheet:

- *"Darcy-cell measurements"* and includes all data logged in LabView for measurements 13-43.

K Risk assessment

K.1 Risk assessment

NTNU	Risk assessment	Prepared by	Number	Date	
		HSE section	HMSRV2603E	04.02.2011	
HSE/KS		Approved by		Replaces	
		The Rector		01.12.2006	

Unit: *Department of Geoscience and Petroleum* **Date:** 20.01.18

Line manager:

Participants in the identification process (including their function):

Runa Aronsen Solberg (Master's Thesis student), Roger Overå (Staff engineer, in charge of reservoir laboratory).

Short description of the main activity/main process:

Master project for student Runa Aronsen Solberg. Project title: "*Modification of existing permeameters to estimate hydraulic conductivity of groundwater in unconsolidated sand in the laboratory*".

Signatures: *Responsible supervisor:* Kaldhin Rønnaug *Student:* Runa Solberg

Activity from the identification process form	**Potential undesirable incident/strain**	**Likelihood:**	**Consequence:**			**Risk Value (human)**	**Comments/status Suggested measures**
		Likelihood (1-5)	Human (A-E)	Environment (A-E)	Economy/ material (A-E)		
Moving around inside the laboratory.	Damage to personell due to slippery floor, falling from ladder or bench.	3	B	A	A	B3	Stay inside marked guidelines when leaving your work station. Always two people present when using a ladder.
Moving around inside the laboratory.	Damage to personell du to chemicals.	1	B	A	A	B1	Use required clothing; laboratory coat, glasses and shoes.
Equipment falling on the floor or personell.	Damage to personell or other equipment.	4	A	A	A	A4	Follow laboratory procedures and apparatus manuals. Use required shoes.
Wrong/improper use of equipment.	Damage to personell or equipment.	3	A	B	B	A3	Use protective gear. Follow laboratory procedures and apparatus manuals.
Wrong/improper use of gas flask.	Damage to tubes.	1	A	A	B	A1	Follow laboratory procedures and apparatus manuals.

K.2 Risk value table

Risk value = Likelihood (1, 2 ...) x consequence (A, B ...). Risk value A1 means very low risk. Risk value E5 means very large and serious risk

Likelihood		Consequence					
Value	Criteria	Grading		Human	Environment	Economy/material	
1	**Minimal**: Once every 50 year or less	E	Very critical	May produce fatality/ies	Very prolonged, non-reversible damage	Shutdown of work >1 year.	
2	**Low**: Once every 10 years or less	D	Critical	Permanent injury, may produce serious health damage/sickness	Prolonged damage. Long recovery time.	Shutdown of work 0.5-1 year.	
3	**Medium**: Once a year or less	C	Dangerous	Serious personal injury	Minor damage. Long recovery time	Shutdown of work < 1 month	
4	**High**: Once a month or less	B	Relatively safe	Injury that requires medical treatment	Minor damage. Short recovery time	Shutdown of work < 1week	
5	**Very high**: Once a week	A	Safe	Injury that requires first aid	Insignificant damage. Short recovery time	Shutdown of work < 1day	

K.3 Matrix for risk assessment

MATRIX FOR RISK ASSESSMENT

CONSEQUENCE						
	Very critical	E1	E2	E3	E4	E5
	Critical	D1	D2	D3	D4	D5
	Dangerous	C1	C2	C3	C4	C5
	Relatively safe	B1	B2	B3	B4	B5
	Safe	A1	A2	A3	A4	A5
		Minimal	Low	Medium	High	Very high
		LIKELIHOOD				

Explanation of the colors used in the risk matrix.

Color	Description
Red	Unacceptable risk. Safety measures must be implemented.
Yellow	Measures to reduce risk shall be considered.
Green	Acceptabel risk.